

INCI DOGAN CINAR

Mathematical modeling and computer simulation of simultaneous heat and mass transfer during drying of food particles

(Under the Direction of Romeo T. Toledo)

The purpose of this dissertation was to design and simulate a mathematical model for the process of simultaneous heat and mass transfer during fluidized bed and tunnel drying for both thawed and infused rabbiteye blueberries. Two different simulation models, namely the diffusional and Luikov models, were formulated and solved using a finite element method (FEM). Blueberries were considered as homogenous pieces and modeled using spherical geometry.

Moisture and temperature distributions in both blueberries during either tunnel or fluidized bed drying were described by a set of coupled non-linear heat and mass transfer equations. Non-linearities in these models were introduced by the use of moisture or temperature dependent transport parameters and material properties.

The Luikov model considered both liquid water and vapor diffusion whereas the diffusional model assumed only liquid water transfer and surface evaporation.

The finite element formulation was developed using Galerkin's weighted residual technique. Numerical solution of these models took into account non-linearities. Coupling effects, which improves the predictions, were presented in governing equations and boundary conditions.

Simulation data was verified by the experimental drying data for both thawed and infused berries in tunnel and fluidized bed dryers. Initial moisture content of thawed berries was 578.99 kg water/100kg DM and of infused berries was 127.87 kg water/100kg DM. Tunnel drying was done at 60 °C with air velocity of 4 m/s and 0% relative air humidity. The temperature of the fluidized bed dryer was 170 °C for thawed berries and 150 °C for infused berries with an air velocity of 12 m/s and relative air humidity of 0%.

The Luikov model gave better approximations to the moisture distribution due to its ability to account for the vapor diffusion.

INDEX WORDS: Rabbiteye blueberries, simultaneous heat and mass transfer, mathematical modeling, computer simulation

MATHEMATICAL MODELING AND COMPUTER SIMULATION OF
SIMULTANEOUS HEAT AND MASS TRANSFER DURING DRYING OF
FOOD PARTICLES

by

INCI DOGAN CINAR

B.S., University of Ankara, Turkey, 1991

M.S., University of Ankara, Turkey, 1993

M.S., Clemson University, 1996

A Dissertation Submitted to the Graduate Faculty of The University of Georgia in Partial

Fulfillment of the Requirements for the Degree

DOCTOR OF PHILOSOPHY

ATHENS, GEORGIA

2002

© 2002

Inci Dogan Cinar

All Rights Reserved

MATHEMATICAL MODELING AND COMPUTER SIMULATION OF
SIMULTANEOUS HEAT AND MASS TRANSFER DURING DRYING OF
FOOD PARTICLES

by

INCI DOGAN CINAR

Approved:

Major Professor: Romeo T. Toledo

Committee:

Yen-Con Hung
William L. Kerr
Rakesh Singh
Garrett L. Van Wicklen

Electronic Version Approved:

Gordhan L. Patel
Dean of the Graduate School
The University of Georgia
May 2002

I dedicate this dissertation to my husband Ozer, my daughter Irem Burcak, and my
parents.

ACKNOWLEDGMENTS

I would like to thank to my major Professor Dr. Romeo T. Toledo for his guidance, interest and support during the course of this research. I also express my sincere appreciation to Drs. Garrett Van Wicklen, William Kerr, Rakesh Singh, and Yen-Con Hung for serving on my advisory committee.

My deepest appreciation to my husband and daughter, my parents, sister, and brother and to my dearest friend Victoria Baramidze for their unconditional love, support and understanding throughout my entire stay in the United States.

Finally, I would like to thank Kahramanmaras Sutcu Imam University, Turkey and the Graduate School of the University of Georgia for financing my doctoral studies at the University of Georgia.

TABLE OF CONTENTS

	Page
ACKNOWLEDGEMENTS	v
LIST OF TABLES	viii
LIST OF FIGURES	ix
CHAPTERS	
1 INTRODUCTION	1
2 LITERATURE REVIEW	4
Historical Development of Drying Process	4
Theoretical Aspects.....	6
Osmotic Dehydration	14
Fluidized Bed Drying.....	17
Mathematical Models.....	17
Boundary Conditions	25
Finite Element Method	28
Model Validation	29
Engineering Properties.....	29
3 THEORETICAL ANALYSIS	37
Experimental Design.....	37
Engineering Properties.....	38
Governing Equations and Boundary Conditions	41
Finite Element Formulation	49
Solution Procedures	60

Element Equations	61
Simulation	64
4 MODEL VERIFICATION	65
Verification of Diffusional Model	67
Verification of Luikov Model	81
Model Application	88
Sensitivity Analysis	90
Effect of Initial Conditions on Drying	97
5 SUMMARY AND CONCLUSIONS	106
NOTATIONS	109
APPENDICES	111
A Matlab Code for Diffusional Model	111
B Matlab Code for Luikov Model	113
C Flow diagram for procedure used in diffusional and Luikov Models	115
REFERENCES	116

LIST OF TABLES

Table 4.1. Material and transport properties for both thawed and infused berries in tunnel drying	68
Table 4.2. Material and transport properties for both thawed and infused berries in fluidized bed drying	69
Table 4.3. Effective diffusivity equations for both thawed and infused blueberries (M = moisture content, kg water/kg DM)	70

LIST OF FIGURES

Figure 4.1. Initial element grid of a single blueberry (1/4 section)	66
Figure 4.2. Refined element grid of a single blueberry (1/4 section)	67
Figure 4.3. Comparison of predicted and experimental moisture contents of thawed blueberries during tunnel drying at 60 °C	71
Figure 4.4. Comparison of predicted and experimental moisture contents of infused blueberries during tunnel drying at 60 °C	72
Figure 4.5. Predicted temperature histories for thawed (Part A) and infused (Part B) blueberries during tunnel drying at 60 °C	74
Figure 4.6. Comparison of predicted and experimental moisture contents of thawed blueberries during fluidized bed drying at 170°C	75
Figure 4.7. Comparison of predicted and experimental moisture contents of infused blueberries during fluidized bed drying at 150°C	76
Figure 4.8. Predicted temperature histories for thawed (Part A) and infused (Part B) berries during fluidized bed drying	77
Figure 4.9. The Predicted moisture distributions of berries during drying using the diffusional model (A: thawed berries during tunnel drying, B: infused berries during tunnel drying, C: thawed berries during FB drying, D: infused berries during FB drying)	78
Figure 4.10. The predicted temperature distributions of berries during drying using the diffusional model (A: thawed berries during tunnel drying, B: infused berries during tunnel drying, C: thawed berries during FB drying, D: infused berries during FB drying)	79
Figure 4.11. Comparison of predicted and experimental moisture contents of thawed blueberries during tunnel drying at 60 °C	82
Figure 4.12. Comparison of predicted and experimental moisture contents of infused blueberries during tunnel drying at 60 °C	83
Figure 4.13. Comparison of predicted and experimental moisture contents of thawed blueberries during fluidized bed drying at 170 °C	84

Figure 4.14. Comparison of predicted and experimental moisture contents of infused blueberries during fluidized bed drying at 150 °C	85
Figure 4.15. The predicted moisture distributions of berries during drying using the Luikov model (A: thawed berries during tunnel drying, B: infused berries during tunnel drying, C: thawed berries during FB drying, D: infused berries during FB drying).	86
Figure 4.16. The predicted temperature distributions of berries during drying using the Luikov model (A: thawed berries during tunnel drying, B: infused berries during tunnel drying, C: thawed berries during FB drying, D: infused berries during FB drying).	87
Figure 4.17. Comparison of predicted and experimental moisture contents of thawed berries during tunnel drying at 110°C using both the diffusional and the Luikov models	89
Figure 4.18. Comparison of predicted and experimental moisture contents of infused berries during tunnel drying at 110°C using both the diffusional and the Luikov models.	90
Figure 4.19. The predicted moisture contents of the infused berries for different Deff during tunnel drying using the diffusional model	91
Figure 4.20. The predicted moisture contents of the infused berries for different Deff during tunnel drying using the Luikov model.....	92
Figure 4.21. The predicted moisture contents of the infused berries for different Deff during fluidized bed drying using the diffusional model.....	92
Figure 4.22. The predicted moisture contents of the infused berries for different Deff during fluidized bed drying using the Luikov model.....	93
Figure 4.23. The predicted moisture contents of the infused berries for different hm values during tunnel drying using the diffusional model.....	94
Figure 4.24. The predicted moisture contents of the infused berries for different hm values during tunnel drying using the Luikov model.	94
Figure 4.25. The predicted moisture contents of the infused berries for different hm values during fluidized bed drying using the diffusional model.....	95
Figure 4.26. The predicted moisture contents of the infused berries for different hm values during fluidized bed drying using the Luikov model	96

Figure 4.27. Effect of initial berry temperature on the predicted moisture content of berries during drying using the diffusional model (A: thawed berries during tunnel drying, B: infused berries during tunnel drying, C: thawed berries during FB drying, D: infused berries during FB drying).....	98
Figure 4.28. Effect of initial berry temperature on the predicted temperature of berries during drying using the diffusional model (A: thawed berries during tunnel drying, B: infused berries during tunnel drying, C: thawed berries during FB drying, D: infused berries during FB drying).....	99
Figure 4.29. Effect of initial berry moisture content on the predicted moisture content of berries during drying using the diffusional model (A: thawed berries during tunnel drying, B: infused berries during tunnel drying, C: thawed berries during FB drying, D: infused berries during FB drying).....	100
Figure 4.30. Effect of initial berry moisture content on the predicted temperature of berries during drying using the diffusional model (A: thawed berries during tunnel drying, B: infused berries during tunnel drying, C: thawed berries during FB drying, D: infused berries during FB drying).....	101
Figure 4.31. Effect of initial berry temperature on the predicted moisture content of berries during drying using the Luikov model (A: thawed berries during tunnel drying, B: infused berries during tunnel drying, C: thawed berries during FB drying, D: infused berries during FB drying).....	102
Figure 4.32. Effect of initial berry temperature on the predicted temperature of berries during drying using the Luikov model (A: thawed berries during tunnel drying, B: infused berries during tunnel drying, C: thawed berries during FB drying, D: infused berries during FB drying).....	103
Figure 4.33. Effect of initial berry moisture content on the predicted moisture content of berries during drying using the Luikov model (A: thawed berries during tunnel drying, B: infused berries during tunnel drying, C: thawed berries during FB drying, D: infused berries during FB drying).....	104
Figure 4.34. Effect of initial berry moisture content on the predicted temperature of berries during drying using the Luikov model (A: thawed berries during tunnel drying, B: infused berries during tunnel drying, C: thawed berries during FB drying, D: infused berries during FB drying).....	105

CHAPTER 1

INTRODUCTION

Drying is one of the most common methods of food preservation. During drying, the behavior of materials depends on the heat and mass transfer characteristics of the product being dried. The mechanism of heat and mass transfer is complicated therefore it has been a subject of intense research for years. The analysis of heat and mass transfer in food system is very important because food properties change with temperature and moisture content. A knowledge of temperature and moisture distribution in the product eases product and/or process design and quality control. Mathematical models and simulation help providing the required temperature and moisture information. Defining the optimum values for drying parameters usually requires costly instruments and lengthy tests. Models facilitate the scientific process design and minimize costs and energy requirements. Therefore, computer based simulation eases the investigation of such complicated food systems. Good understanding of existing drying theory supported by experimental data is the key for further modeling development.

There are many models in the literature for temperature and moisture predictions during drying of foods. However, very few researchers have attempted to study the coupled heat and mass transfer process in food systems. Most of the past work on heat and mass transfer modeling during drying either considered constant material properties (Haghighi and Segerlind, 1988), used a simplified one dimensional model or solved heat and mass transfer equations separately (Sokhansaj and Gustafson, 1979).

This research concentrates on two main models, namely Luikov's model and Diffusional model, to solve heat and mass transfer equations simultaneously with variable material properties. In Luikov's model, all the transport phenomena are given by the effects of moisture content and temperature by applying irreversible thermodynamics. Therefore, it makes a process easy to understand, but it is more difficult to obtain the coefficients in the governing transfer equations. Also some coefficients (e.g., phase change coefficient) are not physical properties of food but are process variables. Therefore, in the literature more simplified models such as the diffusional model are used. The validity of the model is greatly dependent on the variable effective moisture diffusivity coefficient (D_{eff}). D_{eff} is usually assumed to be a function of either temperature or moisture content or more precisely both moisture and temperature (Nsonzi and Ramaswamy, 1998; Ramaswamy and Nsonzi, 1998; Markowski, 1997; Igbeka, 1982; Sharaf-Eldeen and Hamdy, 1979; Zogzas et al., 1996; Itaya et al., 1995; Fortes and Okos, 1981). However, these relationships are empirical. Also, incorporation of the coupling effect of temperature in the diffusion model is still a question.

Solutions of governing heat and mass transfer equations require solution techniques for a set of partial differential equations. For this purpose, the finite element method (FEM) was chosen since it has the capability to solve non-linear problems with boundary conditions.

This research concentrates on the six major steps for developing a fundamental drying model (Waananen et al., 1993).

- 1) The identification of controlling resistances (energy versus mass, internal versus external) (if there is no forced convection external resistance, with increasing moisture content (> 1 kg water/kg dry solid) energy transfer is controlling).

- 2) The identification of moisture transfer mechanisms (diffusion, capillary flow, etc.).
Water contents above saturation cause capillary movement whereas at low moisture content vapor diffusion occurs.
- 3) Development of mathematical descriptions of drying process along with structural and thermodynamic assumptions.
- 4) The determination of all material properties, transfer coefficients and isotherm relationships
- 5) The solution of resulting equations
- 6) The validation of model predictions

The purpose of this research is to analyze and predict moisture and temperature histories and distributions of the thawed and infused blueberries during both tunnel and fluidized bed drying using the Luikov model and the diffusional model. The finite element method will be used to solve non-linear set of partial differential equations. Therefore, it will provide moisture and temperatures histories and distributions regarding the both thawed and infused berry behavior under drying conditions. It is hypothesized that the main mechanisms of moisture transport within the blueberry are either liquid diffusion (the diffusional model) or both liquid and vapor diffusion (the Luikov model).

The major objectives of this research in steps are:

- To create an input file which contains material and transport properties required for the model solutions.
- To model the non-linear simultaneous heat and mass transfer during both tunnel and fluidized bed drying conditions using finite element method.
- To predict moisture and moisture and temperature histories and profiles for thawed and infused blueberries.
- To verify the model predictions using experimental data.

CHAPTER 2

LITERATURE REVIEW

Historical Development of Drying Process

Food drying (dehydration) can be defined as a process in which water is removed to slow down the growth of spoilage microorganisms and the occurrence of deteriorative chemical reactions. Drying is one of the oldest food preservation techniques. It is not certain when the use of dehydration for food preservation began, but its initial development was entirely empirical. However, the process eventually evolved within a scientific based environment. Today dehydration is used not only to preserve, but also to reduce the cost or difficulty of packaging, handling, storing and transporting by converting a wet perishable food into a dry or semi-moist solid. It also reduces the food weight and sometimes the volume (Canovas and Mercado, 1996).

Up until the end of the 18th century, the food industry used the most primitive drying operations which required only warmth and wind. During the 19th century, the scale and production rate rose considerably leaving these methods incompatible as a viable commercial practice. Improvements began with the invention of the papermaking machine. By the end of the 19th century prototypes of the radiant heat drier, the vacuum drier and the pneumatic conveying drier that are in use today were patented.

Theoretical principles behind these developments started with Fisher (1921) who developed drying data on woolen fabrics. He calculated empirical relationships for three different periods of drying and concluded that the drying curves for both colloidal and non-colloidal materials were similar. Ten years later, Sherwood and Cornings (1931) measured the drying rate of a completely wet material spread over small trays in a wind

tunnel. Lewis (1934) elucidated two independent processes of moisture transfer; one being evaporation of water from surface of the solid and a second involving diffusion of liquid water from the interior to the surface. Gilliland and Sherwood (1937) introduced a diffusion equation to calculate constant drying rate time from experimentally derived values of diffusion coefficients. Sherwood later stated that the liquid movement, internal vapor diffusion within the solid, diffusion through the external air boundary layer and eddy diffusion into the bulk air may be treated as diffusional resistances. Krischer (1978) considered moisture arriving to the surface from the interior as a sum of vapor phase movement due to diffusion and liquid motion due to capillarity. He then derived differential equations for simultaneous movement of moisture in both phases in one direction in a homogenous solid from the fact that there is a discontinuity within the material where the capillary movement, if present, might end and vapor diffusion begins. Capillary conductivity and diffusional resistance coefficient were also described in the equations. Krischer's findings were used as a basis for modern drying technology although capillary conductivity was highly dependent on the solid's structure. Values varied six orders of magnitude between solids, even for the same material over a whole moisture content range. The diffusional resistance coefficient can also become large and variable, especially for non-granular solids. Therefore, for materials having complex structure, the diffusion equation with concentration dependent coefficient (D) has been preferentially expressed in the form of Equation 2.1.

$$\frac{\partial c}{\partial t} = \frac{\partial}{\partial x} (D \frac{\partial c}{\partial x}) \quad 2.1$$

Krischer was one of the first to understand the importance of simultaneous heat and mass transfer in drying. He was able to get solutions for temperature and

concentration fields as a function of time using Henry's linear coupling relationship between temperature and moisture concentration. Philip and de Vries (1966) used a more general approach incorporating terms for temperature gradients in liquid and vapor movement within a porous material. Luikov (1966) used irreversible thermodynamics to divide the moisture transfer into two parts: one due to a moisture gradient driving force characterized by "moisture diffusivity", and another due to temperature gradient. Luikov's model combined both of Krischer's capillarity and diffusion parameters, thus reducing the number of variable coefficients to one. Luikov assumed that moisture moved as vapor entirely by an evaporation-condensation mechanism and was driven by thermal gradients. Bulk vapor filtration was also taken into account in which case a pressure gradient driving force was included. Luikov also noted that moisture may transfer from a material of low moisture content to another of higher moisture content if the latter was more hygroscopic, therefore it was unsatisfactory to use the moisture gradient as a driving force (Keey, 1980).

Theoretical Aspects

Drying not only affects the water content of the product, but also other physical and chemical characteristics such as water activity, sorption isotherms, microbial spoilage, enzymatic, non-enzymatic reactions, and destruction of nutrients and flavor (Canovas and Mercado, 1996). Water is mainly removed by the use of air which provides the necessary sensible heat and latent heat of vaporization and acts as a carrier gas to remove water vapor from the evaporation surface (Brennan and Butters, 1990).

High quality dried product with a reasonable cost can be achieved if dehydration is relatively rapid. Factors that affect total drying time are 1) product size and geometry, 2) product geometrical arrangement in relation to drying air, 3) properties of the drying

air, and 4) characteristics of drying equipment (Jayaraman and Das Dupta, 1992). Vega-Mercado et al. (2001) and Ratti (2001) provided general information on the fundamentals of drying, engineering aspects and commercial applications.

Since drying is a complex phenomenon, many mechanisms have been presented to explain internal transport and surface evaporation of water in foods. Depending on the application, different mechanisms for moisture transport predominate. For simultaneous heat and mass transfer the possible mechanisms for internal moisture transfer are: (a) liquid movement due to capillary forces, (b) liquid diffusion due to concentration gradients, (c) liquid diffusion through pores due to vapor pressure gradients, and (d) vapor flow due to total pressure difference (Rossen and Hayakawa, 1977). For a moist porous solid, the rate of phase change is much faster than heat and mass transfer rates thus liquid content, partial vapor pressure and temperature are in equilibrium in the material. Partial vapor pressure equals the saturation value when the proportion of water in the liquid phase is larger than the maximum equilibrium moisture content in sorption (Berger and Pei, 1973).

Liquid or vapor flow due to total pressure gradient is caused by external pressure, shrinkage, high temperatures and capillarity. Effusion (Knudsen) flow has importance in high vacuum conditions (as in freeze drying) and only exists when the mean high path of vapor molecules is close to the order of the pore diameter. Liquid movement due to gravity is generally neglected since it has no significant effect on food drying (Fortes and Okos, 1980).

Liquid diffusion is considered by many researchers as the principal flow mechanism in the drying of solids and is given by Fick's equation.

$$\frac{\partial M}{\partial t} = \nabla(D_{\text{eff}} \nabla M) \quad 2.2$$

Where M = mass content (db) D_{eff} = effective diffusion coefficient

D_{eff} is assumed to be either constant or linearly dependent on temperature and/or concentration. Arrhenius type dependency on temperature is: $K = K_0 \exp(-E_a/RT)$. Hougén et al. (1940) concluded that the diffusion equation could be applied to the drying of starches and gelatin. The diffusion equation could be misleading in some cases where the driving forces for diffusion are pressure related instead of concentration. However, any error can be compensated for if calculations are made by numerical integration techniques. Liquid diffusion due to a concentration gradient alone does not take into account shrinkage, case hardening, or sorption isotherm (Fortes and Okos, 1980; Canavos and Mercado, 1996).

Fortes and Okos (1980) defined capillarity as “flow of a liquid through the interstices and over the surface of a solid due to molecular attraction between solid and liquid”. The capillary liquid flow can be expressed as (Canavos and Mercado, 1996)

$$1/A \frac{\partial x}{\partial t} = J_L = -k_H \nabla \phi \quad 2.3$$

Where ϕ = pressure difference between water and air at the water-air interphase
present in capillary

k_H = permeability

x = moisture content

A = exposed drying area

$$k_H = (\sigma \cos\theta) / (4r^2 f(r) n) \int r^2 f(r) dr \quad 2.4$$

Where σ = surface tension

θ = contact angle

$f(r)$ = differential curve for distribution of pore size as a function of
radius r

According to evaporation-condensation theory, water vapor flowing within the product condenses near the evaporation surface. Therefore the rate of condensation is equal to the rate of evaporation from the surface providing there is no accumulation of water in the pores near the surface. The theory takes into account simultaneous heat and mass transfer in a continuous network of pores. Canovas and Mercado (1996) derived the Lewis number from heat and mass balance.

The Lewis number (Le) determines whether the heat transfer equation should be considered. If $Le > 60$ the mass transfer equation is sufficient to describe the drying process, while heat transfer predominates when $Le < 60$ (Young 1969).

A diffusional internal mass transfer mechanism, which incorporates liquid, vapor, and surface diffusion, has been assumed in many modeling studies. Van den Berg (1981) hypothesized at surface diffusion of water in starch molecules as a molecular jump from one adsorbed site to another. For granular solids, the main mechanism was found to be the capillary movement of water at levels above the saturation point. At temperatures very close to or higher than the boiling point of water, there occurs rapid vapor generation which may cause significant total pressure gradients along with partial vapor pressure gradients. Same situation may be seen during moderate temperature vacuum

drying and high temperature convective drying. One might also consider the cross effects between drying forces; in coupled heat and mass transfer conditions temperature gradients can cause mass transfer (Soret effect) and mass concentration gradients can cause heat flow (Dufour effects), when irreversible thermodynamics is used as the basis for the model (Waananen et al., 1993).

At high moisture, diffusion of liquid water might also be considered in the model as diffusivity decreases significantly in the presence of water soluble sugars or salts. At lower moisture contents, transport is mainly by vapor diffusion through the pores and cracks that are developed during drying. In the latter, the effective diffusivity of water is strongly dependent on the porosity of the material, which is reduced sharply by water soluble carbohydrates (Marousis et al., 1989). Therefore the lowest diffusivity values were found in homogenous gel like foods at low moistures, and the highest in highly porous, freeze dried, or extruded foods (Saravacos, 1995).

In convective air drying, the mechanisms that have to be considered are moisture diffusion in the solid towards the surface, vaporization and convective transfer of vapor into the air stream and conductive heat transfer within the material and heat transfer from air to the solid surface. Each mechanism is formulated by a driving force and transport coefficient such as the moisture diffusion coefficient, and the boundary layer mass and heat transfer coefficients and thermal conductivity (Maroulis et al., 1995).

Bruin and Luyben (1980) published a detailed review on drying of food materials explaining all possible mechanisms along with heat and mass transfer equations and changes in food materials during dehydration.

For multicomponent foods, the situation is more complex. Adsorption and desorption of moisture (sorption isotherm) needs to be determined to find which component is the rate limiting within a moisture change. Hong et al. (1986) found that

the rate limiting component was the one having the lowest effective diffusion coefficient. They stated that in multicomponent foods moisture transfers from the component having higher water activity to the one at lower water activity. Moisture sorption isotherms are very important in describing the relationship between water activity and equilibrium moisture content of foods, and are used for calculation of drying time, ingredient mixing and packaging predictions and moisture change during storage. Each isotherm is unique in the range of specified water activity because: (1) water activity depression of food is caused by a combination of factors and each might be predominant in any given range, (2) hygroscopic properties of components may change due to physical and/or chemical interactions, and (3) changes in dimensions and transfer properties may affect sorption/desorption rate during processes (Lomauro et al., 1985).

The amount and state (free or bound) of water molecules in a food matrix plays a primary role in sorption isotherms. Free water held in interstitial spaces and pores of material by pure physical forces (surface tension), exhibits liquid-like properties of water. Bound water is a sorbent or solute-associated water and held by water-solid interactions on mono layer and water-water interactions on multiple layers. A generalized moisture sorption isotherm can be divided into three regions: (1) Region A; corresponds to monomolecularly adsorbed water at hydrophilic, charged and polar groups of food components. The water has an enthalpy of vaporization greater than pure water, therefore is unavailable for chemical reactions. (2) Region B (transition region); adsorbed additional layers over the monolayer. (3) Region C; contains water that has properties similar to that of free water and corresponds to condensation of water in capillaries of a porous food structure (McMinn and Magee, 1999 and Karathanos, 1999).

When a porous material is dried from a high enough initial moisture content, the surface is covered with a continuous layer of free water and evaporation occurs at the

surface. Moisture is transferred internally due to capillary flow of free water (water inside of pores) through the voids. Drying rate is determined by external conditions (temperature, humidity, air flow rate) only. This period is called the constant rate period. The surface remains saturated with liquid water because the rate of water movement to surface is equal to the rate of evaporation from the surface and surface temperature remains constant at the wet bulb temperature of the drying air. The water phase is continuous as long as the free water content is greater than a critical value. For a 2-dimensional porous medium, the critical value is 50 % of the saturated free water content. For a 3-dimensional porous medium, it is ~30 % (Chen and Pei, 1983).

The rate of mass transfer is given by

$$(\partial w/\partial t)_c = -k_g A (P_s - P_a) = -k_g A (H_s - H_a) \quad 2.5$$

Where

$(\partial w/\partial t)_c$ = drying rate

k_g = mass transfer coefficient

A = drying surface area

P_s = water vapor pressure at surface

P_a = partial pressure of water vapor in air

H_s = relative humidity at surface

H_a = relative humidity of air

The rate of heat transfer is

$$(\partial T/\partial t) = h_c A (T_a - T_s) \quad 2.6$$

Where

h_c = heat transfer coefficient for convection area for heat transfer

T_a = dry bulb temperature of air

T_s = surface temperature

At the constant rate period, the rate of drying can be determined using either heat or mass transfer equations. Generally heat transfer equations give a more reliable estimation than mass transfer equations (Jayaraman and Das Gupta, 1992). The constant rate drying time can be derived by equating heat transfer and mass transfer equations since there is equilibrium between heat and mass transfer (Brennan and Butters, 1990).

When the critical water content is reached, discontinuous wet patches start to form within the solid. The mass transfer coefficient and surface free water content decrease marking the start of the first falling rate (Chen and Pei, 1983). At the first falling rate period the surface temperature rises due to a new heat balance and slowly creeps towards the dry bulb temperature of the air. Free water exists on surfaces while dry patches may contain bound water. Subsequently, the drying rate falls. The second falling rate starts when the evaporation front moves into the solid and the drying rate falls further. The mass concentration of surface water is its maximum sorptive value, no surface free water exists. Inside the evaporation front, voids contain free water and the main moisture transfer is by capillary flow. During the falling rate period, the drying rate is controlled by moisture transfer within the solid and therefore takes the major portion of drying time (Brennan and Butters, 1990; Chen and Pei, 1983). In falling rate period, at high moisture levels, external resistance to mass and moisture transport such as temperature, gas velocity, total pressure, and partial vapor pressure can be controlling, while at low moisture, the drying rate is controlled by internal factors such as moisture

diffusivity (Cronin and Kearney, 1998). The sample temperature is measured during drying to identify whether a process is controlled by energy or mass transfer. As long as the sample temperature is equal to wet bulb temperature of air, the process is energy transfer controlled. When the sample temperature exceeds the wet bulb temperature of air, mass transfer is the controlling mechanism. Also, if the reciprocal of the overall transfer coefficient is close to the reciprocal of external mass transfer coefficient, external mass transfer control is suggested (Waananen et al., 1993). Heat and mass transfer equations for falling rate are given by Brennan and Butter (1990), Chen and Pei (1983), and Suzuki et al. (1974) for different material geometries. They presented derivations of drying rate equations for constant and falling rate periods along with the initial and boundary condition equations.

During the falling rate period, the average drying time can be estimated from Fick's second law of diffusion (Jayaraman and Das Gupta, 1992). The mechanism of moisture migration is capillary flow at the first falling rate period whereas at the second falling rate period evaporation occurs below the surface and vapor diffusion occurs from the evaporation site to the surface (Ramaswamy and Nsonzi, 1998; Sabarez and Price, 1999). Solutions acquired by modeling of simultaneous heat, water and vapor diffusion were studied by Thorvaldsson and Janestad (1999). Although drying is described by both constant and falling rate periods, the constant rate period is very short and therefore not often observed in food drying (Zogzas and Maroulis, 1996).

Osmotic Dehydration

Osmotic dehydration was first proposed by Ponting et al. in 1966 (Spiazzi and Mascheroni, 1998). It can be defined as the removal of water from a cell through the cell membrane by lowering the water activity on the other site of the semipermeable

membrane (Yao and Le Maguer, 1996). Hypertonic solutions (generally sugar or salt solutions) having higher osmotic pressure than the food are used in the process to lower the water activity of the food (Jayaraman and Das Gupta, 1992). Recently, osmotic dehydration has gained increasing attention as a potential alternative or supplementary process to conventional air drying. Specifically, in the food industry, although osmotic dehydration itself cannot provide a sufficiently low moisture content for shelf stability, osmotic dehydration can be used as a pretreatment before air drying to reduce the water content of food to 30-70% of the original amount. The main advantages of osmotic dehydration are (1) high quality product and low operation cost, (2) shorter air drying time, (Since the process is carried out at a constant low temperature, it is isothermal and does not involve internal phase change), (3) limited heat damage, and (4) improved textural quality, flavor enhancement and color stabilization (Karathanos et al., 1995; Yao and Le Maquer, 1996; Simal et al., 1997).

During osmotic dehydration, there is a two-way mass transfer between the product and low water activity solution: 1) water, along with natural substances (e.i., sugars, vitamins, pigments), is transferred from food to the solution (water loss), and 2) solute migrates from solution to the food (solute gain). Thus, there occurs a shrinkage and weight loss of product. This is complex mass transfer since both transfers occur simultaneously (Karathanos and Kostaopoulos, 1995). These two fluxes take place under strong non-equilibrium conditions. Diffusing solute enters into the extracellular volume. Depending on the solute characteristics, the solute may or may not penetrate the cell membrane and the intracellular volume. This penetration creates a chemical potential across the cell membrane, which in turn draws water out into the extracellular volume. Therefore two simultaneous counter flows exist (Yao and Le Maguer, 1996).

Water loss and solute gain depend on operating conditions, cellular tissue type and the form in which the product is pretreated. Highly concentrated solutions (60-70% by weight) result in considerable product weight loss and low solute gain, whereas low concentrations result in solute gain by product (impregnation). Solutes of high molecular weight cause water loss rather than solid gain (Spiazzi and Mascheroni, 1997).

During mass transfer in osmotic dehydration two resistances exist: 1) external (temperature, concentration of osmotic solution, contact time), and 2) more complex internal (nature of food, size, shape, cell tissue structure, membrane permeability, shrinkage). Generally, external resistances are negligible compared to internal resistances. Processing conditions (temperature, type and concentration of solution, contact time) has an effect on final product quality (Nsonzi and Ramaswamy, 1998).

Two basic approaches on modeling the osmotic dehydration are: 1) macroscopic (assumes tissue is homogenous, therefore properties of cell wall, cell membrane and vacuole are lumped), and 2) microscopic (recognizes heterogeneity and complex cell structure is given by simplified conceptual model. Yao and Le Maguer (1996) presented a new conceptual model to describe the mass transfer in 2 layers representing intracellular and extracellular volumes and semi-permeable membrane that separates two layers. Mathematical modeling of the osmotic dehydration process has been carried out by many researchers. Review of this research can be found in Jayaraman and Das Gupta (1992); Nsonzi and Ramaswamy (1998); Simal et al. (1997); Yao and Le Maguer 1994 and 1997. The numerical solution (finite element analysis) of osmotic dehydration process is reviewed by Yao and Le Maguer (1994 and 1997) for one dimensional transfer of potato tubers.

Fluidized Bed Drying

The fluidized bed dryer is one of the popular types of dryers, and is used in every area of drying. Advantages of fluidized bed drying depend on improving the rate of heat and mass transfer. High drying rates are important at the start of the process. High thermal efficiency can be achieved by recycling the exhaust air that will be far from saturation. Final material moisture content is controlled by adjusting the air inlet temperature. Air flow rates are adjusted according to the fluidization requirements. Therefore, a series of experiment are taken to determine the minimum fluidization velocity for a given food material.

The limiting factor for drying is the equilibrium moisture content of the product under drying conditions. Theoretically, evaporation must be equal to or less than the amount of water that the air can hold without reaching saturation (relative to food desorption isotherm) and energy for the latent heat is what remains from the transferred energy after providing the sensible heat (Kiranoudis et al., 1997; Ferrao et al., 1998; Temple et al., 2000).

Mathematical Models

Drying is a complicated process involving simultaneous heat and mass transfer phenomena. Coupled phenomena complicate the analysis of drying that, to date, there is no commonly applied theoretical model to describe simultaneous heat and mass transfer (Rovedo et al., 1995). Many models have been presented for air drying of foods, but experimental data are still needed (Maroulis et al., 1995; Banga and Singh, 1994). Model development helps maximize the product quality while maintaining and ensuring the shelf stability of product (Fryer, 1994). Basically heat and mass flux equations are combined with mass and energy balance equations to yield a set of differential equations

which describe heat and mass transfer in foods during drying (Bruin and Luyben, 1980). Some of the modeling assumptions, driving forces and mechanisms were given in tabulated form by Waanen et al. (1993). Sharaf-Eldeen et al. (1987) reviewed the mathematical models for drying and classified them into the following three different types: semitheoretical and empirical models, diffusion models, and simultaneous heat and mass transfer models. Boundary conditions on these differential equations are determined by the type of drying equipment, the way of introducing food material into the drying medium etc. Three types of general boundary conditions were summarized by Fowler (1997). Solutions of these differential equations are often achieved by numerical techniques because of moisture dependent transport properties and time dependent boundary conditions. The finite element method is the most popular. Depending on assumptions, solutions may be simplified. For example, it is reasonable to assume uniform product temperature because the Biot number is small so that temperature dependent diffusivity is used to calculate drying rates in the first falling rate period. Or it is possible to use constant transport properties during initial stages of drying as stated by Bruin and Luyben (1980).

For drying of foodstuffs, there are two typical models to describe the process. Isothermal models assume rapid heat transfer along with slow moisture diffusion. Therefore drying occurs entirely at dry bulb temperature of air. These are used in modeling of foods having low initial moisture content. Uniform temperature-profile models assume infinite thermal conductivity. The temperature is uniform throughout the sample at any time during drying. The method is valid when $Le > 10$. Le is the ratio of thermal diffusivity to the moisture diffusivity (Rovedo et al., 1995).

Other models are also used to describe simultaneous heat and mass transfer in drying of food materials are as follows. In the literature on mathematical modeling of

drying, Luikov's model is frequently seen. Luikov (1975) applied the principles of irreversible thermodynamics which accounts for cross-effects between driving forces. Fick's law is based on proportionality between mass transfer and the concentration gradient whereas Fourier's law between heat transfer and temperature gradient. When there is more than one driving force, Luikov's theory enables the combination of heat and mass transfer. He found a direct relation between mass and heat transfer since there was entropy transfer along with the mass transfer in capillary porous bodies. This interrelation becomes closer when liquid evaporates inside the body (Fortes and Okos, 1980).

The derived equations for Luikov's model are based on the assumptions that air and water transport is simultaneous, no shrinkage or deformation occurs, isotropy is assumed, and direct relation to isotherms is not considered. Luikov used linear law which is "unlike classical theory of molecular transfer, the simultaneous heat and mass transfer is determined by the action not of one corresponding force but the action of all thermodynamic forces" (Rossen and Hayakawa, 1977; Luikov, 1966):

$$J_i = \sum_{k=1}^n L_{ik} X_k \quad i = 1, 2, \dots, n \quad 2.7$$

Where, J_i = i^{th} flux (water, ice, vapor, air)

X_k = k^{th} thermodynamic driving forces

L_{ik} = kinetic coefficients ($L_{ik} = L_{ki}$)

Luikov defined vapor and liquid fluxes in capillary porous bodies as (Canovas and Mercado, 1996):

$$J_v = -D_v \rho_s \nabla X - k_{TV} \rho_s \nabla T \quad 2.8$$

$$J_L = -D_L \rho_s \nabla X - k_{TL} \rho_s \nabla T \quad 2.9$$

Where, D_v, D_L = diffusion coefficients of vapor and liquid, respectively

k_{TV}, k_{TL} = thermal moisture diffusivities of vapor and liquid, respectively

X = thermodynamic driving force

In the case of intense moisture evaporation inside the body, there is an increase in pressure which causes a filtration effect and the equations include an additional pressure term.

Detailed derivations of equations and solutions can be found in Luikov (1975), Rossen and Hayakawa (1977), and Saravacos and Mercado (1996). Tsukada et al. (1991) used a modified Luikov model for strain-stress analysis of cylindrically formed starch granules under transient state simultaneous heat and mass transfer conditions that also considered volumetric changes. Total moisture flux was determined by the sum of concentration, temperature and pressure gradients. Crack formation was also analyzed.

Husain et al. (1973) modified coupled heat and mass transfer equations for single kernel drying of rough rice including variable diffusivity and solutions were obtained numerically. Good agreement with experimental data was found.

Zhou et al. (1994) and Mukherjee (1997) used Luikov's model to describe the drying process and measurements of coefficients in the model were given in detail. Songtao et al (1999) used Luikov's model to predict the cross-effect of heat and mass

transfer by applying thermal and moisture gradient coefficients. Pandey et al. (1999) investigated the analytical solutions of Luikov's equations for capillary porous bodies.

Harmanthy (1969) derived a model with equations for falling rate period of porous body heat and mass transfer. Considering only vapor diffusion and convective boundary conditions, a set of second order nonlinear differential equations was solved numerically. King (1968) presented simultaneous heat and mass transfer analysis for dehydrated foods using a variable diffusivity expressed as an equation having temperature and moisture content as variables (Rossen and Hayakawa, 1977). Whitaker et al. (1969) concluded that evaporation of water resulted in absorption of heat, thus heat and mass transfer should be considered simultaneously. Chen and Johnson (1969) and Husain et al. (1973) used modified Luikov equations for simultaneous heat and mass transfer in the drying of biological materials.

In Philip and De Vries (from Canovas and Mercado, 1996) model, a set of equations were derived to describe moisture and heat transfer in porous materials considering combination of moisture and temperature gradients. The mechanistic approach assumes vapor diffusion and capillary movement. Their model proposed vapor flux which results in condensation on one front and evaporation on the other resulting in capillary flow which equals the rate of condensation and evaporation. General expression of vapor flux (J_v) is:

$$J_v = -\varepsilon_a D_{atm} [P/(P - P_v)] \nabla \rho_v \quad 2.10$$

Where,

D_{atm} = molecular diffusivity of water vapor in air

ε = tortuosity factor

P = pressure

a = volumetric air content

ρ_v = density of water vapor

The authors presented an expression of chemical potential ($\Delta\mu$) in a capillary to show the separate effects of isothermal and thermal components of vapor transfer. At high moisture contents liquid diffusivities are the most important variables, whereas at low moisture contents vapor diffusivities becomes important. A limitation of this model is that equations are valid in the capillary flow region where there is liquid continuity in pores and capillaries (Fortes and Okos, 1980; Canovas and Mercado, 1996).

In the Krischer and Kast model, capillary flow is the main moisture transport mechanism in the drying of wet porous materials. They proposed a multimechanism model which considered simultaneous migration of moisture by capillary flow and vapor diffusion. It was assumed that the vapor pressure is equal to saturation value in the region of moisture content that is greater than maximum sorptive value (the Clausius-Clapeyron equation is used for coupling) whereas in sorption region, experimental desorption isotherms are used for P_v determination (Chen and Pei, 1983).

Berger and Pei's (1973) model is based on Krischer's basic theories. Assumptions are: (1) internal moisture transfer is due to capillary flow (due to concentration gradient, ΔC) and vapor diffusion (due to ΔP), whereas internal heat transfer is due to heat conduction and latent heat of phase change, (2) at any material moisture content, partial P_v and temperature are in equilibrium, and (3) vapor pressure is equal to the saturation value at moisture contents higher than the maximum sorptional

value, thus Classius-Clapeyron equation is used. For the sorptional region of moisture content, the sorption isotherm is determined experimentally.

Berger and Pei (1973) also described the boundary conditions for numerical solutions of equations. They give the dimensionless parameters and their significance in tabulated form. Berger and Pei's model was used by Wang and Brennan (1995) for slab-shaped potato. The latter included modified form of model to incorporate variable thermal properties and solutions were done by Finite difference method.

Sokhansanj and Bruce (1987) assumed liquid diffusion to surface and evaporation only at the surface for grains (Haghighi and Segerling, 1988). Balaban and Pigott (1988) and also Banga and Singh (1994) listed the literature on models for air drying of biological materials. Kiranoudis et al (1992) used mechanistic heat and mass transfer model in which transport coefficients were determined by empirical equations. Mahmutoglu et al. (1995) studied transient simultaneous heat and mass transfer in dehydration of apricots using exponential and Page equations. Their model considered shrinkage and thermal conductivity, and specific heat were taken to be moisture dependent.

Although there are many models for simultaneous heat and mass transfer, most are not applicable to composite foods since moisture concentrations are used as the driving force and different foods have different chemical affinities to moisture. Sakai and Hayakawa (1992 and 1993) developed a computerized model based on chemical potential as mass transport potential. Cylindrical composite samples of starch and sucrose were dried in forced air dryer. Haghighi and Segerling (1988) modeled simultaneous heat and mass transfer in an isotropic sphere using finite element method. Kumar et al. (1982) developed their model from an orthogonal expansion technique for n-layer cylindrical body having discontinuous moisture contents at interfaces. Tomas and Skansi (1996)

defined kinetic modeling based on heat and mass accumulation of air as well as the material.

Chiang and Petersen (1987) experimentally measured the temperature and moisture profiles during apple drying by the use of gamma ray densitometry (for moisture profile) and thermocouples (for temperature profile). Shrinkage was determined by the distance which the evaporation front has receded from initial surface. These experimental measurements can be successfully used in model development and validated by comparing experimental and predicted data.

Hayakawa and Furuta (1989) modified Luikov's model by expressing local pressure change in terms of local temperature change, vaporization ratio and shrinkage and solved numerically by finite difference method. In 1992, they developed a new model by modifying Luikov's model to represent two-dimensional heat and mass transfer in food with volumetric changes. Numerical solutions were achieved using the finite difference method.

Ghious et al. (1997) proposed a model derived from physical and transport properties along with heat and mass balances for unsteady state conditions for fruits and vegetables. Numerical solutions were given by using the central finite difference method.

Wang and Chen (1999) used a diffusion model for heat and mass transfer in porous material (banana) during low intensity convection drying.

Many researchers have proposed liquid diffusion to be the principle flow mechanism in drying solids (Fortes and Okos, 1980). This theory gained interest among food and grain researchers. In the models diffusion is assumed to be the rate controlling mechanism during drying of biological products (Pabis and Henderson, 1961; Henderson and Perry, 1967; Young and Whitaker, 1971; Husain et al., 1973; Mahmutoglu et al., 1995). Even the moisture diffusion equation alone is inadequate. Absorption or

evolution of water by a solid results in evolution or absorption of heat. This heat causes changes in the temperature to consequently affect the ability of solid to absorb or lose water. Therefore transfer of moisture and heat is coupled and should be considered simultaneously.

Rovedo et al. (1995) divided the diffusional models into two categories: isothermal and uniform temperature profile models. Isothermal diffusional models (having contour lines for temperature gradient) assume rapid heat transfer and relatively slow moisture diffusion (e.g., drying of low initial moisture content foods, such as grains) whereas uniform temperature models assume infinite thermal conductivity (uniform temperature throughout the drying material).

Thorvaldsson and Janestad (1999) further developed a model for simultaneous heat, water, vapor diffusion based on Fourier's and Fick's laws separating liquid and vapor diffusion. Their predictions had well agreed well with experimental data. Chou et al. (2000) developed a model incorporating both liquid and vapor diffusion along with heat transfer. Chang and Weng (2000) and Hernandez et al. (2000) worked on the analytical solution to coupled heat and mass transfer in porous material and compared results with the experimental results for wood slab, cassava, and mangos.

Boundary Conditions

Determination of temperature and moisture profiles necessitates the solution of proper heat and mass transfer equations. However, such solution depends on the physical conditions existing at the boundaries of the system. The number of boundary conditions is equal to the order of transfer equation in spatial coordinates whereas the number of initial conditions is equal to the order of transfer equation in time.

Incoropera and DeWitt (1996) and Fowler (1997) defined three main types of boundary conditions for the heat transfer equation as:

1) Constant surface temperature

$$T(0,t) = T_s \quad 2.11$$

2) Constant surface heat flux

a.) Finite heat flux (Neumann conditions)

$$-k \left(\frac{\partial T}{\partial x} \right)_{x=0} = q_s'' \quad 2.12$$

b.) Adiabatic (insulated) surface

$$\frac{\partial T}{\partial x} = 0 \quad 2.13$$

3) Convective surface condition

$$-k \left(\frac{\partial T}{\partial x} \right)_{x=0} = h [T_\alpha - T(0,L)] \quad 2.14$$

Where,

T_s = surface temperature

k = thermal conductivity

q_s'' = heat flux

h = convective heat transfer coefficient

In particular, according to a mass balance, the total moisture transported to the surface is equal to amount evaporated from the surface into drying air. Therefore, mass flux, J_m , is (Fortes and Okos, 1980):

$$J_m = h_m (P_{vs} - P_{va}) = h_m (c_s - c_a) \quad 2.15$$

Where,

h_m = mass transfer coefficient

P_{vs} = water vapor pressure at surface

P_{va} = water vapor pressure of air

c_s = concentration of water in solid

c_a = concentration of water in air

In a heat balance, the amount of heat supplied to the surface equals the sum of heat that penetrates by conduction and that which is absorbed as latent heat for liquid evaporation. Thus heat flux (J_T) is given by:

$$J_T = -K_T \nabla T - L M_{ev} = h_T (T_s - T_a) \quad 2.16$$

Where,

K_T = thermal conductivity

L = heat of vaporization

M_{ev} = rate of moisture evaporation

h_T = heat transfer coefficient

Finite Element Method

In the analysis of various complex heat and mass transfer models, analytical solutions are not available, therefore iterative numerical solutions (finite element method in particular) are needed. Finite element method is a very popular and powerful numerical technique for solving differential equations. In the method, any continuous quantity (e.g., moisture, temperature) can be approximated by a discrete model composed of a set of piecewise continuous functions defined over domains (elements) (Segerlind, 1984). Elements are connected at nodal points along their boundaries and their equations are obtained by minimizing a functional of physical problem. Accuracy of the solution is dependent on the size and the distribution of these elements. Puri and Anantheswaran (1993) reviewed the use of the finite element method in food processing and a summary was given in tabulated form indicating modeling conditions and applications. They stated that the finite element method had the advantages of handling: (1) spatial variation of material properties, (2) irregular shapes, and (3) non-linear problems, varying element size and mixed boundary value problems. However, the finite element equations are usually complex requiring significant computer time. The finite element method has been used by many researchers for different food processing operations (Adriana et al., 1995; Wu and Irudayaraj, 1996; Irudayaraj and Wu, 1997 and 1999; Hong et al., 1986; Haghghi and Segerlind, 1988; Haghghi et al., 1990). Detailed information on adaptive and stochastic finite element method during drying can be found in Haghghi and Aguirre (1999).

Model Validation

Limited data on simultaneous heat and mass transfer model validation is available in the literature. Maroulis et al. (1995) and Kiranoudis et al. (1992) calculated relative standard deviations between predicted and experimental data.

$$S X^2 = \Sigma e_{xi}^2 / N \quad 2.17$$

$$S T^2 = \Sigma e_{Ti}^2 / N \quad 2.18$$

Where,

e_{xi} = relative moisture deviation = $(X_p - X_e) / X_e$

X_p = predicted moisture content

X_e = experimental moisture

e_{Ti} = relative temperature deviation = $(T_p - T_e) / T_e$

T_p = predicted temperature

T_e = experimental temperature

N = number of drying experiments

Engineering Properties

Calculations of thermophysical properties of foods can be found in Miles et al. (1983) in great detail. Below is the data gathered from the literature regarding model development.

Heat Transfer Properties

Thermal Conductivity (k): for solid foods, k is a strong function of porosity (ϵ). Moisture content, temperature and fiber direction of material also have an effect (Saravacos and Kostaropoulos, 1996). Balaban and Pigot (1988) determined thermal conductivity experimentally and expressed the moisture and temperature dependency for ocean perch. Maroulis et al. (1990), Maroulis et al. (1991), and Saravacos and Kostaropoulos (1995) suggested a structural model to predict thermal conductivity of starch based foods from the thermal conductivity of solid (λ_s) and gas phases (λ_a) and porosity (ϵ) of material. For granular-porous solids (parallel model):

$$\lambda = \epsilon \lambda_a + (1-\epsilon) \lambda_s \quad 2.19$$

For gelatinized starch materials (series model):

$$1/\lambda = \epsilon / \lambda_a + (1-\epsilon) / \lambda_s \quad 2.20$$

Where λ_s (porous) = 0.139 W/mK

$$\lambda_s$$
 (non-porous) = 0.320 W/mK

$$\lambda_a = 0.023 \text{ W/mK for starch based foods.}$$

Thermal Diffusivity (α): is usually determined from thermal conductivity(k, J/msK), bulk density(ρ_b) and specific heat (cp) of the product as (Saravacos and Kostaropoulos,1996)

$$\alpha = k / (\rho_b \text{ cp}) \quad 2.21$$

Voudouris and Hayakawa (1994) described a computerized mathematical model for simultaneous determination of thermal conductivity and thermal diffusivity using data from a point heat source probe.

Mass Transfer Properties

Effective moisture diffusivity (Deff): is an overall transport property of all possible transport mechanisms (molecular diffusion, surface diffusion, capillary flow, hydrodynamic flow) assuming concentration gradient as driving force. For unsteady state, Fick's diffusion equation can be used to determine Deff in one-dimension:

$$\frac{\partial x}{\partial t} = \frac{\partial}{\partial z} [D_{eff} \frac{\partial x}{\partial z}] \quad 2.22$$

Where x = moisture content (db) t=time

A straight line equation of simplified Fick's law is often used to describe drying kinetics of foods as:

$$(M_{avg} - M_e) / (M_i - M_e) = C e^{-KE} \quad 2.23$$

where C = constant

K = dehydration constant (1/h)

Mavg = average moisture content (kg water/kg matter)

Mi = initial moisture content

Me = equilibrium moisture content

This simplified approach is not always applicable due to complex transport mechanism of foods during drying (Jayaraman and Das Gupta, 1992).

In most foods, De_{eff} is not constant and changes considerably as a function of moisture content due to complex physicochemical structure of foods therefore numerical methods are applied for solution. In practice, De_{eff} is determined experimentally from drying rate data (fitting results from solved differential equation to drying data). Saravacos (1995) published effective moisture diffusivity of selected foods including starch gel and granular starch with temperature, percent moisture and technique of determination. He also reported an Arrhenius dependency of De_{eff} with temperature.

$$De_{eff} = De_{eff,o} \text{EXP} (-E_a/RT) \quad 2.24$$

or

$$De_{eff} = De_{eff,o} \text{EXP} (-X_o/X) \text{EXP} (-T_o/T) \quad 2.25$$

Where

E_a = activation energy of diffusion

R = universal gas constant

X = moisture content

T = temperature

X_o = reference moisture content

T_o = reference temperature

E_a values of some food products were tabulated by Saravacos (1995). More detailed data on De_{eff} was given by Suzuki et al. (1974). They presented exact and numerical solutions of the transport equation considering both constant and variable De_{eff}

for the wet material in the constant and falling rate periods under both high and low intensity drying conditions.

The fundamental equation for moisture movement in a block wet material was described by Fick's law for unsteady moisture distribution in the constant rate period of drying.

$$\frac{\partial M}{\partial t} = \frac{\partial}{\partial x} [D(M) \frac{\partial M}{\partial x}] \quad 2.26$$

Where, M = moisture content

With initial and boundary conditions:

$$M = M_I \text{ at } t = 0 \quad 2.27$$

$$D \frac{\partial M}{\partial x} = N_i \text{ at } x = 0 \text{ (at surface)} \quad 2.28$$

$$\frac{\partial M}{\partial x} = 0 \text{ at } x = b \text{ (at bottom)} \quad 2.29$$

Where, N_i = relative drying rate per unit surface

b = depth of food material

Time of constant rate period was determined by solving above equations using condition of critical points $M(x=0, t=t_c) = M_{sc}$ where M_c = critical moisture content calculated from mass balance:

$$M_c / M_I = 1 - (N_i t_c / M_{ib}) \quad 2.30$$

Initial and boundary conditions for the falling rate period are different since evaporation zone has withdrawn into the material. For a receding evaporation plane, initial and boundary conditions are as follows:

$$M = M(x, t=t_c) \quad 2.31$$

$$D \frac{\partial M}{\partial x} = f \cdot N_i \text{ at } x = \varepsilon(t) \quad 2.32$$

$$\frac{\partial M}{\partial x} = 0 \text{ at } x=b \quad 2.33$$

$M(x, t=t_c)$ = solution of 1st and 4th equations (above) at $t=t_c$

f = characteristic drying rate

ε = depth of evaporated plane where:

$$d\varepsilon/dt = [-2D (\partial^2 M / \partial x^2)_{x=\varepsilon}] / [\partial M / \partial x_{x=\varepsilon}] \quad 2.34$$

Knowing ε , f can be calculated as

$$f = 1 / \{ 1 + [\gamma \text{ Bi} (\varepsilon/b)] \} \quad 2.35$$

Where, Bi = Biot number

γ = evaporative resistance coefficient (calculated from moisture saturation curve and has values between 0.1 and 0.5).

In more simplified form, Luikov suggested that the expression of Fick's Law of diffusion can be used for analytical solution of any geometrical shape by modifying Fourier number (Fo) = $\text{Deff} \cdot t / R^2$ and using as a shape factor in the original equation (Alvarez et al., 1995).

Balaban (1989) stated that the De_{eff} is constant down to the critical moisture content. Below this point De_{eff} decreases to one fifth of its original value. Critical point was determined experimentally.

Tong and Lund (1990) determined De_{eff} in porous materials as a function of temperature and moisture content. Vagenas and Karathanas (1991 and 1993) determined De_{eff} for granular materials and published structural models for estimation of effective moisture diffusivity in tabulated form. More detailed analytical solutions of moisture diffusivity equations can be found in Zogzas et al. (1994).

Surface mass transfer coefficient (h_m): According to Saravacos and Kostanopoulos (1996), there are three moisture transfer coefficients (k_c , k_y , k_p) that can be used to define moisture transfer rate or flux [J (kg/m²sec)] depending on driving force

$$J = k_c (C_s - C_a) = k_y (Y_s - Y_a) = k_p (P_s - P_a) \quad 2.36$$

Where, C_s , C_a = moisture concentration of solid surface and air (kg/m³)

Y_s , Y_a = moisture fraction (kg water/ kg dry air)

P_s , P_a = vapor pressure of water (Pa)

These coefficients for simple geometry and air flow conditions can be determined by semi-empirical equations. For example, h_m of flat plate with turbulent air flow parallel to surface can be given as (Balaban and Pigot, 1988).

$$h_m = 8.92 \cdot 10^{-3} V_o (Re)^{-0.2} [C / (C - C_{air})] \quad 2.37$$

Where, V_o = air velocity

Re = Reynolds number

C = water concentration at surface

C_{air} = water concentration in air

Maroulis et al. (1991) used externally controlled drying model to predict heat and mass transfer coefficients simultaneously. They used a non-linear regression procedure to fit model to experimental data. Saravacos (1995) presented the methods to estimate moisture transfer coefficients as experimental, regression analysis of drying rate data, empirical equations and heat and mass transfer analogies. Interestingly, he stated that in porous foods, surfactants spreads the liquid water to a larger surface and thus increase the rate of evaporation in the early stages of drying. Markowski (1998) developed a new equation for the mass transfer coefficient during carrot drying. Numerical solutions were obtained by finite element method with Neuman type boundary condition.

Moisture filtration coefficient (k_p): Irudayaraj and Wu (1999a) used Luikov's 3 way coupled heat, mass and pressure transfer model to determine k_p for starch and starch-fructose samples.

CHAPTER 3

THEORETICAL ANALYSIS

Experimental Design

The modeling used in this research is based on the process and experimental data developed by Kim (1987). The layout of experimental design from Kim's study is given in the following sections.

Raw Blueberries (*Vaccinium Ashei*)

Berries were obtained from Alma, GA and were frozen and stored until used. Moisture content of frozen berries was determined to be 85.3% (wb) using oven drying method.

Osmotic Pretreatment

Blueberries were mixed with dry crystalline sucrose to facilitate the removal of water from fruits prior to drying. Osmotic pretreatment was done in two stages: In the first stage half of the required sucrose was mixed with thawed berries at 4 °C and held for two days. Fruits were drained on screen and berries were added the second half of sucrose at 4 °C and set for three days. Sugar crystals were recovered from solution by the use of settling tank and recycled into the process. The amount of sucrose required was calculated.

Dehydration Method

For FB drying, a batch of osmotically treated and thawed blueberries (70 grams) was placed into the dryer and exposed to drying air at 170°C for 4 minutes and at 150°C for 8 minutes. The air temperature was kept constant by the use of temperature controller. Drying air was successfully recycled to reach high temperature since the amount of water removal from small batch of berries was low. Thawed and osmotically treated blueberries were also dried in conventional drier at 60°C with 4 m/s air velocity.

Engineering Properties

Density (ρ)

The composite density of both thawed and infused berries was calculated from the individual densities of components as follows (Toledo, 1991).

$$\rho_{\text{water}} = 997.18 + 0.0031439.(T) - 0.0037574.(T^2) \quad 3.1$$

$$\rho_{\text{CH}} = 1599.1 - 0.31046.(T) \quad 3.2$$

$$\rho_{\text{fiber}} = 1311.5 - 0.36579.(T) \quad 3.3$$

where ρ_{water} = density of water (kg/m^3)

ρ_{CH} = density of carbohydrates (kg/m^3)

ρ_{fiber} = density of fiber (kg/m^3)

T = temperature of berry at time t ($^{\circ}\text{C}$)

Therefore the composite density (ρ , kg/m^3) is:

$$\rho = 1 / (\sum X_i / \rho_i) \quad 3.4$$

where X_i = mass fraction of each component namely water, carbohydrate, and fiber (determined experimentally)

Volume (V)

Berries are treated as spheres therefore the volume of an individual berry is given by:

$$V = (4/3).\pi.r^3 \quad 3.5$$

Where r = radius of berry (m)

Specific Heat (Cp)

Specific heat can be predicted from the chemical composition of major components accurately (Toledo,1991) as:

$$C_p = 837.36.SNF + 4186.8.M \quad 3.6$$

where SNF = fraction of solids non fat

M = moisture fraction

Surface Heat Transfer Coefficient (h)

For particles in a gas stream, h is calculated from the dimensionless Nusselt number (Nu) (Toledo, 1991).

$$Nu = h.d/k \quad 3.7$$

where d = characteristics length (diameter, m)

k = thermal conductivity of air

$$Nu = 2 + (0.6.Re^{0.5}.Pr^{0.33}) \quad 3.8$$

$$\text{where } Re = \text{Reynolds number} = (D.v.\rho) / \mu \quad 3.9$$

where D = diameter (m)

\bar{v} = average velocity of air (m/s)

ρ = density of air (kg/m³)

μ = viscosity of air (Pas)

$$\text{Pr} = \text{Prandtl number} = (C_p \cdot \mu) / k \quad 3.10$$

where C_p = specific heat of air (J/kg/K)

Thermal Conductivity (k_q)

The thermal conductivity of air at different drying temperatures was obtained from tabulated values (Toledo, 1991). The thermal conductivity of berries (k_q) was treated as a function of temperature and material composition and given by:

$$k_q = \sum (k_i \cdot X_{vi}) \quad 3.11$$

where X_{vi} = volume fraction of each component

k_i = thermoconductivity of each component

$$k_{\text{water}} = 0.57109 + 0.0017625 \cdot (T) - 6.7306 \cdot 10^{-6} \cdot (T^2) \quad 3.12$$

$$k_{\text{carbohydrate}} = 0.2014 + 0.0013874 \cdot (T) - 4.3312 \cdot 10^{-6} \cdot (T^2) \quad 3.13$$

$$k_{\text{fiber}} = 0.18331 + 0.0012497 \cdot (T) - 3.1683 \cdot 10^{-6} \cdot (T^2) \quad 3.14$$

$$\text{and } X_{vi} = (X_i \cdot \rho) / \rho_i \quad 3.15$$

where X_i = mass fraction of each component

ρ_i = individual densities of each component

ρ = composite density

Effective Moisture Diffusivity (Deff)

Deff is derived from Fick's law of diffusion. It is assumed to be constant for each time step. Analytical solution of Fick's law of diffusion for a sphere was used for the Deff calculation assuming constant Deff at time t (Simal et al., 1996).

Surface mass Transfer Coefficient (hm)

hm is calculated from the dimensionless Sherwood number (Toledo, 1991) as

$$hm = (Sh \cdot D_{wm}) / D \quad 3.16$$

where D_{wm} = diffusivity (kmole/ms)

D = diameter of berry (m)

$$Sh = 2 + 0.6 \cdot Re^{0.5} \cdot Sc^{0.33} \quad 3.17$$

$$\text{where } Sc = \text{Schmidt number} = \mu_{\text{air}} / (\rho_{\text{air}} \cdot D_m) \quad 3.18$$

where D_m = diffusivity of water in the air ($2.20 \cdot 10^{-5} \text{ m}^2/\text{s}$)

Governing Equations and Boundary Conditions

Modeling approaches for numerical solutions (predictions) of internal transport behavior during simultaneous heat and mass transfer processes in materials are quite variable due to the fact that there are wide choices of possible internal moisture transport mechanisms occurring. In this research, two distinct models describing simultaneous heat and mass transfer during drying were developed:

- Diffusional model assuming moisture diffuses to the outer boundaries of berries in liquid form and evaporates only at the surface of the berries.
- Luikov model assuming mass transport is both liquid and vapor form.

This study lays a foundation for quality predictions and design of the drying process.

Diffusional Model

Following derivation of the theoretical equation, it was assumed that the thermal conductivity and diffusion coefficient are dominant, and are thus treated as variables. Other material properties are constants except the specific heat boundary conditions which were calculated based on the assumption that moisture diffuses to the surfaces of the individual blueberry in liquid form and evaporation takes place only at surface of the blueberry as reported in the literature.

The diffusion equation given by Fick's law is used to describe mass transport due to its accuracy in prediction. The blueberry surface is exposed to convective heat transfer whereas the internal parts are heated by conduction. Therefore, this process is defined by heat conduction equations with convective boundary conditions.

The general diffusion equation describing the mass transfer process has the form:

$$(\partial M/\partial t) = \text{div} (D \nabla M) \quad 3.19$$

with the boundary conditions:

$$q_1 = -D (\partial M/\partial r) = h_m (M - M_\infty) \quad 3.20$$

where $D (\partial M/\partial r) = \text{mass flux}$

$$M = M_0 \text{ on } \Omega_2 \quad 3.21$$

where partial domains Ω_1 and Ω_2 make up complete boundary surface.

Heat transfer is given by the heat conduction equation:

$$\rho_c (\partial T/\partial t) = \text{div} (k_q \nabla T) \quad 3.22$$

with the boundary conditions (assuming liquid diffusion and surface evaporation) from heat balance at the surface of the berry:

$$q_2 = -k_q (\partial T/\partial r) = h (T - T_\infty) + V_\rho [\lambda + c_v (T - T_\infty)] (\partial M/\partial t) \text{ on } \Omega_3, \text{ and} \quad 3.23$$

where $k_q (\partial T/\partial r) = \text{heat flux}$

$$T = T_o \text{ on } \Omega_4 \quad 3.24$$

Finally coupling of two sets of equations is given by the time derivative in boundary condition given by equation 3.23. The special feature of equations 3.19 to 3.24 is that the diffusion coefficient, thermal conductivity, and specific heat are treated as solution dependent variables in the calculations.

Luikov Model

The heat and mass transfer in porous materials can be described by the following basic conservation equations (Luikov, 1966).

$$\rho_c (\partial T / \partial t) = - \operatorname{div} j_q - \sum_{i=1}^3 h_i \cdot I_i \quad 3.25$$

where, h_i = specific enthalpy, kJ/kg

I_i = volumetric capacity of source/sink of material i dependent upon phase change

$$\partial(\rho M_i) / \partial t = - \operatorname{div} j_i + I_i \quad 3.26$$

Equation 3.25 refers to the balance of thermal energy where $\sum_{i=1}^3 h_i \cdot I_i$ is the source (or sink) of heat. The moisture in vapor form will be denoted by suffix 1, in liquid form by suffix 2 in solid form by suffix 3, and inert gas by 4. Equation 3.26 refers to the mass balance for any one of the phases present.

The following assumptions were made in simplifying the above equations.

- The mass is present only as liquid and vapor forms (suffixes $i = 1, 2$)

- The temperatures of the liquid, vapor and the dry body are equal at coincident points.
- Molar capillary transfer of bound substance in the solid state is absent ($j_3 = 0$).
- Chemical reactions associated with water loss are not taken into account; hence the source I_4 will be absent (i.e., $I_4 = 0$).

The transfer of heat by conduction is given by Fourier's law as

$$J_q = -k_q \nabla T \quad 3.27$$

Since liquid and vapor transfer is due to moisture gradient and temperature gradient total mass transfer is given by:

$$j_m = j_1 + j_2 = -a_m \rho (\nabla M + \delta \nabla T) \quad 3.28$$

where

$$j_1 = -a_{m1} \rho (\nabla M + \delta_1 \nabla T)$$

$$j_2 = -a_{m2} \rho (\nabla M + \delta_2 \nabla T)$$

a_{m1} = coefficient of vapor diffusion inside the body

a_{m2} = coefficient of liquid diffusion inside the body, and

$\delta_1 = \delta_2 = \delta$ = in the hygroscopic region

Mass of air and vapor in capillaries is negligibly small compared to liquid therefore:

$$\partial(\rho M_1)/\partial t = 0$$

$$\partial(\rho M_1)/\partial t = -\text{div } j_1 + I_1 = 0 \quad 3.29$$

and

$$-I_1 = \text{div } j_1 = I_2 \quad 3.30$$

Summing Equation 3.26 for values of i ($i = 1,2$) we obtain the differential equation for mass transfer in the porous body was obtained as:

$$\partial(\rho M_i)/\partial t = -\text{div} \sum_{i=1}^2 j_i \quad 3.31$$

Note that the sum of all the sources and sinks of the bound substrate is zero.

$$\sum_{i=1}^2 I_i = 0$$

Using 3.27 and 3.30 in equation 3.25, results in

$$\begin{aligned} \rho c (\partial T/\partial t) &= \text{div} (k_q \nabla T) - (h_1 I_1 + h_2 I_2) & 3.32 \\ &= \text{div} (k_q \nabla T) - (h_1 I_1 - h_2 I_1) \\ &= \text{div} (k_q \nabla T) + (h_2 - h_1) I_1 \\ &= \text{div} (k_q \nabla T) - (h_1 - h_2) \text{div } j_1 \\ &= \text{div} (k_q \nabla T) - \lambda \text{div} [-a_{m1} \rho (\nabla M + \delta_1 \nabla T)] \\ &= \text{div} (k_q \nabla T) - \lambda \text{div} [a_m \varepsilon \rho (\nabla M + \delta \nabla T)] & 3.33 \end{aligned}$$

where, $a_{m1} = \varepsilon a_m$, when the source of vapor is dependent on the vaporization of water,

and $\delta = \delta_1 = \delta_2$. Equation 3.33 can be rewritten as

$$\rho c_q (\partial T/\partial t) = \text{div} [(k_q + \lambda \varepsilon \rho \delta a_m) \nabla T + (\lambda \varepsilon \rho a_m) \nabla M] \quad 3.34$$

Similarly, using 3.28 in equation 3.31 we obtain

$$\partial(\rho M_i)/\partial t = -\text{div} (j_1 + j_2)$$

or

$$\partial(\rho M_i)/\partial t = \text{div} [a_m \varepsilon \rho (\nabla M + \delta \nabla T)] \quad 3.35$$

$a_m = a_{m1} + a_{m2}$, ρ , ε , δ , λ and c_m are assumed to be constants, while the mass transfer coefficient is related to the coefficient of moisture conductivity by

$$a_m = D / \rho c_m \quad 3.36$$

Using 3.36, equations 3.34 and 3.35 can be rewritten as

$$\rho c_q (\partial T / \partial t) = \text{div} \{ [k_q + \delta(\lambda \varepsilon D / c_m)] \nabla T + [(\lambda \varepsilon D / c_m)] \nabla M \} \quad 3.37$$

$$\rho (\partial M / \partial t) = \text{div} \{ [\delta D / c_m] \nabla T + [D / c_m] \nabla M \} \quad 3.38$$

A general set of boundary conditions for the system of equations 3.37 and 3.38 is given by

$$T = T_o \text{ on } \Gamma_1 \quad 3.39$$

and

$$k_q (\partial T / \partial n) + j_q + h(T - T_\infty) + (1 - \varepsilon) \lambda h_m \rho (M - M_\infty) = 0 \text{ on } \Gamma_2 \quad 3.40$$

where $k_q (\partial T / \partial n)$ = temperature flux in the direction normal to the surface.

Similarly the boundary conditions for mass transfer can be rewritten as

$$M = M_o \text{ on } \Gamma_3 \quad 3.41$$

and

$$(D / c_m) (\partial M / \partial n) + j_m + [(D / c_m) \delta (\partial T / \partial n)] + [h_m \rho (M - M_\infty)] = 0 \text{ on } \Gamma_4 \quad 3.42$$

where $(D / c_m) (\partial M / \partial n)$ = moisture flux in the direction normal to the surface.

Rewriting the problem defined by equations 3.37 – 3.42 in a generalized form

$$C_q (\partial T / \partial t) = \nabla [(K_q \nabla T) + (K_\varepsilon \nabla M)] \quad 3.43$$

$$C_m (\partial M / \partial t) = \nabla [(K_\delta \nabla T) + (K_m \nabla M)] \quad 3.44$$

With boundary conditions

$$T = T_o \text{ on } \Gamma_1$$

$$k_q (\partial T / \partial n) + J_q^* = 0 \text{ on } T_2, \text{ for heat transfer} \quad 3.45$$

and

$$M = M_o \text{ on } \Gamma_3$$

$$K_m (\partial M / \partial n) + J_m^* = 0 \text{ on } \Gamma_4, \text{ for mass transfer} \quad 3.46$$

where

$$K_q = k_q + [(\delta \lambda \varepsilon D / c_m)] \quad , \quad K_\varepsilon = (\lambda \varepsilon D / c_m)$$

$$K_\delta = (\delta D / c_m) \quad , \quad K_m = (D / c_m)$$

$$C_q = \rho c \quad , \quad C_m = \rho$$

and

$$J_q^* = A_q^* (T - T_\infty) + A_\varepsilon^* (M - M_\infty) + J_q$$

$$J_m^* = A_s^* (T - T_\infty) + A_m^* (M - M_\infty) + J_m$$

$$A_q^* = [k_q + (\delta \lambda \varepsilon D / c_m)] (h / k_q)$$

$$A_\varepsilon^* = [k_q + (\delta \lambda \varepsilon D / c_m)] \{[\lambda h_m \rho (1 - \varepsilon) / k_q]\}$$

$$J_q = [k_q + (\delta \lambda \varepsilon D / c_m)] (j_q / k_q)$$

$$A_\delta^* = - (h / k_q) (D / c_m) \delta$$

$$A_m^* = h m \{ \rho - [\lambda ((1 - \varepsilon) / k_q) (D / c_m) \delta \rho] \}$$

$$J_m = \{ j_m - [(D / c_m) \delta (j_q / k_q)] \}$$

Symmetry of the problem can be achieved by assuming that ε and δ are constant in the range of interest.

For the case of a constant specific mass capacity (c_m), the moisture content (M) is related to the moisture potential by the relationship

$$M = c_m U \quad 3.47$$

using 3.47, equation 3.37 and 3.38 takes the form

$$\rho c_q (\partial T / \partial t) = \text{div} \{ [k_q + \delta (\lambda \varepsilon D / c_m)] \nabla T + (\lambda \varepsilon D) \nabla U \} \quad 3.48$$

$$\rho c_m (\partial U / \partial t) = \text{div} \{ [\delta D / c_m] \nabla T + (D \nabla U) \} \quad 3.49$$

Multiplying throughout equation 3.48 by $[\delta/(c_m k'_q)]$ and equation 3.49 by $[(\varepsilon\lambda)/k'_q]$ respectively yields

$$[(\rho c_q \delta)/(c_m k'_q)] (\partial T/\partial t) = \text{div} \{ [k_q + \delta(\lambda\varepsilon D/c_m)] \delta/(c_m k'_q) \nabla T + (\lambda\varepsilon D \delta/(c_m k'_q)) \nabla U \} \quad 3.50$$

$$[(\rho c_m \varepsilon \lambda)/k'_q] (\partial U/\partial t) = \text{div} \{ [(\delta D \varepsilon \lambda)/(k'_q c_m)] \nabla T + [(D \varepsilon \lambda)/k'_q] \nabla U \} \quad 3.51$$

where k'_q is a constant thermal conductivity.

Introducing dimensionless variables,

$$t = t'/t_0, R = r/l, Z = z/l$$

t_0 and l are taken as reference values. Equations 3.50 and 3.51 may be written as

$$C_q (\partial T/\partial t) = \nabla [(K_q \nabla T) + (K_\varepsilon \nabla U)] \quad 3.52$$

$$C_m (\partial U/\partial t) = \nabla [(K_\delta \nabla T) + (K_m \nabla U)] \quad 3.53$$

where symmetry is now achieved, since the cross coefficients are equal,

$$K_\varepsilon = K_\delta = [(\lambda\varepsilon D \delta)/(c_m k'_q)]$$

$$K_q = \{ [k_q + [\delta\lambda\varepsilon(D/c_m)]] / k'_q \} (\delta/c_m)$$

$$K_m = [(\lambda\varepsilon D)/k'_q]$$

$$C_q = [(\rho c \delta)/(c_m k'_q)] (l^2/t_0)$$

$$C_m = [(\rho c_m \lambda \varepsilon)/k'_q] (l^2/t_0) \quad 3.54$$

Similarly the general set of boundary conditions given by equations 3.39-3.42 can be rewritten as

$$T = T_0 \text{ on } \Gamma_1 \quad 3.55$$

$$k_q (\partial T/\partial n) + j_q + h(T - T_\infty) + (1 - \varepsilon)\lambda h_m \rho c_m (U - U_\infty) = 0 \text{ on } \Gamma_2 \quad 3.56$$

$$U = U_0 \text{ on } \Gamma_3 \quad 3.57$$

$$D (\partial U/\partial n) + j_m + [(D/c_m) \delta (\partial T/\partial n)] + [h_m c_m \rho (U - U_\infty)] = 0 \text{ on } \Gamma_4 \quad 3.58$$

Equation 3.55-3.58 can be expressed in a generalized nondimensional form as

$$\begin{aligned} T &= T_o \text{ on } \Gamma_1 \\ K_q (\partial T / \partial n) + J_q^* &= 0 \text{ on } \Gamma_2 \end{aligned} \quad 3.59$$

$$\begin{aligned} U &= U_\infty \text{ on } \Gamma_3 \\ K_m (\partial U / \partial n) + J_m^* &= 0 \text{ on } \Gamma_4 \end{aligned} \quad 3.60$$

Here J_q^* and J_m^* are now defined as

$$\begin{aligned} J_q^* &= A_q (T - T_\infty) + A_\varepsilon (U - U_\infty) + J_q \\ J_m^* &= A_\delta (T - T_\infty) + A_m (U - U_\infty) + J_m \end{aligned}$$

where

$$\begin{aligned} A_q &= [(k_q + (\varepsilon \lambda \delta (D/c_m))) / k_q'] (\delta / c_m) (hl/k_q) \\ A_m &= [1 - ((1 - \varepsilon) ((\lambda D \delta) / (c_m k_q')))] [(\varepsilon \lambda) / k_q'] [c_m h_m \rho l] \\ A_\varepsilon &= [(k_q + (\varepsilon \lambda k_m \delta)) / k_q'] [\lambda \delta h_m l \rho / k_q] (1 - \varepsilon) \\ A_\delta &= - [(\varepsilon \lambda \delta D) / (c_m k_q')] [(hl) / k_q] \\ J_q &= [(k_q + (\varepsilon \lambda \delta (D/c_m))) / k_q'] (\delta / c_m) (j_q / k_q) \\ J_m &= [(\varepsilon \lambda) / k_q'] \{j_m - [(D \delta) / c_m] (j_q / k_q)\} \end{aligned}$$

Finite Element Formulation

Finite Element Formulation of Diffusional Model

In the finite element formulation for the mass transfer equation, let the dependent variable M be approximated by interpolating functions of the form

$$M = \sum_{j=1}^n M_j(t) N_j(r,z) \quad 3.61$$

where n = total number of nodes in the element. Using the Galerkin weighted residual method, the residual function for equation 3.19 may be written as

$$R = (\partial M / \partial t) - \nabla (D \nabla M) \quad 3.62$$

Multiplying 3.44 by the weighting function N_i and integrating yields

$$\int_{\Omega} N_i R \, d\Omega = \int_{\Omega} N_i [(\partial M / \partial t) - \nabla (D \nabla M)] \, d\Omega$$

Setting the residual function equal to zero,

$$\int_{\Omega} N_i [(\partial M / \partial t) - \nabla (D \nabla M)] \, d\Omega = 0 \quad 3.63$$

3.63 may be rearranged as

$$\int_{\Omega} N_i (\partial M / \partial t) \, d\Omega - \int_{\Omega} N_i [\nabla (D \nabla M)] \, d\Omega = 0 \quad 3.64$$

Differentiating 3.61 with respect to time yields

$$(\partial M / \partial t) = \sum_{j=1}^n \dot{M}_j N_j$$

The first term of equation 3.64 can now be written as

$$\int_{\Omega} N_i (\partial M / \partial t) \, d\Omega = \int_{\Omega} N_i \sum_{j=1}^n \dot{M}_j N_j \, d\Omega = \sum_{j=1}^n \dot{M}_j \int_{\Omega} N_i N_j \, d\Omega \quad 3.65$$

Using Green's theorem the 2nd term of equation 3.64 can be written as

$$\int_S N_i D (\partial M / \partial n) \, dS - \int_{\Omega} [\nabla N_i \cdot (D \nabla M)] \, d\Omega \quad 3.66$$

$D (\partial M / \partial n)$ is the mass flux in the direction normal to the surface. Considering axisymmetry, terms ∇M and ∇N may be expressed in cylindrical coordinates as

$$\nabla M = (\partial M / \partial r) \vec{r} + (\partial M / \partial z) \vec{z} \quad 3.67$$

$$\nabla N = (\partial N / \partial r) \vec{r} + (\partial N / \partial z) \vec{z} \quad 3.68$$

where \vec{r} and \vec{z} are unit vectors in the r and z directions, respectively. Using 3.67 and 3.68, equation 3.66 can be rewritten as

$$\int_S N_i D (\partial M / \partial n) dS - \int_{\Omega} \{[(\partial N_i / \partial r) \vec{r} + (\partial N_i / \partial z) \vec{z}] \cdot [D (\partial M / \partial r) \vec{r} + D (\partial M / \partial z) \vec{z}]\} d\Omega =$$

$$\int_S N_i D (\partial M / \partial n) dS - \int_{\Omega} D \{[(\partial N_i / \partial r)(\partial M / \partial r)] + [(\partial N_i / \partial z)(\partial M / \partial z)]\} d\Omega$$

Using shape function approximation 3.61, the above term becomes

$$\int_S N_i D (\partial M / \partial n) dS - \sum_{j=1}^n M_j \int_{\Omega} D \{[(\partial N_i / \partial r)(\partial N_j / \partial r)] + [(\partial N_i / \partial z)(\partial N_j / \partial z)]\} d\Omega \quad 3.69$$

Substituting 3.69 and 3.65 into equation 3.64 results in

$$\sum_{j=1}^n M_j \int_{\Omega} N_i N_j d\Omega - \int_S N_i D (\partial M / \partial n) dS - \sum_{j=1}^n M_j \int_{\Omega} D \{[(\partial N_i / \partial r)(\partial N_j / \partial r)] +$$

$$[(\partial N_i / \partial z)(\partial N_j / \partial z)]\} d\Omega = 0 \quad 3.70$$

For axisymmetric problems, $d\Omega = 2\pi r dr dz$, $ds = 2\pi r dl$ and equation 3.70, becomes

$$2\pi \sum_{j=1}^n M_j \int N_i N_j r dr dz - 2\pi \int N_i D (\partial M / \partial n) r dl - 2\pi \sum_{j=1}^n M_j \int D \{[(\partial N_i / \partial r)(\partial N_j / \partial r)] +$$

$$[(\partial N_i / \partial z)(\partial N_j / \partial z)]\} r dr dz = 0 \quad 3.71$$

The convective boundary condition for moisture from equation 3.20 is

$$q_1 = D (\partial M / \partial r) = -h_m (M - M_{\infty}) = -h_m M + h_m M_{\infty} = -C_1 M + C_2$$

where

$$C_1 = h_m, \text{ constant}$$

$$C_2 = h_m M_\infty, \text{ constant}$$

Using equation 3.20 in 3.71 we have the following

$$\sum_{j=1}^n M_j \int 2\pi N_i N_j r dr dz - (N_i C_1) \left(\sum_{j=1}^n M_j N_j \right) r dl - \int 2\pi N_i C_2 r dl - \sum_{j=1}^n M_j \int 2\pi D \{ [(\partial N_i / \partial r)(\partial N_j / \partial r)] + [(\partial N_i / \partial z)(\partial N_j / \partial z)] \} r dr dz = 0 \quad 3.72$$

$$\sum_{j=1}^n M_j \int 2\pi N_i N_j r dr dz - \sum_{j=1}^n M_j \left\{ \int 2\pi D \{ [(\partial N_i / \partial r)(\partial N_j / \partial r)] + [(\partial N_i / \partial z)(\partial N_j / \partial z)] \} r dr dz + \int 2\pi C_1 N_i N_j r dl \right\} - \int 2\pi N_i C_2 r dl = 0 \quad 3.73$$

Equation 3.73 can be written in a simplified form as

$$\sum_{j=1}^n M_j c_{ij} + \sum_{j=1}^n M_j k_{ij} - f_i = 0 \quad 3.74$$

where

$$c_{ij} = 2\pi \int N_i N_j r dr dz \quad 3.75$$

is the element capacitance matrix,

$$k_{ij} = \int 2\pi D \{ [(\partial N_i / \partial r)(\partial N_j / \partial r)] + [(\partial N_i / \partial z)(\partial N_j / \partial z)] \} r dr dz + \int 2\pi C_1 N_i N_j r dl \quad 3.76$$

is the element conductance matrix, and

$$f_i = 2\pi \int N_i C_2 r dl \quad 3.77$$

is the element force factor

Assembling the element matrices in equation 3.74 using 3.75, 3.76, and 3.77 the global matrix equation can be written as

$$[C_1] \{M\} + [K_1(M)] \{M\} - \{F_1\} = 0 \quad 3.78$$

where, $[K_1(M)]$ is obtained by superposition of element matrices from 3.76.

In the finite element formulation for heat transfer equation, using the shape function for the dependent variable T,

$$T = \sum_{j=1}^n T_j(t) N_j(r,z) \quad 3.79$$

Following the diffusion equation formulation procedure, we can rewrite equation 3.70 by replacing the mass transfer parameters by heat transfer parameters as

$$\begin{aligned} \sum_{j=1}^n \dot{T}_j \int_{\Omega} \rho c N_i N_j d\Omega - \int_S N_i k_q (\partial T / \partial n) dS - \sum_{j=1}^n T_j \int_{\Omega} k_q \{[(\partial N_i / \partial r)(\partial N_j / \partial r)] + \\ [(\partial N_i / \partial z)(\partial N_j / \partial z)]\} d\Omega = 0 \end{aligned} \quad 3.80$$

where, \dot{T} is time derivative of T and $k_q (\partial T / \partial n)$ is the temperature flux in the direction normal to the surface. Using axisymmetric assumption equation 3.22 becomes,

$$\begin{aligned} 2\pi\rho c \sum_{j=1}^n \dot{T}_j \int N_i N_j r dr dz - 2\pi \int N_i k_q (\partial T / \partial n) r dl - 2\pi \sum_{j=1}^n T_j k_q \int D \{[(\partial N_i / \partial r)(\partial N_j / \partial r)] \\ + [(\partial N_i / \partial z)(\partial N_j / \partial z)]\} r dr dz = 0 \end{aligned} \quad 3.81$$

The boundary condition given by equation 3.23 is

$$k_q (\partial T / \partial r) = h (T_{\infty} - T) - V\rho [\lambda + c_v (T_{\infty} - T)] (\partial M / \partial t) \quad 3.82$$

Using a forward difference approximation for $(\partial M / \partial t)$ in 3.23

$$k_q (\partial T / \partial r) = (hT_{\infty} - hT) - V\rho [\lambda + c_v (T - T_{\infty})] [(M_{t+\Delta t} - M_t) / \Delta t] \quad 3.83$$

Defining,

$$M_{ave} = [(M_t + M_{t-1}) / \Delta t] \quad 3.84$$

Then equation 3.83 becomes

$$k_q (\partial T / \partial r) = (hT_\infty - hT) - V\rho c_v M_{ave} + V\rho c_v M_{ave} T - V\rho c_v M_{ave} T_\infty \quad 3.85$$

or,

$$\begin{aligned} k_q (\partial T / \partial r) &= -(h - V\rho c_v M_{ave})T + (h - V\rho c_v M_{ave})T_\infty - V\rho \lambda M_{ave} \\ &= -C_3 T + C_4 \end{aligned} \quad 3.86$$

where

$$C_3 = (h - V\rho c_v M_{ave}) = \text{constant}$$

and

$$C_4 = (h - V\rho c_v M_{ave})T_\infty - V\rho \lambda M_{ave} = \text{constant}$$

Substituting equation 3.85 into the second term of 3.81 yields an expression similar to 3.73

$$\begin{aligned} \sum_{j=1}^n \dot{T}_j \int 2\pi\rho c N_i N_j r dr dz - \sum_{j=1}^n T_j \{ \int 2\pi k_q \{ [(\partial N_i / \partial r)(\partial N_j / \partial r)] + [(\partial N_i / \partial z)(\partial N_j / \partial z)] \} r dr dz \\ + \int 2\pi C_3 N_i N_j r dl \} - \int 2\pi N_i C_4 r dl = 0 \end{aligned} \quad 3.87$$

Equation 3.87 can be written in a simplified form as

$$\sum_{j=1}^n \dot{T}_j c_{ij}' + \sum_{j=1}^n T_j k_{ij}' - f_i' = 0 \quad 3.88$$

where

$$c_{ij}' = 2\pi\rho c \int N_i N_j r dr dz \quad 3.89$$

is the element capacitance matrix,

$$k_{ij}' = 2\pi \int \{ [(\partial N_i / \partial r)(\partial N_j / \partial r)] + [(\partial N_i / \partial z)(\partial N_j / \partial z)] \} r dr dz + 2\pi \int C_3 N_i N_j r dl \quad 3.90$$

is the element temperature conductance matrix, and

$$f_i' = 2\pi \int N_i C_4 r dl \quad 3.91$$

is the temperature component of the element force vector.

The global matrices can be obtained by assembling the element matrices in equation 3.87, hence

$$[C_2] \{\dot{T}_j\} + [K_2(T)] \{T\} - \{F_2\} = 0 \quad 3.92$$

Finite Element Formulation of Luikov Model

The dependent variables, temperature and moisture potential, can be approximated in terms of the nodal values, T_j and U_j , respectively, by interpolating functions:

$$T \approx \bar{T} = \sum_{j=1}^n N_j(R, Z) T_j(t) \quad 3.93$$

$$U \approx \bar{U} = \sum_{j=1}^n N_j(R, Z) U_j(t) \quad 3.94$$

where, N_j 's are the shape functions as defined by Segerlind (1984) and \bar{T} and \bar{U} are the element temperature and moisture approximations respectively.

Rearranging equation 3.52 yields

$$\nabla [(K_q \nabla T) + (K_\varepsilon \nabla U)] - C_q (\partial T / \partial t) = 0 \quad 3.95$$

Substituting the approximations given by 3.93 and 3.94 into equation 3.95 results in

$$\nabla [(K_q \nabla \bar{T}) + (K_\varepsilon \nabla \bar{U})] - C_q (\partial \bar{T} / \partial t) = 0 \quad 3.96$$

Using the Galerkin method and requiring the integral of the weighed errors over the domain to be zero, then multiplying throughout 3.96 by N_i and setting the integral over the domain to zero,

$$\int_{\Omega} N_i \{ \nabla [(K_q \nabla \bar{T}) + (K_\varepsilon \nabla \bar{U})] - C_q (\partial \bar{T} / \partial t) \} d\Omega = 0 \quad 3.97$$

or

$$\int_{\Omega} N_i \{ [\nabla (K_q \nabla \bar{T}) + \nabla (K_\varepsilon \nabla \bar{U})] - C_q (\partial \bar{T} / \partial t) \} d\Omega = 0 \quad 3.98$$

or

$$\int_{\Omega} \{ [N_i \nabla (K_q \nabla \bar{T}) + N_i \nabla (K_\varepsilon \nabla \bar{U})] - N_i C_q (\partial \bar{T} / \partial t) \} d\Omega = 0 \quad 3.99$$

Using Green's Theorem 3.99 becomes

$$\begin{aligned} & \int_{\Gamma} N_i K_q (\partial \bar{T} / \partial n) d\Gamma - \int_{\Omega} [\nabla N_i \cdot (K_q \nabla \bar{T})] d\Omega + \int_{\Gamma} N_i K_\varepsilon (\partial \bar{U} / \partial n) d\Gamma - \\ & \int_{\Omega} [\nabla N_i \cdot (K_\varepsilon \nabla \bar{U})] d\Omega - \int_{\Omega} N_i C_q (\partial \bar{T} / \partial t) d\Omega = 0 \end{aligned} \quad 3.100$$

In cylindrical coordinates (R,Z), considering axisymmetry, ∇T and ∇U are written as

$$\nabla T = (\partial T / \partial R) \vec{R} + (\partial T / \partial Z) \vec{Z} \quad 3.101$$

$$\nabla U = (\partial U / \partial R) \vec{R} + (\partial U / \partial Z) \vec{Z} \quad 3.102$$

Using 3.101 and 3.102, equation 3.100 can be rewritten as

$$\begin{aligned} & \int_{\Gamma} N_i K_q (\partial \bar{T} / \partial n) d\Gamma - \int_{\Omega} \{ [(\partial N_i / \partial R) \vec{R} + (\partial N_i / \partial Z) \vec{Z}] \cdot [K_q (\partial \bar{T} / \partial R) \vec{R} + K_q (\partial \bar{T} / \partial Z) \vec{Z}] \} d\Omega + \\ & \int_{\Gamma} N_i K_\varepsilon (\partial \bar{U} / \partial n) d\Gamma - \int_{\Omega} \{ [(\partial N_i / \partial R) \vec{R} + (\partial N_i / \partial Z) \vec{Z}] \cdot [K_\varepsilon (\partial \bar{U} / \partial R) \vec{R} + K_\varepsilon (\partial \bar{U} / \partial Z) \vec{Z}] \} d\Omega \\ & - \int_{\Omega} N_i C_q (\partial \bar{T} / \partial t) d\Omega = 0 \end{aligned} \quad 3.103$$

Substituting 3.93 and 3.94 in equation 3.103

$$\int_{\Gamma} N_i K_q (\partial \bar{T} / \partial n) d\Gamma - \sum_{j=1}^n T_j \int_{\Omega} K_q \{[(\partial N_i / \partial R)(\partial N_j / \partial R)] + [(\partial N_i / \partial Z)(\partial N_j / \partial Z)]\} d\Omega +$$

$$\int_{\Gamma} N_i K_{\varepsilon} (\partial \bar{U} / \partial n) d\Gamma - \sum_{j=1}^n U_j \int_{\Omega} K_{\varepsilon} \{[(\partial N_i / \partial R)(\partial N_j / \partial R)] + [(\partial N_i / \partial Z)(\partial N_j / \partial Z)]\} d\Omega -$$

$$\sum_{j=1}^n \bar{T}_j \int_{\Omega} N_i N_j C_q d\Omega = 0 \quad 3.104$$

or

$$\sum_{j=1}^n \bar{T}_j \int_{\Omega} N_i N_j C_q d\Omega + \sum_{j=1}^n T_j \int_{\Omega} K_q \{[(\partial N_i / \partial R)(\partial N_j / \partial R)] + [(\partial N_i / \partial Z)(\partial N_j / \partial Z)]\} d\Omega +$$

$$\sum_{j=1}^n U_j \int_{\Omega} K_{\varepsilon} \{[(\partial N_i / \partial R)(\partial N_j / \partial R)] + [(\partial N_i / \partial Z)(\partial N_j / \partial Z)]\} d\Omega -$$

$$\int_{\Gamma} N_i \{ [K_q (\partial \bar{T} / \partial n)] + [K_{\varepsilon} (\partial \bar{U} / \partial n)] \} d\Gamma = 0 \quad 3.105$$

In matrix form equation 3.105 becomes

$$[C]\{\bar{T}\} + [K_h(T)]\{T\} + [K_u(U)]\{U\} + \{F\} = 0 \quad 3.106$$

where the element matrices are

$$[C]_{ij} = \sum_{j=1}^n \int_{\Omega} [N_i N_j] C_q d\Omega \quad 3.107$$

$$[K_h]_{ij} = \sum_{j=1}^n \int_{\Omega} K_q \{[(\partial N_i / \partial R)(\partial N_j / \partial R)] + [(\partial N_i / \partial Z)(\partial N_j / \partial Z)]\} d\Omega \quad 3.108$$

$$[K_u]_{ij} = \sum_{j=1}^n \int_{\Omega} K_{\varepsilon} \{[(\partial N_i / \partial R)(\partial N_j / \partial R)] + [(\partial N_i / \partial Z)(\partial N_j / \partial Z)]\} d\Omega \quad 3.109$$

$$\{F\}_i = - \sum_{j=1}^n \int_{\Gamma} N_i \{ [K_q (\partial \bar{T} / \partial n)] + [K_{\varepsilon} (\partial \bar{U} / \partial n)] \} d\Gamma \quad 3.110$$

Using 3.59 and 3.60 in equation 3.110 and noting that $(K_\epsilon / K_m) = (\delta/c_m)$ 3.110 results in

$$\begin{aligned} \{F\}_i &= \sum_{j \in \mathcal{H}} \int_{\Gamma} N_i \{J_q^* + [(\delta/c_m)K_m (\partial \bar{U} / \partial n)]\} d\Gamma \\ &= \sum_{j \in \mathcal{H}} \int_{\Gamma} N_i \{J_q^* + [(K_\epsilon / K_m) J_q^*]\} d\Gamma \end{aligned} \quad 3.111$$

For equation 3.53 an expression similar to equation 3.106 can be obtained by following the same procedure as above. Hence using the shape function approximation for U and T equation 3.53 can be written as

$$\nabla [(K_\delta \nabla \bar{T}) + (K_m \nabla \bar{U})] - C_m (\partial \bar{U} / \partial t) = 0 \quad 3.112$$

Minimizing the residual of the functional with respect to the weighting function N_i , we have

$$\int_{\Omega} N_i \{ \nabla [(K_\delta \nabla \bar{T}) + (K_m \nabla \bar{U})] - C_m (\partial \bar{U} / \partial t) \} d\Omega = 0 \quad 3.113$$

$$\int_{\Omega} \{ [N_i \nabla (K_\delta \nabla \bar{T})] + [N_i \nabla (K_m \nabla \bar{U})] - C_m N_i (\partial \bar{U} / \partial t) \} d\Omega = 0 \quad 3.114$$

Using Green's Theorem the integral in equation 3.114 becomes

$$\begin{aligned} \int_{\Gamma} N_i K_\delta (\partial \bar{T} / \partial n) d\Gamma - \int_{\Omega} [\nabla N_i \cdot (K_\delta \nabla \bar{T})] d\Omega + \int_{\Gamma} N_i K_m (\partial \bar{U} / \partial n) d\Gamma - \\ \int_{\Omega} [\nabla N_i \cdot (K_m \nabla \bar{U})] d\Omega - \int_{\Omega} N_i C_m (\partial \bar{U} / \partial t) d\Omega = 0 \end{aligned} \quad 3.115$$

Using 3.93 and 3.94 equation 3.115 can be written as,

$$\begin{aligned}
& \int_{\Gamma} N_i K_{\delta} (\partial \bar{T} / \partial n) d\Gamma - \int_{\Omega} \{[(\partial N_i / \partial R) \bar{R} + (\partial N_i / \partial Z) \bar{Z}]. [K_{\delta} (\partial \bar{T} / \partial R) \bar{R} + K_{\delta} (\partial \bar{T} / \partial Z) \bar{Z}]\} d\Omega + \\
& \int_{\Gamma} N_i K_m (\partial \bar{U} / \partial n) d\Gamma - \int_{\Omega} \{[(\partial N_i / \partial R) \bar{R} + (\partial N_i / \partial Z) \bar{Z}]. [K_m (\partial \bar{U} / \partial R) \bar{R} + K_m (\partial \bar{U} / \partial Z) \bar{Z}]\} d\Omega \\
& - \int_{\Omega} N_i C_m (\partial \bar{U} / \partial n) d\Omega = 0 \tag{3.116}
\end{aligned}$$

or

$$\begin{aligned}
& \int_{\Gamma} N_i K_{\delta} (\partial \bar{T} / \partial n) d\Gamma - \sum_{j=1}^n T_j \int_{\Omega} K_{\delta} \{[(\partial N_i / \partial R)(\partial N_j / \partial R)] + [(\partial N_i / \partial Z)(\partial N_j / \partial Z)]\} d\Omega + \\
& \int_{\Gamma} N_i K_m (\partial \bar{U} / \partial n) d\Gamma - \sum_{j=1}^n U_j \int_{\Omega} K_m \{[(\partial N_i / \partial R)(\partial N_j / \partial R)] + [(\partial N_i / \partial Z)(\partial N_j / \partial Z)]\} d\Omega - \\
& \sum_{j=1}^n \bar{U}_j \int_{\Omega} N_i N_j C_m d\Omega = 0 \tag{3.117}
\end{aligned}$$

Equation 3.117 can be rewritten as

$$\begin{aligned}
& \sum_{j=1}^n \bar{U}_j \int_{\Omega} N_i N_j C_m d\Omega + \sum_{j=1}^n T_j \int_{\Omega} K_{\delta} \{[(\partial N_i / \partial R)(\partial N_j / \partial R)] + [(\partial N_i / \partial Z)(\partial N_j / \partial Z)]\} d\Omega + \\
& \sum_{j=1}^n U_j \int_{\Omega} K_m \{[(\partial N_i / \partial R)(\partial N_j / \partial R)] + [(\partial N_i / \partial Z)(\partial N_j / \partial Z)]\} d\Omega - \\
& \int_{\Gamma} N_j \{ [K_{\delta} (\partial \bar{T} / \partial n)] + [K_m (\partial \bar{U} / \partial n)] \} d\Gamma = 0 \tag{3.118}
\end{aligned}$$

In matrix form equation 3.118 becomes

$$[C']\{\bar{U}\} + [K'_h(T)]\{T\} + [K'_u(U)]\{U\} + \{F'\} = 0 \tag{3.119}$$

where the element matrices are

$$[C']_{ij} = \sum_{j=1}^n \int_{\Omega} [N_i N_j] C_m d\Omega \tag{3.120}$$

$$[K'_h]_{ij} = \sum_{j \neq i} \int_{\Omega} K_{\delta} \{[(\partial N_i / \partial R)(\partial N_j / \partial R)] + [(\partial N_i / \partial Z)(\partial N_j / \partial Z)]\} d\Omega \quad 3.121$$

$$[K'_u]_{ij} = \sum_{j \neq i} \int_{\Omega} K_m \{[(\partial N_i / \partial R)(\partial N_j / \partial R)] + [(\partial N_i / \partial Z)(\partial N_j / \partial Z)]\} d\Omega \quad 3.122$$

$$\{F'\}_i = - \int_{\Gamma} N_i \{ [K_{\delta} (\partial \bar{T} / \partial n)] + [K_m (\partial \bar{U} / \partial n)] \} d\Gamma \quad 3.123$$

Using 3.59 and 3.60 in equation 3.123 and noting that $[K_{\delta} (\partial T / \partial n)] = [K_{\delta} (J^*_q / K_q)]$, we obtain

$$\{F'\}_i = \int_{\Gamma} N_i \{ J^*_m + [J^*_q (K_{\delta} / K_q)] \} d\Gamma \quad 3.124$$

Equations 3.106 and 3.119 can be combined to form a system of nonlinear differential equations in the general form as

$$[C_{\phi}] \{ \bar{\phi} \} + [K(\phi)] \{ \phi \} + \{ F\phi \} = 0 \quad 3.125$$

Solution Procedures

Finite element solution of a time-dependent problem involves solving a system of first order differential equations in the time domain. Global capacitance ($[C]$) and global conductance ($[K]$) matrices are temperature and moisture dependent, so that solution by iterative time marching schemes is required. Non-linearities are due to temperature and moisture dependent material properties.

A system of equations defined in the finite element formulation section can be given in the following form, using mean value theory for temperature and moisture (Seegerlind, 1984):

$$([C] + \theta \Delta t [K]) \{ \phi \}_b = ([C] - (1-\theta) \Delta t [K]) \{ \phi \}_a + \Delta t ((1-\theta) \{ F \}_a + \theta \{ F \}_b) \quad 3.126$$

Out of four possible choices of solution procedures, purely forward difference method was selected. This method is unconditionally stable and calculated values do not oscillate around the correct values. Details of the solution procedure can be found in Segerlind (1984). Having known values of ϕ (temperature or moisture) at time t , the solution at time $t + \Delta t$ can be obtained by:

$$\phi_{t+\Delta t} = [A] [P]^{-1} \{\phi_t\} + [P]^{-1} \{F_t\} \Delta t \quad 3.127$$

where

$$[A] = ([C] \pm \Delta t [K])$$

$$[P] = [C]$$

Element Equations

Element Shape Functions

Based on finite element method, a single blueberry can be divided into n triangular elements. In this research, linear triangular element having straight sides and three nodes, namely i , j , and k (one at each corner) was used. Labeling and numbering of nodes was done using a counter clockwise order starting from node i . If moisture and temperature (ϕ) within each element can be approximated by an interpolation polynomial as

$$\phi = \alpha_1 + \alpha_2 x + \alpha_3 y \quad 3.128$$

Then nodal values for nodes i , j , and k are

$$\phi_i = \alpha_1 + \alpha_2 X_i + \alpha_3 Y_i \quad 3.129$$

$$\phi_j = \alpha_1 + \alpha_2 X_j + \alpha_3 Y_j \quad 3.130$$

$$\phi_k = \alpha_1 + \alpha_2 X_k + \alpha_3 Y_k \quad 3.131$$

where (X_i, Y_i) , (X_j, Y_j) , and (X_k, Y_k) are the coordinates of respective nodes.

Solving for

$$\alpha_1 = (1/2A) \{[(X_j Y_k) - (X_k Y_j)]\phi_i + [(X_k Y_i) - (X_i Y_k)]\phi_j + [(X_i Y_j) - (X_j Y_i)]\phi_k\} \quad 3.132$$

$$\alpha_2 = (1/2A) \{(Y_j - Y_k)\phi_i + (Y_k - Y_i)\phi_j + (Y_i - Y_j)\phi_k\} \quad 3.133$$

$$\alpha_3 = (1/2A) \{(X_k - X_j)\phi_i + (X_i - X_k)\phi_j + (X_j - X_i)\phi_k\} \quad 3.134$$

where

$$2A = \begin{vmatrix} 1 & X_i & Y_i \\ 1 & X_j & Y_j \\ 1 & X_k & Y_k \end{vmatrix} \quad 3.135$$

and A = area of the triangle

Substituting for the α values and rearranging the 3.128

$$\phi = N_i \phi_i + N_j \phi_j + N_k \phi_k \quad 3.136$$

where N is the shape functions whose values are

$$N_i = (1/2A) [a_i + (b_i x) + (c_i y)] \quad 3.137$$

$$N_j = (1/2A) [a_j + (b_j x) + (c_j y)] \quad 3.138$$

$$N_k = (1/2A) [a_k + (b_k x) + (c_k y)] \quad 3.139$$

With $a_i = X_j Y_k - X_k Y_j$

$$a_j = X_k Y_i - X_i Y_k$$

$$a_k = X_i Y_j - X_j Y_i$$

$$b_i = Y_j - Y_k$$

$$b_j = Y_k - Y_i$$

$$b_k = Y_i - Y_j$$

$$c_i = X_k - X_j$$

$$c_j = X_i - X_k$$

$$c_k = X_j - X_i$$

Numerical Integration

Numerical integration of the governing equations are given by Segerlind (1984). The method results in the following element matrices for 2 dimensional triangular elements:

$$kD = (Dx/(4*Aii))*[bi^2 bi*bj bi*bk;bi*bj bj^2 bj*bk;bi*bk bj*bk bk^2]+... \\ (Dy/(4*Aii - kD))*[ci^2 ci*cj ci*ck;ci*cj cj^2 cj*ck;ci*ck cj*ck ck^2] \quad 3.140$$

$$kG = ((G*Aii)/12)*[2 1 1;1 2 1;1 1 2] \quad 3.141$$

$$kstf = kD+kG \quad 3.142$$

$$f = Qmass*Aii*ones(3,1)/3 \quad 3.143$$

Element matrices of boundary conditions are given by:

$$km = ((Mmass*Lij)/6)*[2 1 0;1 2 0;0 0 0] \\ =((M*Ljk)/6)*[0 0 0;0 2 1;0 1 2] \\ =((M*Lik)/6)*[2 0 1;0 0 0;1 0 2] \quad 3.144$$

$$fs = ((S*Lij)/2)*[1;1;0]$$

$$=((S*Ljk)/2)*[0;1;1]$$

$$=((S*L_{ik})/2)*[1;0;1] \text{ for the sides } ij, jk \text{ and } ik \text{ respectively.} \quad 3.145$$

Simulation

Mathematical simulation of the drying process was done by using a MATLAB program (Version 5.3, Mathworks, Inc.). MATLAB is an interactive system and programming language for general computations allowing the use of matrix system of equations for numeric problems. The MATLAB code was written for temperature and moisture data analysis. The code itself takes the values of constants and dependent variables as inputs. Data processing can be given in steps as:

- Triangulation of the whole domain
- Calculation of conductance and capacitance matrices and force vectors for each element
- Creating global matrices and vectors
- Inclusion of all the boundary conditions
- Numerical solution

CHAPTER 4

MODEL VERIFICATION

Finite element programs derived from the theoretical formulation were written to calculate moisture and temperature histories and distributions during both tunnel and fluidized bed drying for both thawed and infused blueberries. Computer codes were written in MATLAB (5.3 Student version). Temperature and moisture histories were predicted for each node of the each element and average values of temperature and moisture were calculated. Predicted results (finite element solutions) were then compared with experimental (measured) data for model validation.

Temperature and moisture histories and distributions were obtained by solving both the diffusional model given by equations 3.19 and 3.23 and the Luikov model given by equations from 3.43 to 3.46. Systems of non-linear differential equations were converted into matrix equations for the finite element solutions.

In both models, each blueberry was treated as an isotropic sphere, which is symmetric with respect to its center. A quarter of a berry was considered for the solutions due to symmetry. Initial discretization of this domain was done using separate computer code and a two dimensional finite element grid in cylindrical coordinates was created as shown in Figure 4.1. This initial (coarse) grid consisted of seven linear triangular elements with a total of eight nodes and was refined for better approximations of the temperature and moisture histories and distributions. Refinement code takes each triangular element and divides it into four triangular elements from the middle of each initial vertex. The refined mesh is shown in Figure 4.2. Solution to the set of simultaneous heat and mass transfer equations required a set of boundary conditions. In

this research, convective boundary conditions were used along the outer surface ($r = 0.71$ cm) assuming the fluxes along the axis were zero (due to symmetry) contributing to the isolated boundary. Therefore complete definition of the boundaries was achieved.

Nodal temperatures and moisture contents were predicted using both models for both thawed and infused blueberries. Based on nodal values, the average moisture content and temperature values were calculated to represent the whole blueberries.

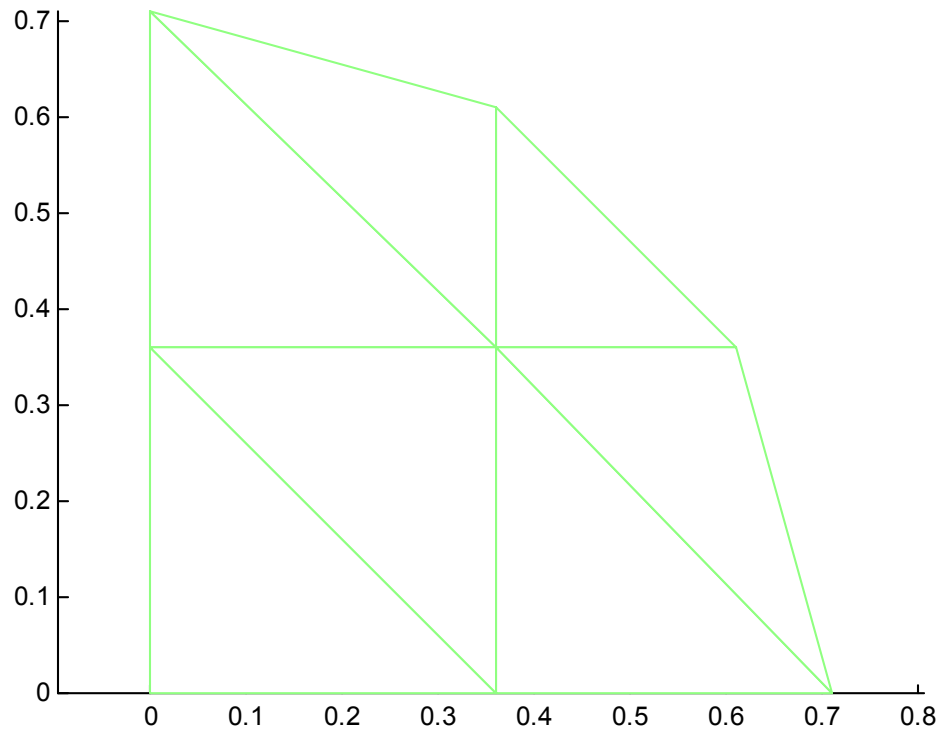


Figure 4.1. Initial element grid of a single blueberry (1/4 section)

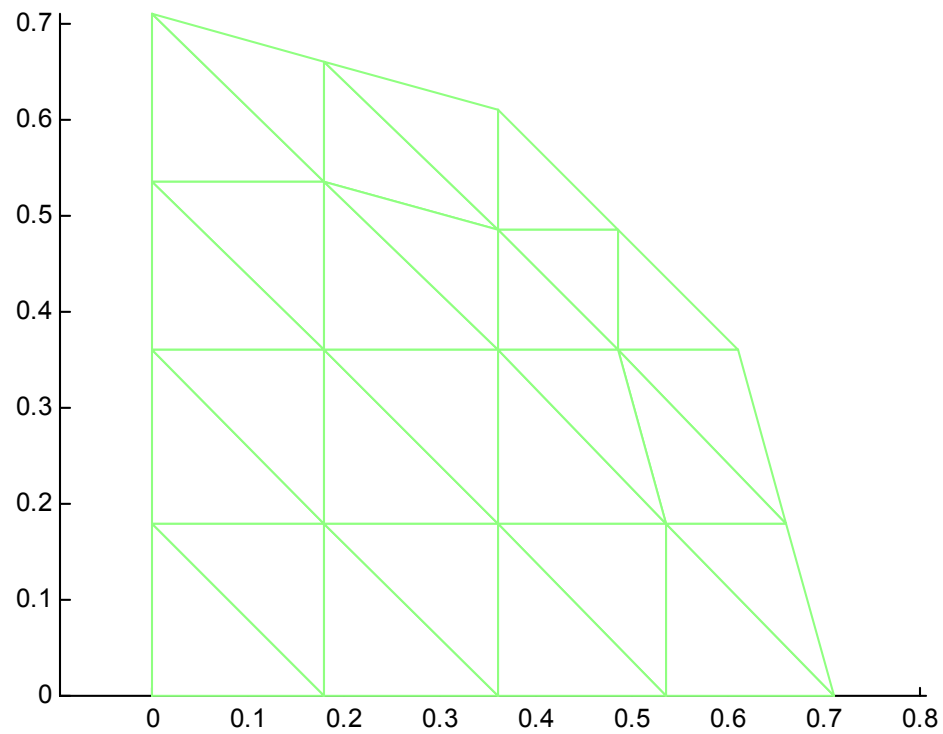


Figure 4.2. Refined element grid of a single blueberry (1/4 section)

Verification of Diffusional Model

Material and transport properties for both thawed and infused berries in tunnel drying and fluidized bed drying were calculated and reported in Table 4.1 and Table 4.2, respectively.

Table 4.1. Material and transport properties for both thawed and infused berries in tunnel drying (* values obtained from Kim, 1987).

Parameters	Units	Thawed Berries	Infused Berries
Convective Mass Transfer Coefficient (h_m)	m^2/s	0.03225	0.03225
Initial Density (ρ)	kg/m^3	1070*	1190*
Specific Heat (c)	$J/kg.K$	3593.9	3470
Volume (V)	m^3	$1.4984.10^{-6}$	$1.4984.10^{-6}$
Latent Heat of Evaporation (λ)	J/kg	$2.3586.10^6$	$2.3586.10^6$
Convective Heat Transfer Coefficient (h)	$W/m^2.K$	31.8656	31.8656
Drying Air Temperature (T)	$^{\circ}K$	333 (60 $^{\circ}C$)*	333 (60 $^{\circ}C$)*
Relative Humidity of Air (RH)	%	0*	0*
Thermal Conductivity of Air (k)	$W/m.K$	0.0288	0.0288
Reynolds Number (Re)	–	2991.43*	2991.43*
Drying Air Velocity (V)	m/s	4	4
Viscosity of Air at Drying Air Temp. (μ)	Pas	$20.085.10^{-6}$	$20.085.10^{-6}$
Specific Heat of Air at Drying Air Temp. (c_{air})	$J/kg.K$	1009	1009
Density of Air at Drying Air Temp. (ρ_{air})	kg/m^3	0.998	0.998

Table 4.2. Material and transport properties for both thawed and infused berries in fluidized bed drying (* values obtained from Kim, 1987).

Calculated Parameters	Units	Thawed Berries	Infused Berries
Convective Mass Transfer Coefficient (h_m)	m^2/s	0.03632	0.03949
Initial Density (ρ)	kg/m^3	1070*	1190*
Specific Heat (c)	$J/kg.K$	3593.9	3470
Volume (V)	m^3	$1.4984.10^{-6}$	$1.4984.10^{-6}$
Latent Heat of Evaporation (λ)	J/kg	$2.0539.10^6$	$2.1147.10^6$
Convective Heat Transfer Coefficient (h)	$W/m^2.K$	106.7618	106.8125
Drying Air Temperature (T)	$^{\circ}K$	443 (170 $^{\circ}C$)*	423 (150 $^{\circ}C$)*
Relative Humidity of Air (RH)	%	0*	0*
Thermal Conductivity of Air (k)	$W/m.K$	0.0369	0.0355
Reynolds Number (Re)	–	5459.04	5907.60
Drying Air Velocity (V)	m/s	12	12
Viscosity of Air at Drying Air Temp. (μ)	Pas	$24.87.10^{-6}$	$24.82.10^{-6}$
Specific Heat of Air at Drying Air Temp. (c_{air})	$J/kg.K$	1015	1014
Density of Air at Drying Air Temp. (ρ_{air})	kg/m^3	0.796	0.833

The diffusional model uses two additional variable parameters namely effective diffusivity and thermal conductivity. D_{eff} is assumed to be the strong function of moisture content whereas thermal conductivity (k_q) is dependent on the temperature. Since the D_{eff} data for blueberries was not available in the literature, numerical calculations were made. Although D_{eff} was variable during drying, it was constant for each time step. Therefore Fick's law of diffusion equation was solved using MATLAB (Simal et al., 1996). Experimental moisture values were used for calculating the regression equations for the D_{eff} . Table 4.3 gives the D_{eff} equations as a function of moisture content for both blueberries and for both drying method. These effective diffusivity equations were used in the diffusional model for estimation of the predicted values of moisture and temperature distributions.

Table 4.3. Effective diffusivity equations for both thawed and infused blueberries (M = moisture content, kg water/kg DM).

	D_{eff} (m^2/s) Equations	r^2
<u>Thawed Blueberry</u>		
Tunnel Drying	$-2.10^{-9} M^2 + 10^{-8} M + 2.10^{-9}$	0.9926
Fluidized Bed Drying	$-8.10^{-9} M^3 + 5.10^{-8} M^2 - 10^{-8} M + 7.10^{-9}$	0.9970
<u>Infused Blueberry</u>		
Tunnel Drying	$2.10^{-9} M^3 - 3.10^{-6} M^2 + 2.10^{-9} M + 3.10^{-11}$	0.9961
Fluidized Bed Drying	$-6.10^{-8} M^3 + 8.10^{-8} M^2 - 10^{-8} M + 10^{-9}$	0.9825

Comparison of the predicted and experimental moisture contents for thawed berries during tunnel drying are given in Figure 4.3. As seen, predicted moisture content was slightly under the experimental values for the first 8 hours of drying with the relative standard deviation of 0.1923. Closer agreement between experimental and predicted values was observed after 8 hours.

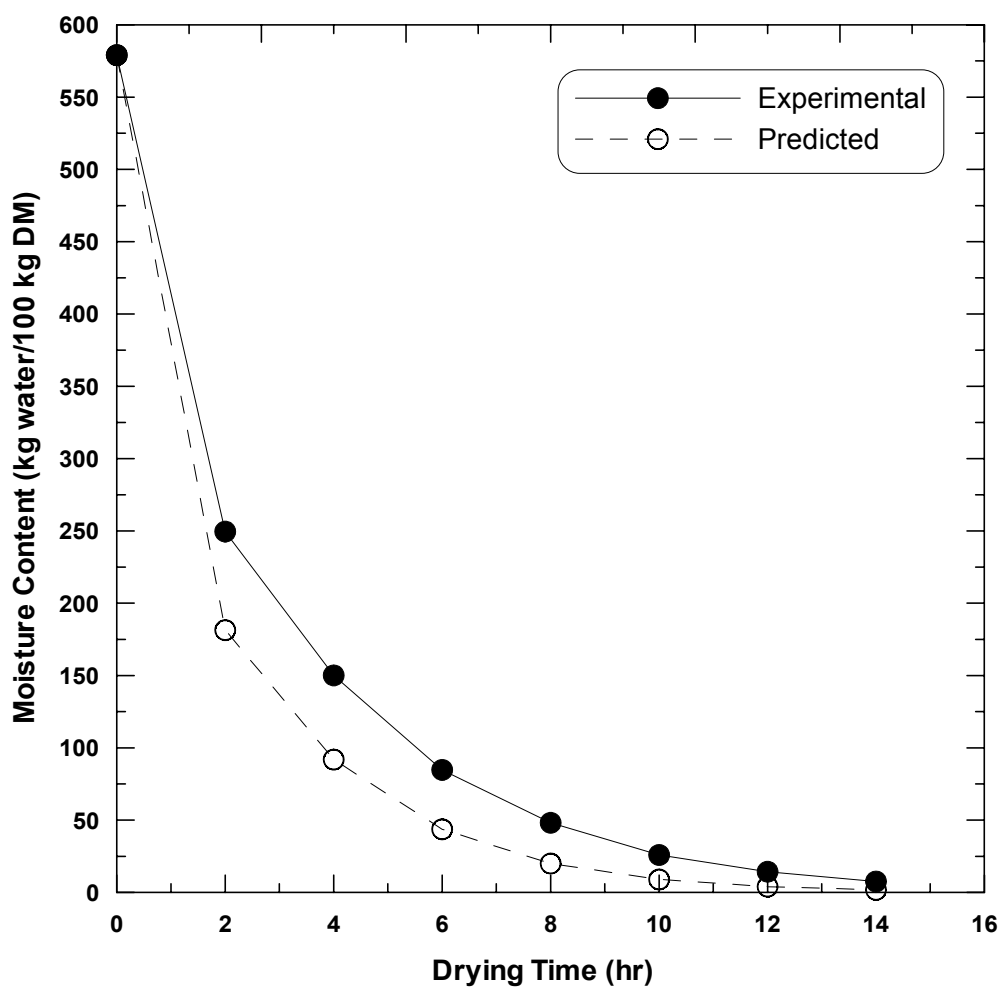


Figure 4.3. Comparison of predicted and experimental moisture contents of thawed blueberries during tunnel drying at 60 °C.

Figure 4.4 shows moisture content comparison of infused berries during tunnel drying. For the first 8 hours of drying predicted values were below the experimental values. After 8 hours predicted values were higher than the experimental values. Relative standard deviation throughout the entire drying was 0.1926.

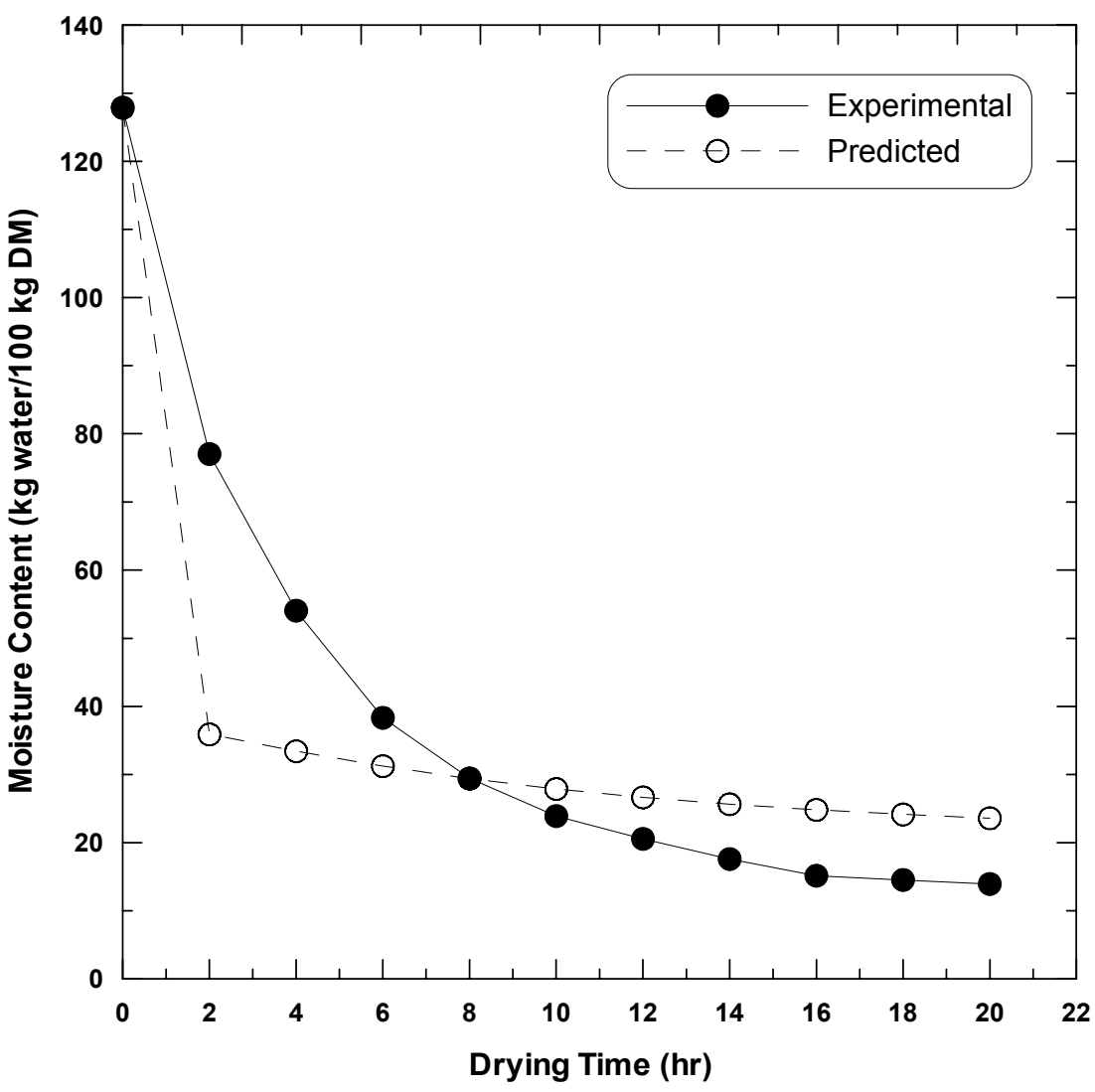


Figure 4.4. Comparison of predicted and experimental moisture contents of infused blueberries during tunnel drying at 60 °C.

There was no temperature history available for the experimental data. However, predicted temperature histories for both thawed and infused berries in tunnel dryer was given in Figure 4.5a and 4.5b assuming that good agreement between predicted and experimental moisture contents also resulted in good approximation of temperature histories since the system of heat and mass transfer equations were solved simultaneously. Any possible error in predicted temperature history was supposed to be reflected on the predicted moisture content. As seen in Figure 4.5, the temperature of the berry reached to equilibrium temperature after the first 2 hours of drying.

Predicted moisture contents of both thawed and infused berries during fluidized bed drying were also compared with the experimental moisture contents. Predicted moisture contents for thawed blueberries in the fluidized bed dryer at 170 °C were in good agreement with the experimental values with the relative standard deviation of 0.1293 as seen in Figure 4.6. There might have been an experimental error on determining moisture content at 80 sec which gave sharp decrease on the moisture plot. Predicted values were higher in the first 160 sec, and then the experimental values became greater. Model predictions provided smooth drying curve on drying data. Figure 4.7 summarizes the same comparison for infused blueberries. Predicted values were higher than experimental values during the entire drying with the relative standard deviation of 0.2677, although drying curves followed the same trend.

Temperature histories of both blueberries for fluidized bed drying were given in Figures 4.8a and 4.8b. As expected, there was sharp increase in the temperature towards the equilibrium temperature.

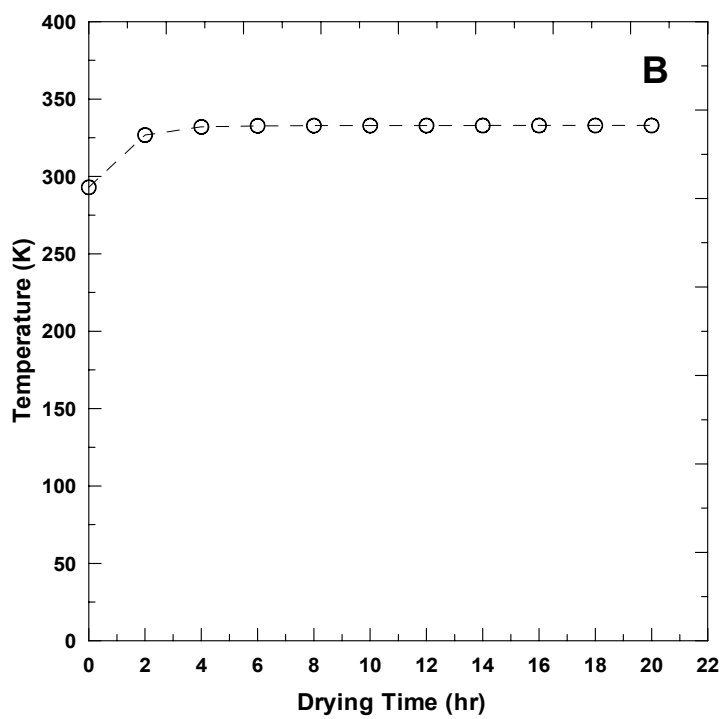
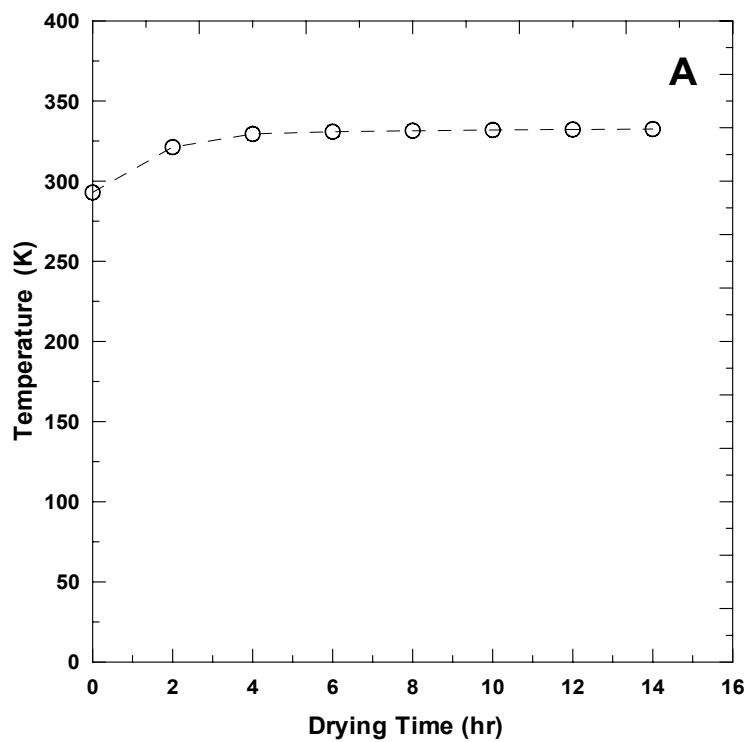


Figure 4.5. Predicted temperature histories for thawed (Part A) and infused (Part B) blueberries during tunnel drying at 60 °C.

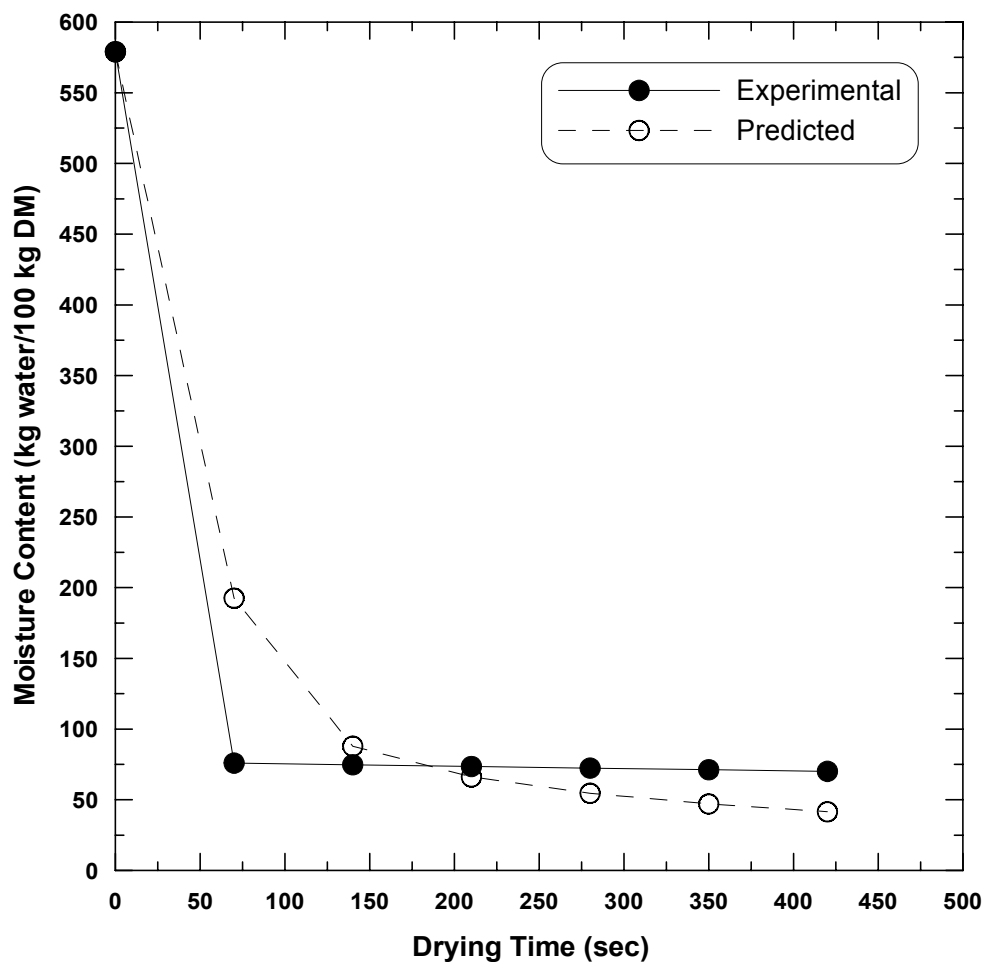


Figure 4.6. Comparison of predicted and experimental moisture contents of thawed blueberries during fluidized bed drying at 170°C.

Also, the predicted moisture distributions of both berries in both dryers using the diffusional model were given by Figure 4.9. As expected, the predicted moisture contents for both berries and both dryers were the lowest on the surface of the berry ($r=R$) followed by the mid-section ($r=R/2$) and the center. Moisture gradients in these sections were greater for the infused berries in both dryer suggesting that the infused sugar slowed the moisture transfer.

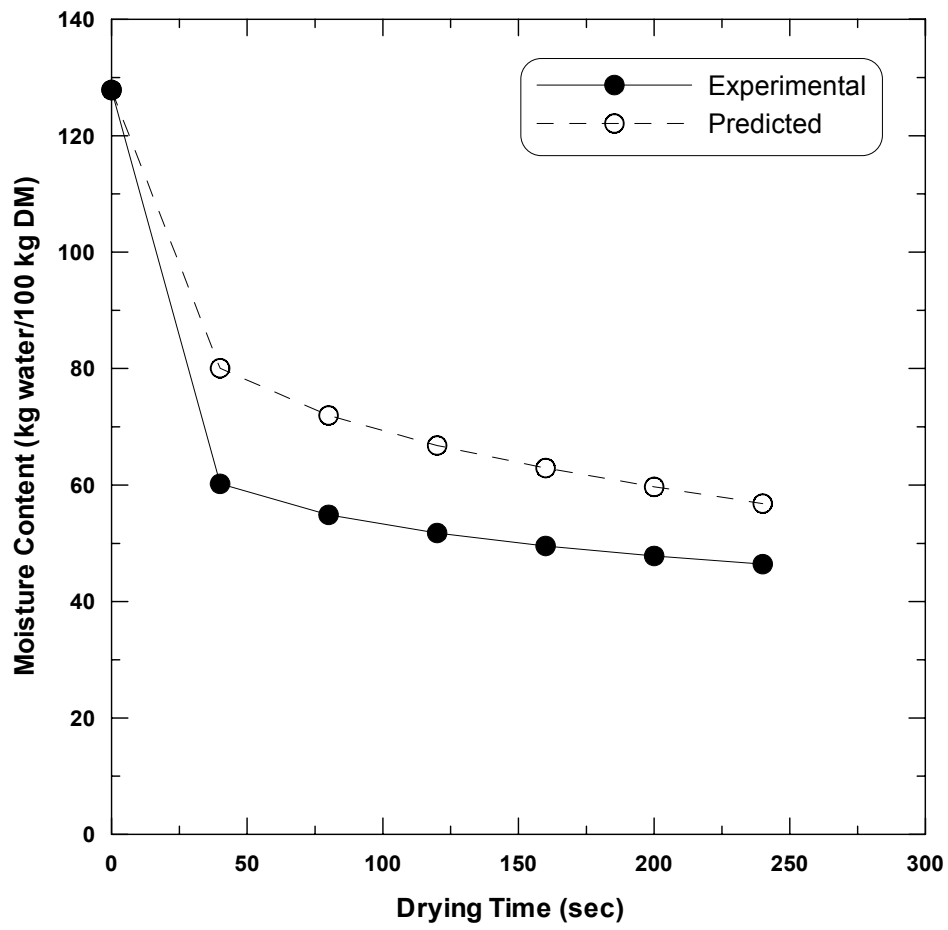


Figure 4.7. Comparison of predicted and experimental moisture contents of infused blueberries during fluidized bed drying at 150°C.

Finally, Figure 4.10 shows the predicted temperature distributions of both berries in both dryers using the diffusional model. The predicted temperature distributions resulted in the lowest temperature gradient on the surface of the berry followed by the mid-section and the center. Smooth curves were obtained for the tunnel drying, because the extended period of drying results in temperature equilibrium.

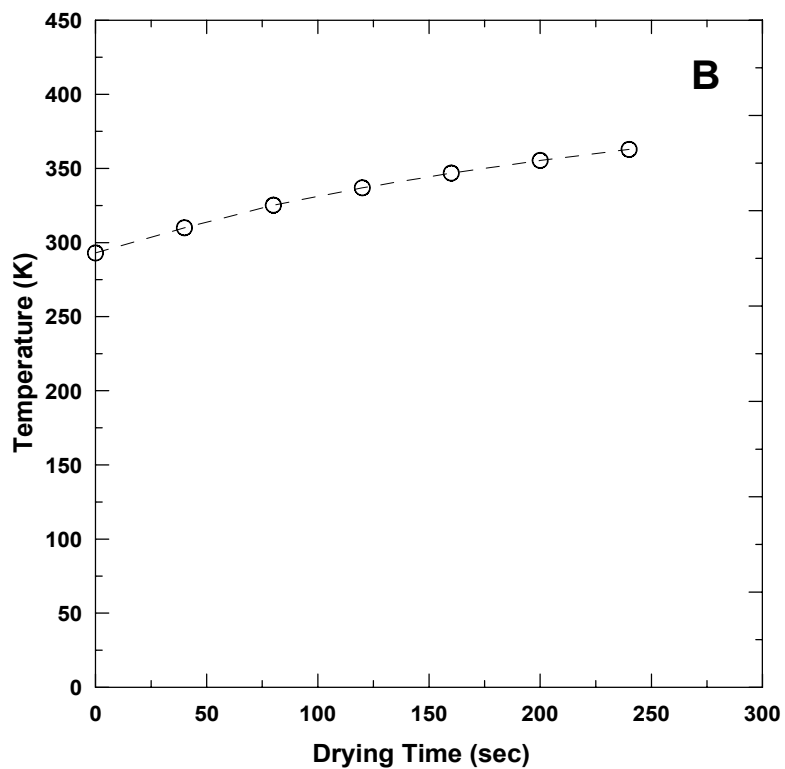
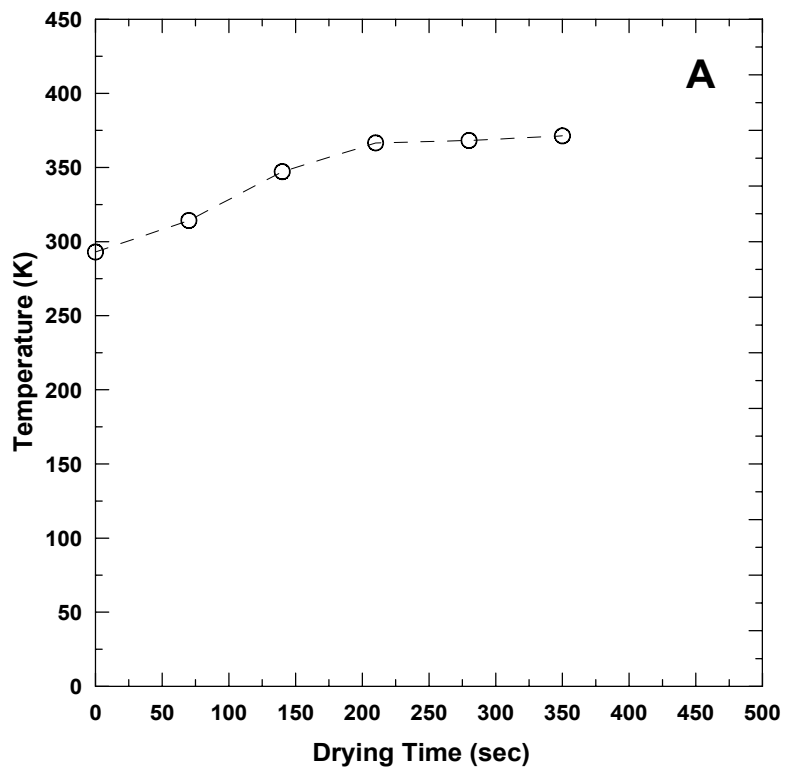


Figure 4.8. Predicted temperature histories for thawed (Part A) and infused (Part B) berries during fluidized bed drying.

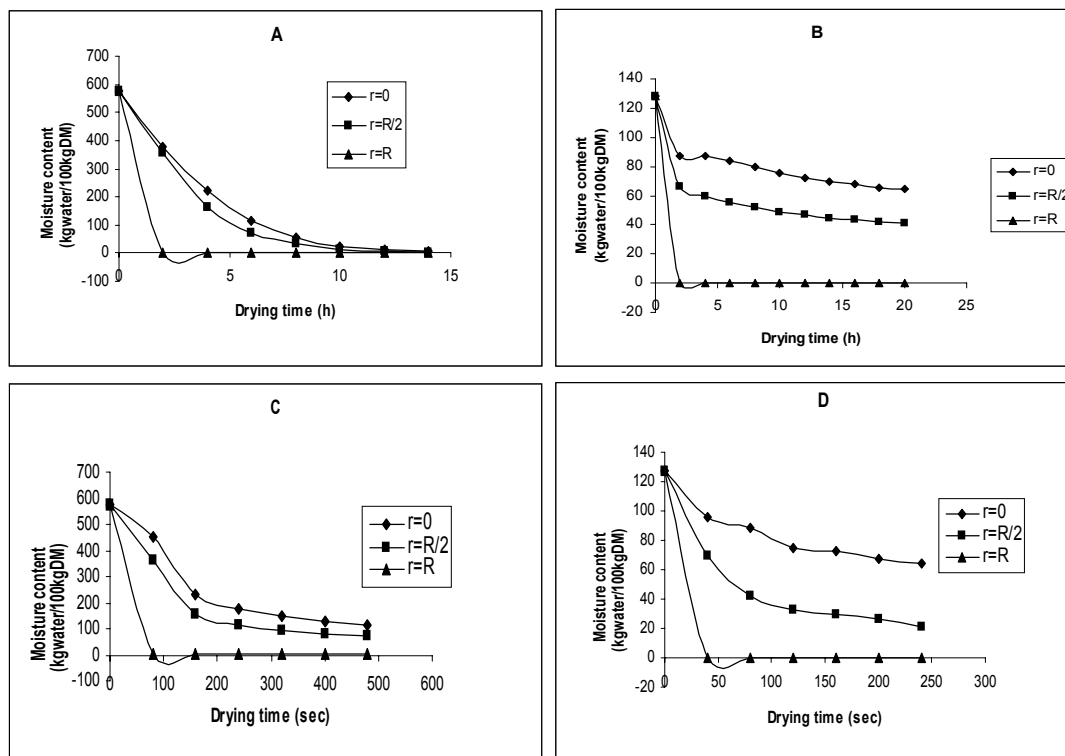


Figure 4.9. The Predicted moisture distributions of berries during drying using the diffusional model (A: thawed berries during tunnel drying, B: infused berries during tunnel drying, C: thawed berries during FB drying, D: infused berries during FB drying).

In general, there was a sharp decrease in the predicted moisture content in the first initial phase of drying for both thawed and infused blueberries in both the tunnel and the fluidized bed dryers, and then it remained constant. This indicates that the moisture transport rate for the initial stage of drying was higher at higher moisture content and it was slowed down by the relative increase in the sugar concentration as water is removed. Also there might be a second falling rate period where the drying rate significantly slows due to lower moisture content of the both blueberries. The high initial drying rate for both berries in both dryers indicates the gradient of moisture (driving force for moisture

transfer) was high. In each time interval during drying this gradient decreased below the previous level, therefore, the moisture content decrease started to level off. At lower temperatures in tunnel drying, the rate of liquid moisture loss is very rapid and water depletion near surface occurs quickly. Therefore the rate of moisture diffusion within the berry is not enough to replenish the fast evaporation from the surface to drying medium resulting in further decrease of the drying rate. All these findings were in agreement with results from Jia and Sun (2000), Chen and Pei (1983), Husain et al. (1972), and Whitaker and Young (1972).

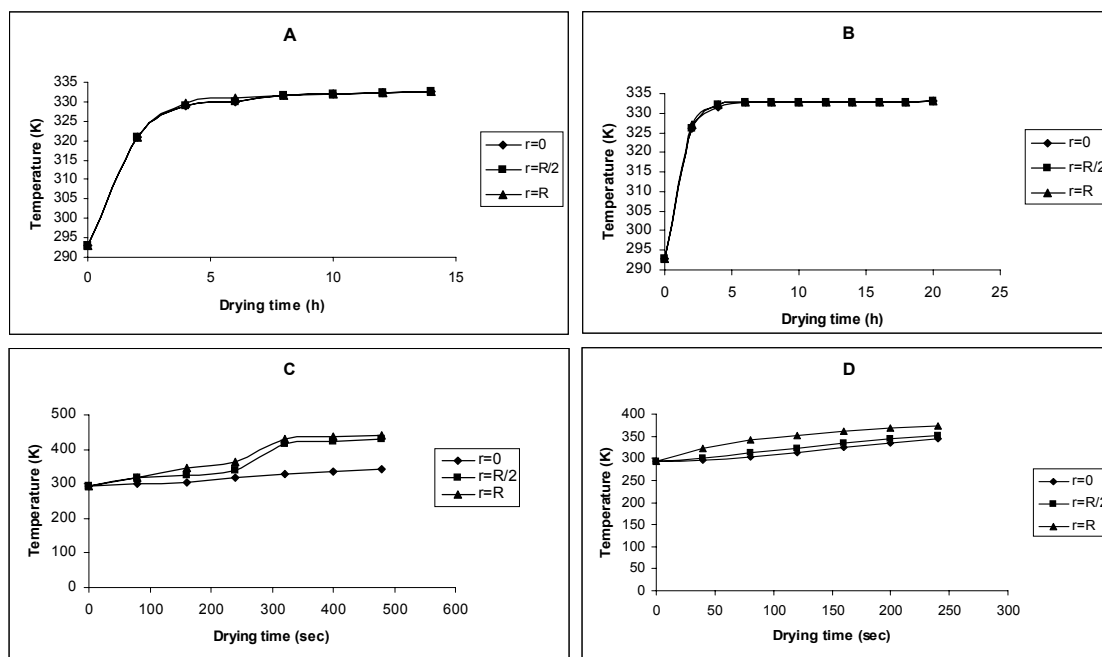


Figure 4.10. The predicted temperature distributions of berries during drying using the diffusional model (A: thawed berries during tunnel drying, B: infused berries during tunnel drying, C: thawed berries during FB drying, D: infused berries during FB drying).

The diffusional model fits the experimental data better at lower temperature drying (tunnel drying) than that at higher temperature drying (fluidized-bed drying). This is consistent with the expectations, because the diffusional model only considers liquid diffusion and evaporation on the surface of the blueberries. But in high temperatures in the fluidized bed dryer, vapor diffusion could occur but was not accounted for in the diffusional model, thus predicted values are lower than the experimental values. Fortes and Okos (1981), Chen and Pei (1983), Mahmutoglu et al. (1995), and McMinn and Magee (1999) observed the importance of the vapor diffusion along with the liquid diffusion. Furthermore, Haghghi and Segerlind (1988) and Fusco et al. (1991) stated the limitations of diffusional models for drying of granular or porous materials indicating that other mechanisms such as capillarity, gravity, and external pressure (shrinkage) might be important.

As for the temperature histories, it is interesting to note that the berry temperature did not reach the drying air temperature for both the tunnel and fluidized bed dryer. A possible reason for this might be that water evaporation from the berry surface might have caused the evaporative cooling thus keeping the equilibrium temperature below the drying air temperature. This finding is supported by the research of Chang and Weng (2000).

This rapid temperature rise in blueberries could cause thermally induced flavor changes which would damage berry quality. Therefore, if higher drying air temperatures are used, the drying time should be controlled carefully because maximum temperature gradients occur in the initial phase of drying.

Overall, the diffusional model provides reasonable approximation of the experimental drying data for both drying methods and for both berry samples. Plots show realistic moisture contents and effective diffusion coefficients. The diffusional

model obviously works better for lower temperature drying data. It could be valuable for predicting drying rates of different food materials. The diffusional model is even more useful at longer drying times at lower drying air temperature where the process accounts for predominant liquid diffusion to the surface.

Verification of Luikov Model

Material and transport properties for both blueberries in both drying from Tables 4.1 and 4.2 were also used in Luikov model. There were three additional parameters namely phase conversion criteria (ϵ), thermo-gradient coefficient (δ), and mass capacity (cm). These three parameters were considered as constants, but their values were not available for the blueberries in the literature. Also, experimental determination of coefficients was not possible. Therefore values for the specified vegetables and grains were used as the starting point (Zhoce et al., 1994; Mukherjee et al., 1997; Irudayaraj et al., 1992; Irudayaraj and Wu, 1999b) for parameter estimation. During simulation, two of the variables were kept constant while the third was changed. Predicted moisture contents compared to the experimental data (Irudayaraj and Wu, 1999a). The number which gave the lowest error between predicted and experimental data was used in the simulation. Minimization of the deviation between experimental and predicted data resulted in a phase conversion criteria (ϵ , the ratio of the vapor diffusion coefficient to the total diffusion coefficient of moisture) of 0.8, thermogradient coefficient (δ) of 0.03 and mass capacity (cm) of 0.003. Comparison of predicted and experimental moisture contents of thawed berries during tunnel drying at 60 °C were given in Figure 4.11. The Luikov model agreed well with the experimental data. Predicted values were slightly under the experimental data with the relative standard error of 0.0258.

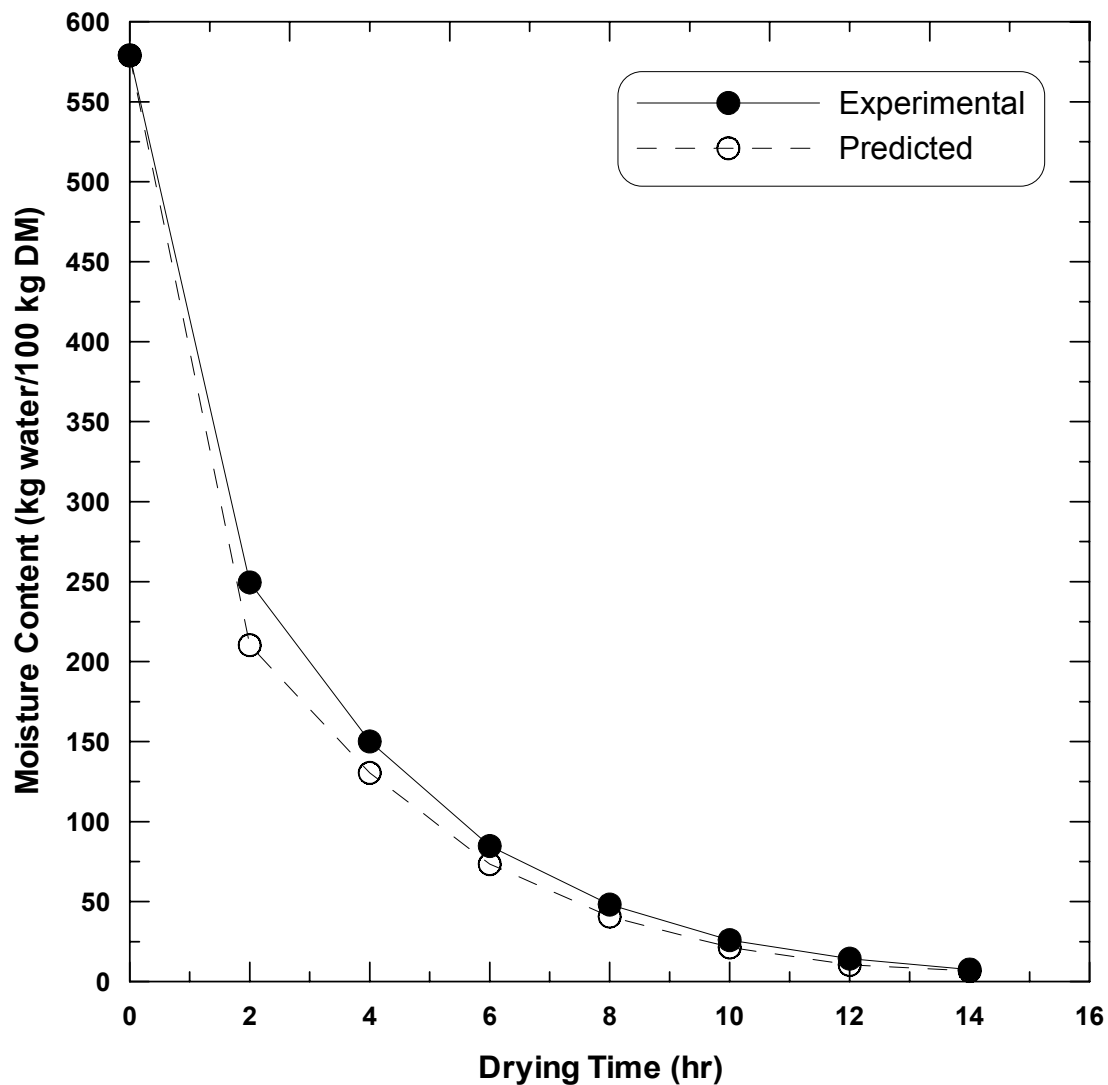


Figure 4.11. Comparison of predicted and experimental moisture contents of thawed blueberries during tunnel drying at 60 °C

Figure 4.12 gives the comparison of the predicted and experimental moisture contents of infused blueberries during tunnel drying at 60 °C. Predicted and experimental values agreed well throughout the drying with the relative standard error of 0.0278. Predicted moisture values were slightly under the experimental moisture values.

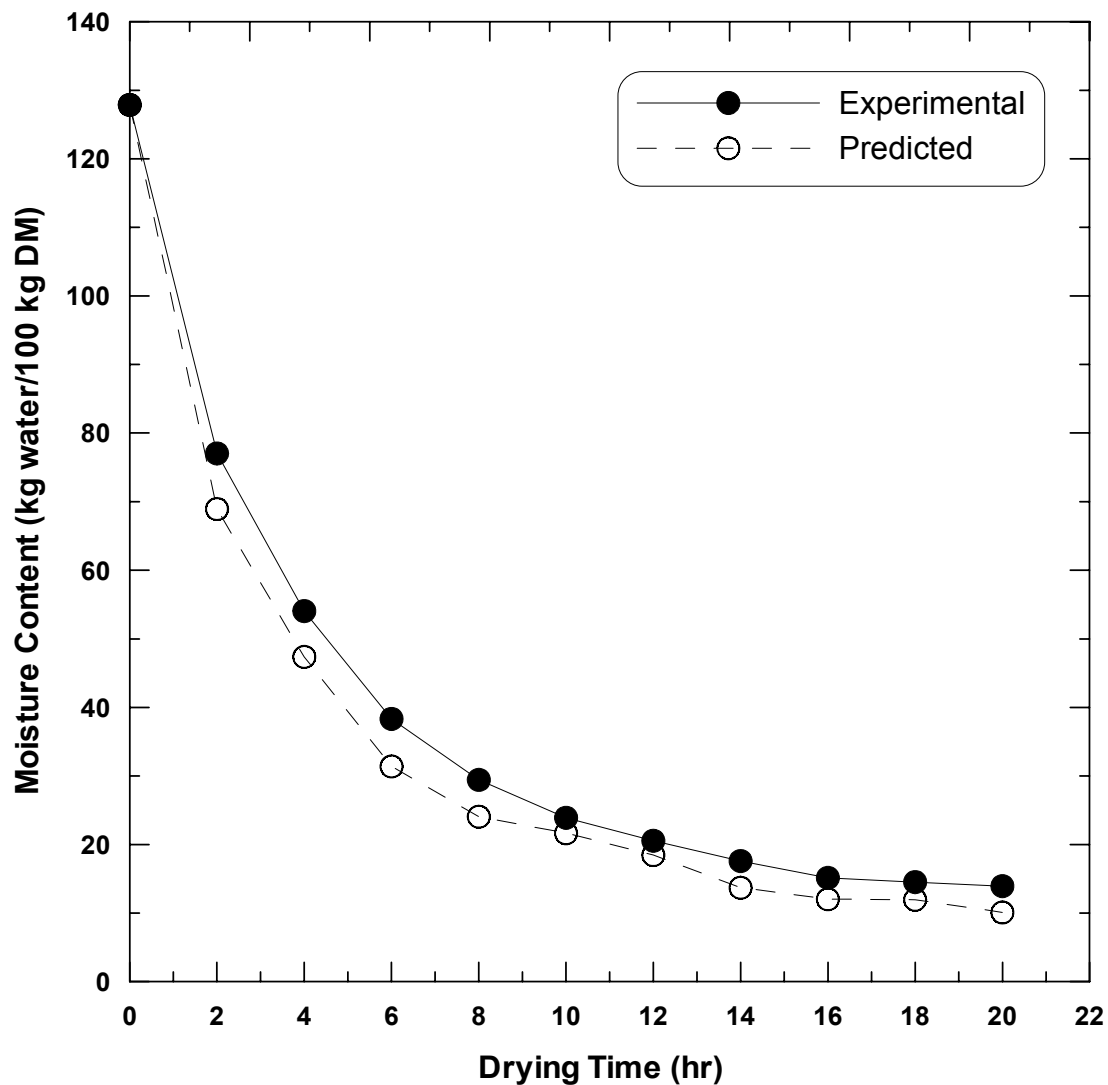


Figure 4.12. Comparison of predicted and experimental moisture contents of infused blueberries during tunnel drying at 60 °C

Figure 4.13 is the summary of the comparison between predicted and experimental moisture contents of the thawed blueberries during fluidized bed drying at 170 °C. Predicted moisture values were slightly under the experimental moisture values with the relative standard error of 0.0236.

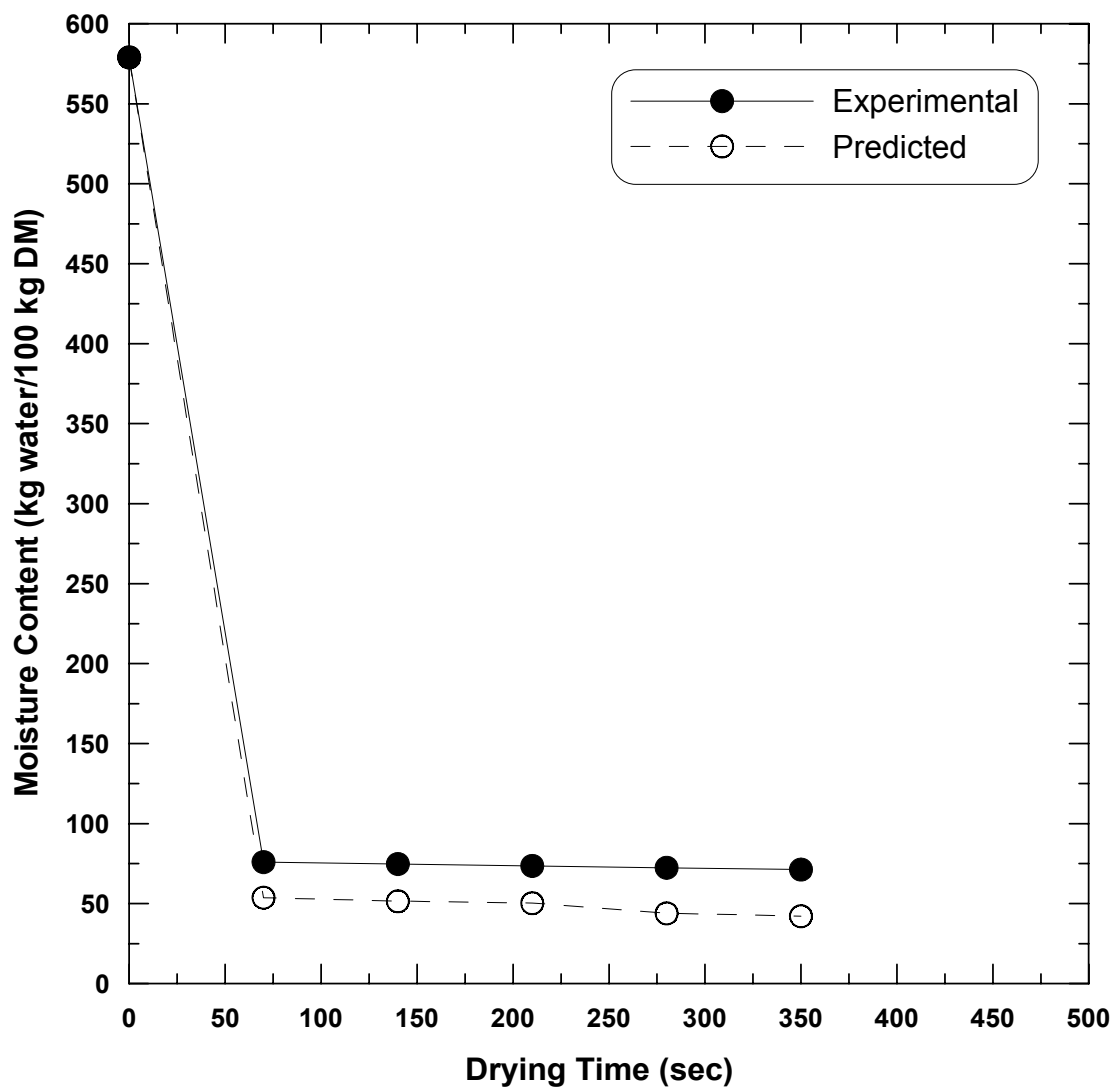


Figure 4.13. Comparison of predicted and experimental moisture contents of thawed blueberries during fluidized bed drying at 170 °C

Finally the comparison between predicted and experimental moisture contents of the infused berries during fluidized bed drying at 150 °C was given in Figure 4.14. Predicted moisture values resulted in the relative standard error of 0.0372 when compared to the experimental moisture values.

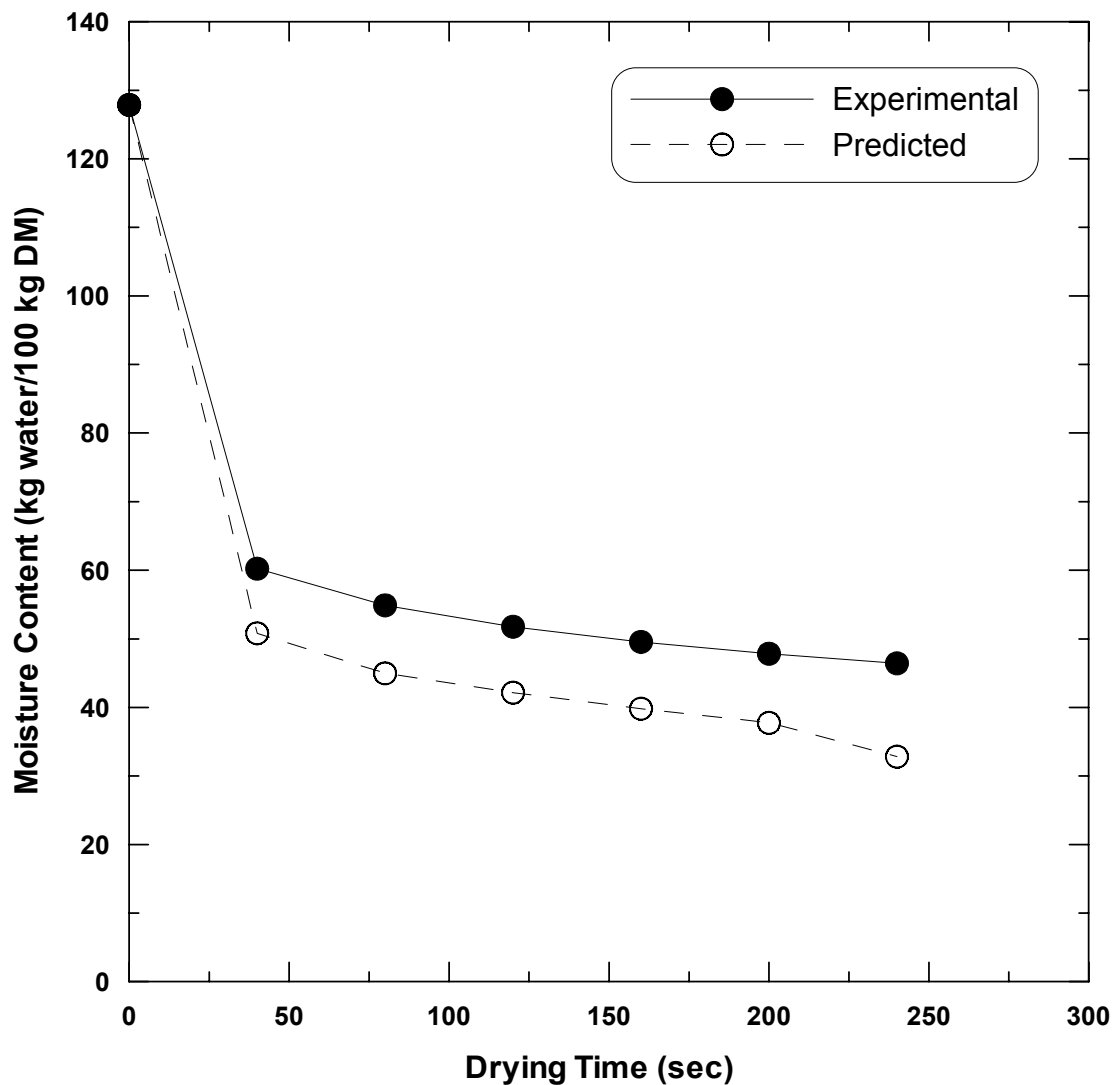


Figure 4.14. Comparison of predicted and experimental moisture contents of infused blueberries during fluidized bed drying at 150 °C

Figure 4.15 gives the predicted moisture distributions of both berries in both dryers using the Luikov model. The predicted moisture distributions for both berries and both dryers were the lowest on the surface, the mid-section and the center, respectively. As seen in the diffusional model, the moisture gradients for the infused berries in both

dryers were greater, because the infused sugar slowed the moisture transfer. In all four figures, surface moisture was carried away by the drying air therefore surface moisture distribution quickly reached to equilibrium with the drying air.

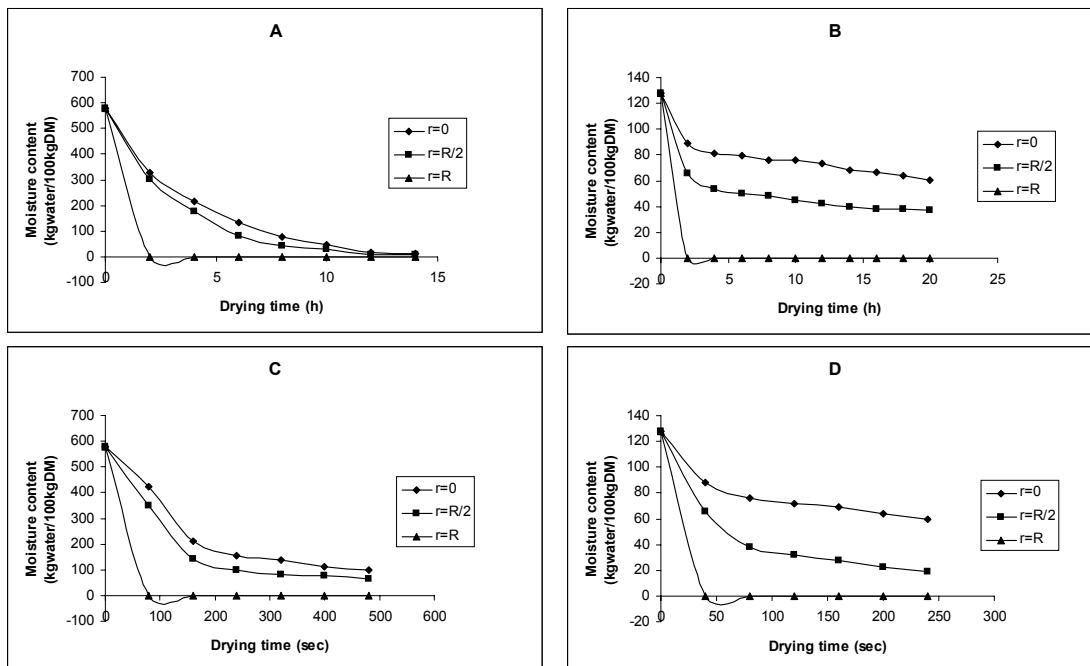


Figure 4.15. The predicted moisture distributions of berries during drying using the Luikov model (A: thawed berries during tunnel drying, B: infused berries during tunnel drying, C: thawed berries during FB drying, D: infused berries during FB drying).

The predicted temperature distributions of both berries in both dryers using the Luikov model are given by Figure 4.16. During tunnel drying, both berries had smoothly reached to the equilibrium temperature after the first hours of drying. Both berries had slight temperature gradients at the surface, the mid-section, and the center, but they also

reached to the equilibrium after 250 sec for thawed berries and 150 sec for the infused berries.

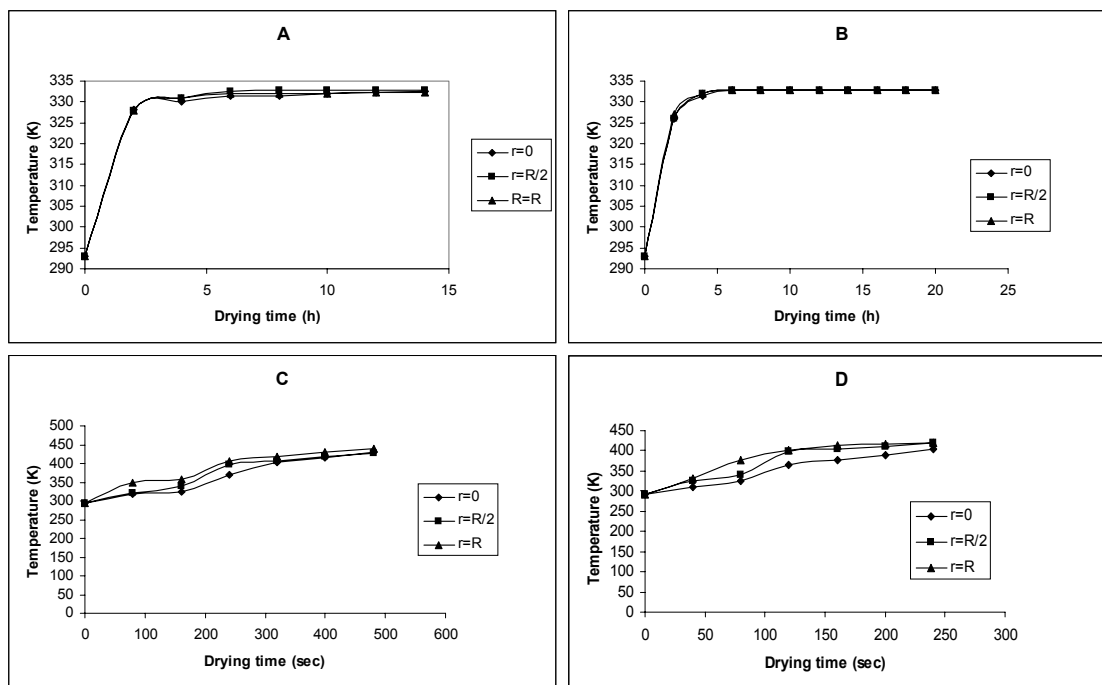


Figure 4.16. The predicted temperature distributions of berries during drying using the Luikov model (A: thawed berries during tunnel drying, B: infused berries during tunnel drying, C: thawed berries during FB drying, D: infused berries during FB drying).

In general, the Luikov model gave better approximations to the experimental moisture data during both drying conditions than the diffusional model. Interestingly, the closer agreements between predicted and experimental moisture contents were observed during tunnel drying at 60 °C for both blueberries than fluidized bed drying. Although the Luikov model accounted for the vapor diffusion along with liquid diffusion, at higher

drying temperatures (above 100 °C) pressure gradient might play an important role in heat and mass transfer and it is the function of the temperature (Luikov, 1975; Wu and Irudayaraj, 1996; Irudayaraj and Wu, 1999b; Irudayaraj and Wu; 1996). Therefore, inclusion of the pressure term in both heat and mass transfer equations may increase the accuracy of the model. But this addition introduces more constants in the system of differential equations therefore a solution would require additional equations.

MODEL APPLICATION

Model applications were done using the separate set of experimental data from Alma experimental station that have been obtained in 2001. For these experiments only the tunnel dryer was used. The temperature of the drying air was 110°C (230°F) and the air velocity was 12 m/s with the relative humidity of 0%. Initial moisture content of the thawed berries was 527.5 kg water/100 kg DM whereas initial moisture content of infused berries was 233.5 kg water/100 kg DM.

Figure 4.17 shows the comparison of the predicted and the experimental moisture contents of thawed berries during the tunnel drying at 110°C using both the diffusional and the Luikov models. Both models resulted in close agreement with the experimental data. Moisture gradient (moisture decrease) for the first 900 sec of drying was higher and it started to remain constant after 900 sec.

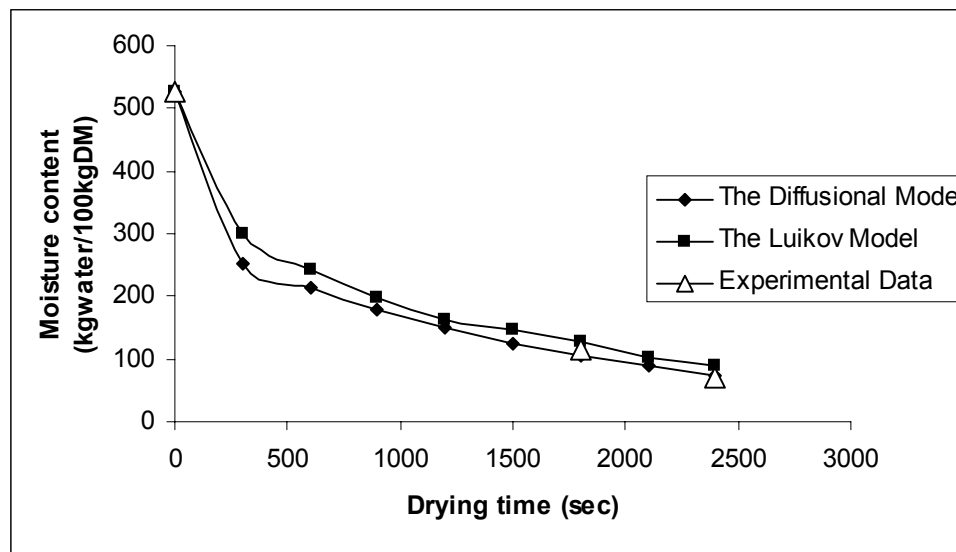


Figure 4.17. Comparison of predicted and experimental moisture contents of thawed berries during tunnel drying at 110°C using both the diffusional and the Luikov models.

The comparison of predicted and experimental moisture contents of infused berries during tunnel drying at 110°C using both models is given by Figure 4.18.. The predicted moisture contents from both models were close although the Luikov model had slightly higher predicted moisture values than the diffusional model. Both models gave very good agreement with the experimental moisture values at 1200 sec. However, both models overestimated the experimental moisture content at the end of drying (1800 sec).

Overall, both the diffusional and the Luikov models resulted in closed agreement with the experimental data points for the moisture contents of both thawed and infused berries.

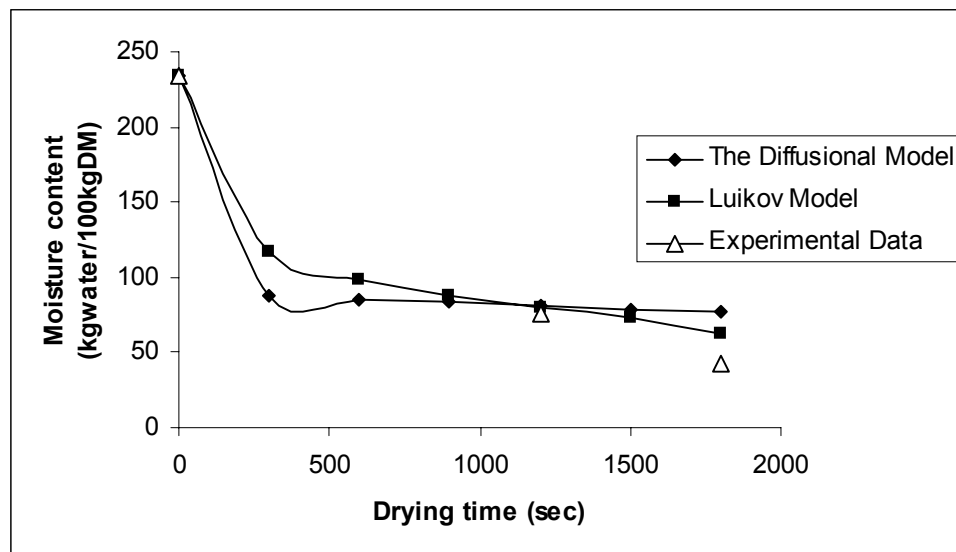


Figure 4.18. Comparison of predicted and experimental moisture contents of infused berries during tunnel drying at 110°C using both the diffusional and the Luikov models.

SENSITIVITY ANALYSIS

Both models use four major parameters, De_{eff} , h_m , k_q , h , to calculate the other material and the transport properties as given in Tables 4.1 and 4.2. Therefore, the effect of these parameters on the both model predictions was studied. The infused berries were chosen as an illustrative example. After the program runs, it has been seen that the De_{eff} and h_m have significant effect on both model predictions whereas k_q and h did not resulted in significant changes in predicted moisture contents.

Figures 4.19 and 4.20 give predicted moisture contents of the infused berries for different De_{eff} values during tunnel drying at 60°C using the diffusional model and the Luikov model, respectively. As seen even the very small changes in the De_{eff} resulted in the significant change on moisture content for the infused berries especially for the first

10 hour of drying. These results indicate that the caution must be taken for the selection of the calculation method of De_{eff} for both models.

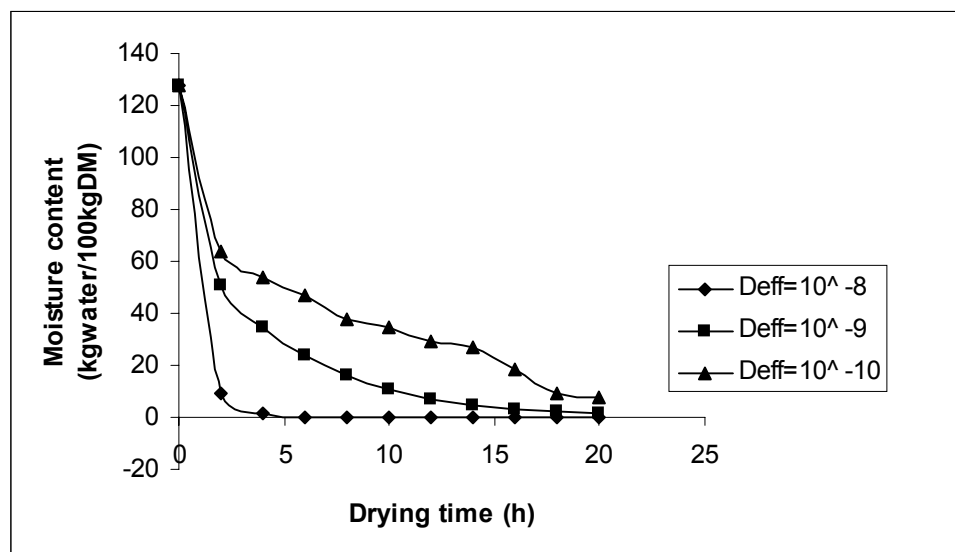


Figure 4.19. The predicted moisture contents of the infused berries for different De_{eff} during tunnel drying using the diffusional model.

The predicted moisture contents of infused berries for different De_{eff} values during FB drying using the diffusional model and the Luikov model are shown in Figures 4.21 and 4.22, respectively. As in tunnel drying, very small changes in De_{eff} resulted in significant amount of changes in moisture predictions for both models. This clearly indicates that the moisture content predictions are very sensitive to even small changes in De_{eff} .

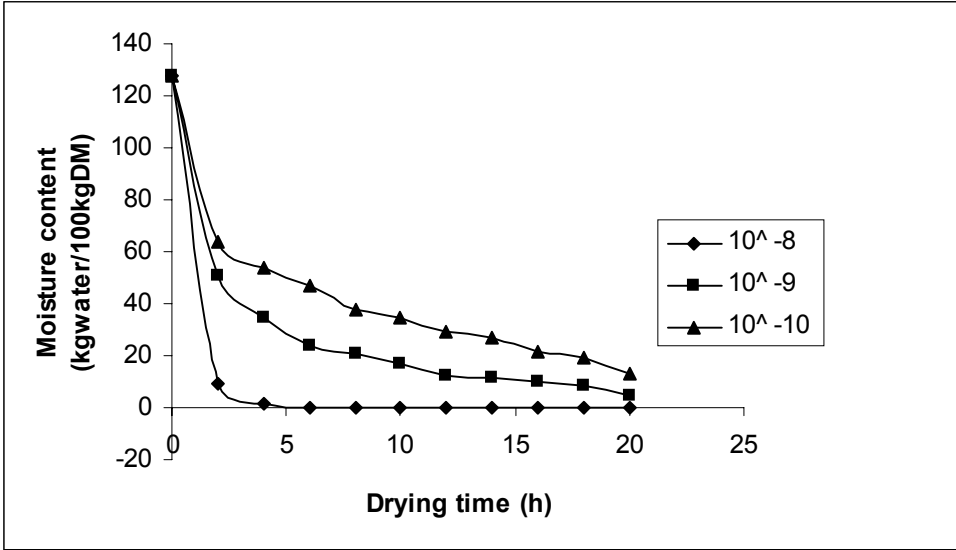


Figure 4.20. The predicted moisture contents of the infused berries for different Deff during tunnel drying using the Luikov model.

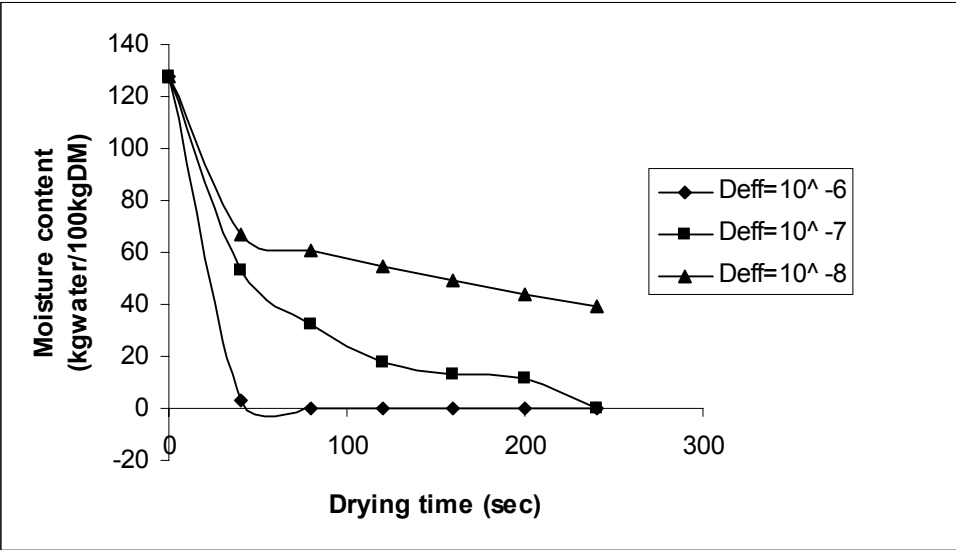


Figure 4.21. The predicted moisture contents of the infused berries for different Deff during fluidized bed drying using the diffusional model.

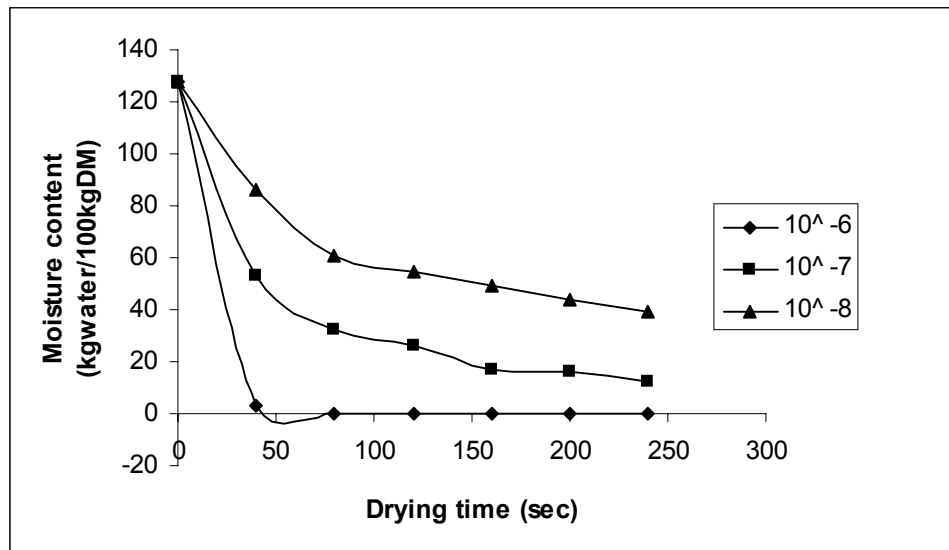


Figure 4.22. The predicted moisture contents of the infused berries for different De_{eff} during fluidized bed drying using the Luikov model.

Overall results show that the moisture content predictions for both models are very sensitive to the De_{eff} changes. Therefore, better approximations to the experimental data can be achieved by the careful selection of the calculation methods of De_{eff} , in another word, moisture and/or temperature dependency of De_{eff} have to be defined and studied for the predictions.

Another important parameter for both model predictions is hm . Figures 4.23 and 4.24 show the predicted moisture contents of infused berries for different hm values during tunnel drying using the diffusional and the Luikov models, respectively.

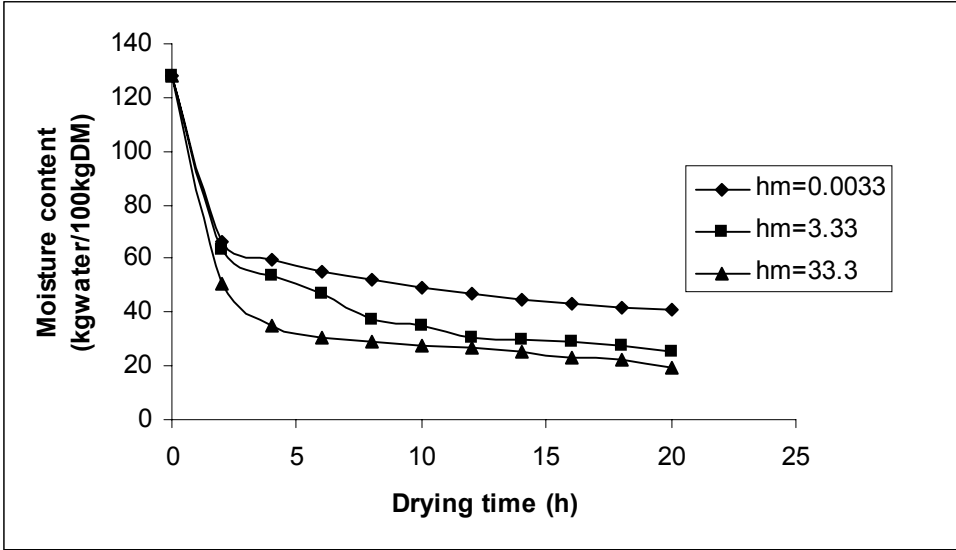


Figure 4.23. The predicted moisture contents of the infused berries for different hm values during tunnel drying using the diffusional model.

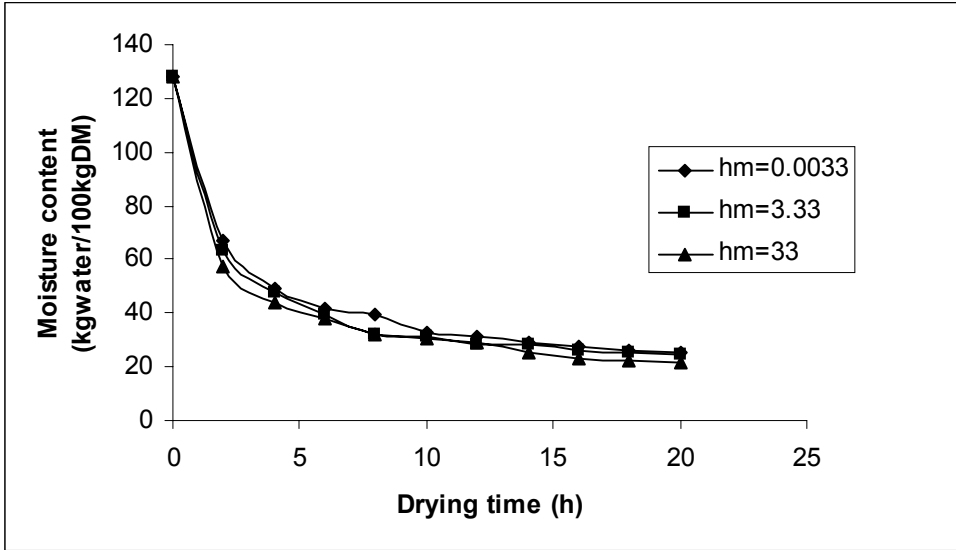


Figure 4.24. The predicted moisture contents of the infused berries for different hm values during tunnel drying using the Luikov model.

The predicted moisture contents were also sensitive to the changes in the h_m although the results were not as drastic as De_{eff} changes. The difference between predicted moisture contents were greater on the first 8 hours of drying for the diffusional model (Figure 4.23). The predicted moisture contents of infused berries using the Luikov model resulted in slight differences for different values of h_m (Figure 4.24). This indicates that the Luikov model for infused berries during tunnel drying is not as sensitive to the h_m changes as the diffusional model.

The predicted moisture contents of infused berries for different h_m values during fluidized bed drying using the diffusional model and the Luikov model are given by Figures 4.25 and 4.26, respectively.

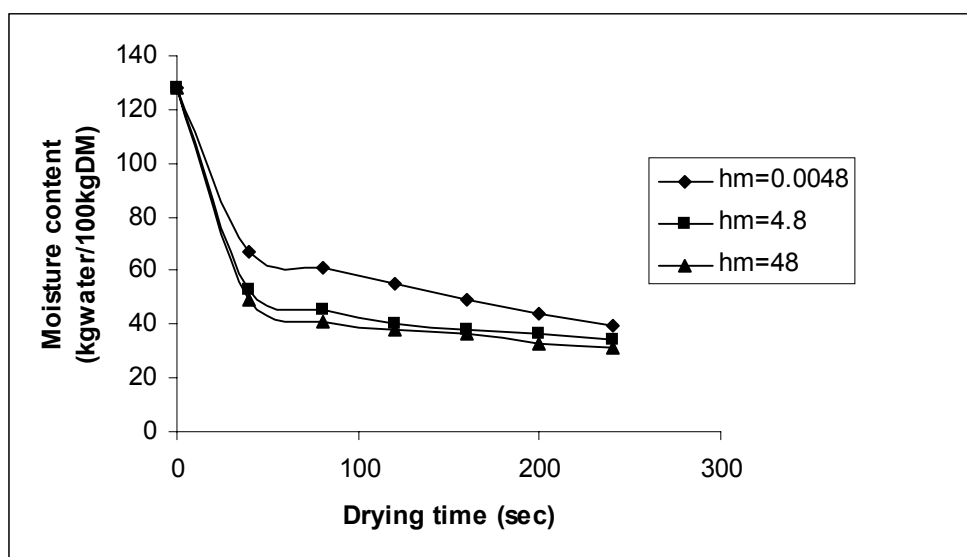


Figure 4.25. The predicted moisture contents of the infused berries for different h_m values during fluidized bed drying using the diffusional model.

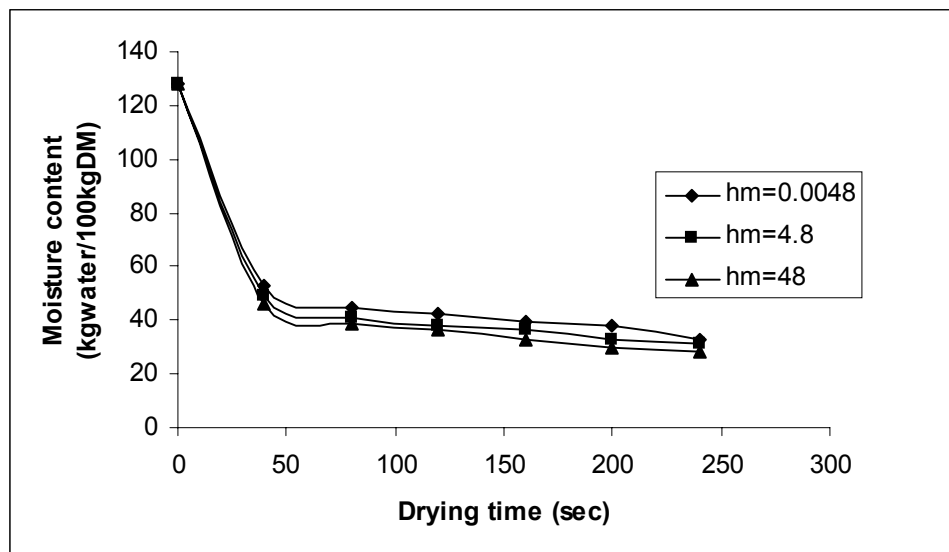


Figure 4.26. The predicted moisture contents of the infused berries for different hm values during fluidized bed drying using the Luikov model.

The diffusional model is sensitive to hm changes during fluidized bed drying of infused berries especially during the first 120 sec as seen in Figure 4.25. The predicted moisture contents became closer at the higher hm values. The Luikov model showed lesser sensitivity to hm changes for fluidized bed drying of infused berries through the entire drying as seen in Figure 4.26.

The closer agreement between the predicted moisture contents for different hm values during fluidized bed drying of infused berries using the Luikov model has been observed.

This sensitivity analysis provides an insight on the importance of De_{eff} and hm on both model predictions. The factor that might affect these two parameters may also be considered. For example, the selection of the drying air velocity will in return affect hm . Because the drying air velocity contributes un the calculation of Re which then is used to

calculate Sh . Finally Sh correlates the hm in the relations given in the section of engineering properties.

EFFECT OF INITIAL CONDITIONS ON DRYING

Effect of initial berry temperature and moisture content on the both temperature and moisture content of the berries during both tunnel and fluidized bed drying were also studied. Set of four initial berry temperature, 5°C, 10°C, 30°C, and 40°C, were chosen for both drying conditions. Initial moisture contents of the thawed berries were chosen to be 378, 478, 500, and 550 kg water/100 kg DM whereas infused berries had the initial contents of 75, 100, 150, and 175 kg water/100 kg DM. All the other material and transport properties were the same as indicated in the Tables 4.1 and 4.2. Both the diffusional model and the Luikov model were used for the simulations to obtain the predicted values of moisture contents and temperatures.

The effect of the initial berry temperature on the predicted moisture content of the both berries during both drying conditions can be seen on Figure 4.27 for the diffusional model. The initial temperature of the both berries did not result in significant change on the predicted moisture contents in the range from 5°C to 40°C.

The effect of the initial berry temperature on the predicted temperature values of berries during both drying conditions using the diffusional model is given in Figure 4.28. The predicted temperature values of the both berries in tunnel drying were reached to equilibrium after 2 hours of drying and the predicted temperature values were very close after 2 hours of drying. Similar results were observed for the fluidized bed drying of both berries. There were slight differences in the predicted temperature values for the initial temperature range of 5°C to 40°C.

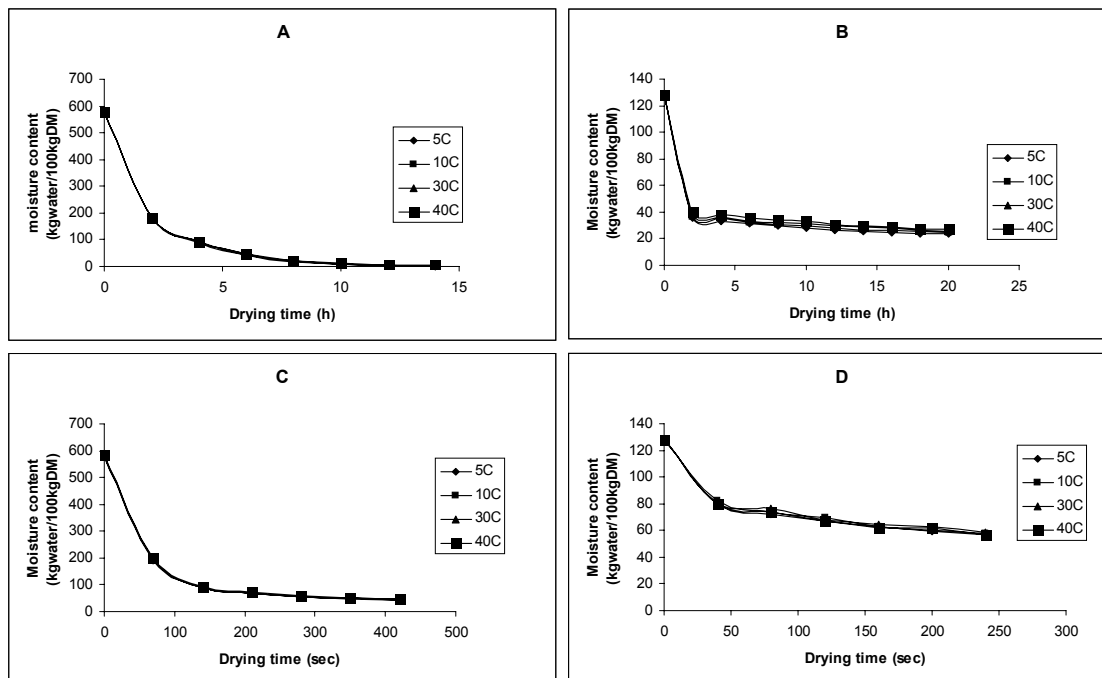


Figure 4.27. Effect of initial berry temperature on the predicted moisture content of berries during drying using the diffusional model (A: thawed berries during tunnel drying, B: infused berries during tunnel drying, C: thawed berries during FB drying, D: infused berries during FB drying).

The effect of the initial berry moisture content on the predicted moisture content of both berries during both drying conditions were also studied for the diffusional model as seen in Figure 4.29. The higher initial moisture contents resulted in the higher predicted moisture contents for each time interval of drying for the both berries during both drying conditions. For the both berries, tunnel drying resulted in closer predicted moisture contents in the range of the initial moisture content values than the fluidized bed drying. During the fluidized bed drying of infused berries, the predicted moisture

contents were higher for the higher initial moisture contents of berries especially for the first 120 sec of drying, after 120 sec the predicted moisture contents were closer.

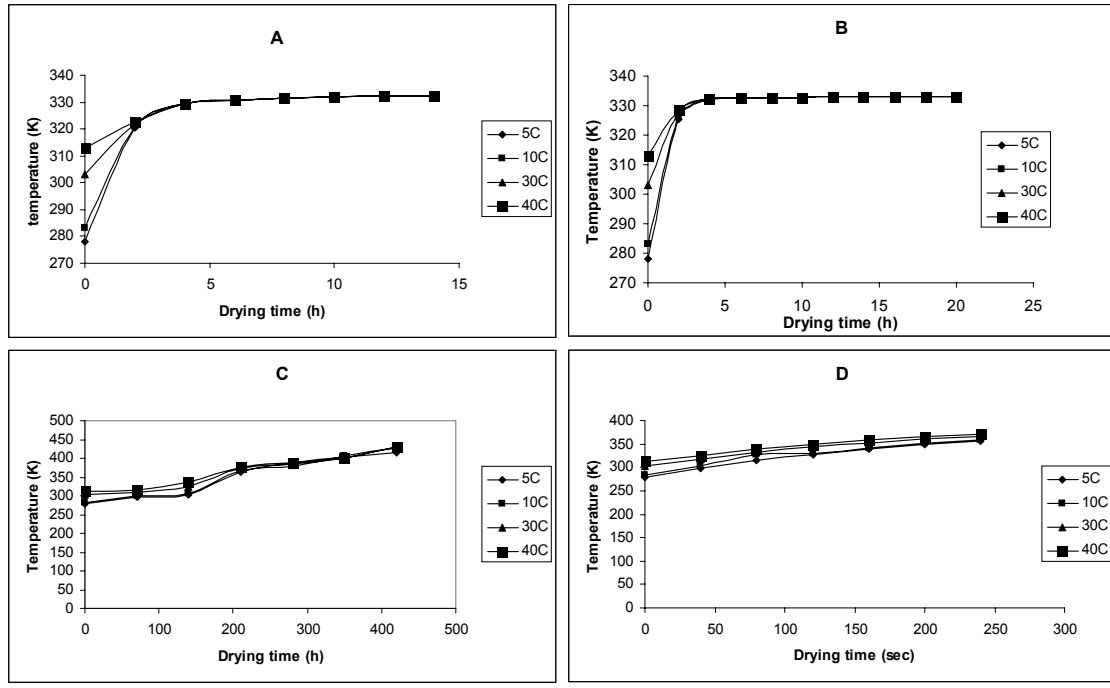


Figure 4.28. Effect of initial berry temperature on the predicted temperature of berries during drying using the diffusional model (A: thawed berries during tunnel drying, B: infused berries during tunnel drying, C: thawed berries during FB drying, D: infused berries during FB drying).

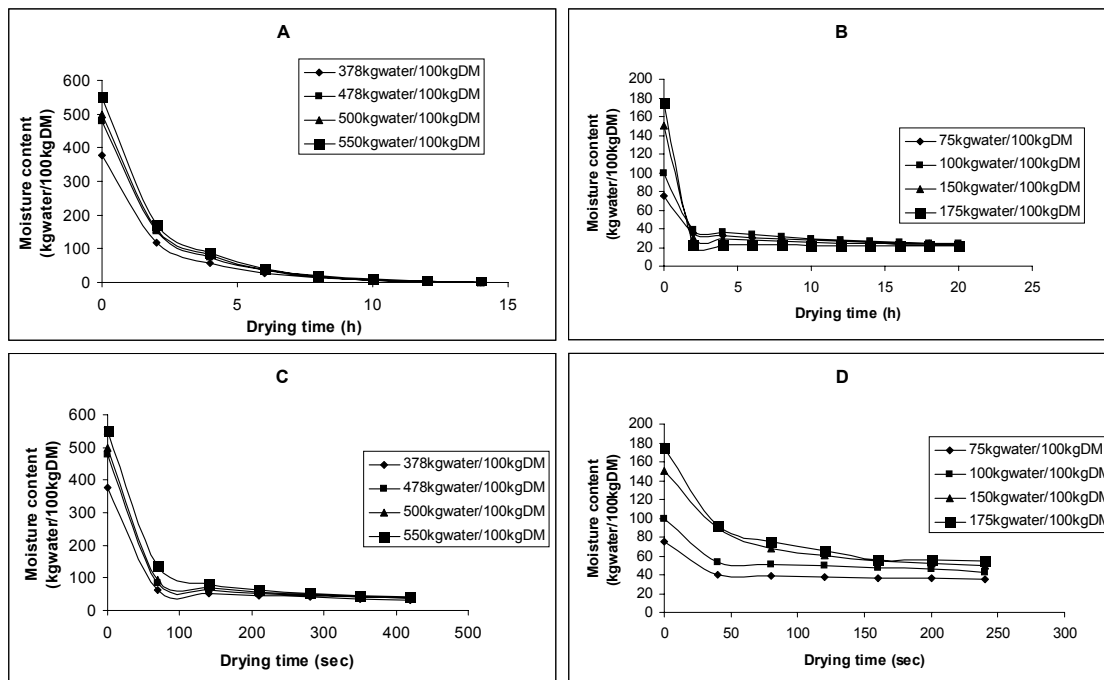


Figure 4.29. Effect of initial berry moisture content on the predicted moisture content of berries during drying using the diffusional model (A: thawed berries during tunnel drying, B: infused berries during tunnel drying, C: thawed berries during FB drying, D: infused berries during FB drying).

Figure 4.30 shows the effect of the initial berry moisture contents on the predicted temperature of both berries during both drying conditions using the diffusional model. Results indicated that the difference in the initial moisture contents of the berries did not have significant effect on the predicted temperature values. In tunnel drying both berries reached to equilibrium temperature after 2 hours of drying.

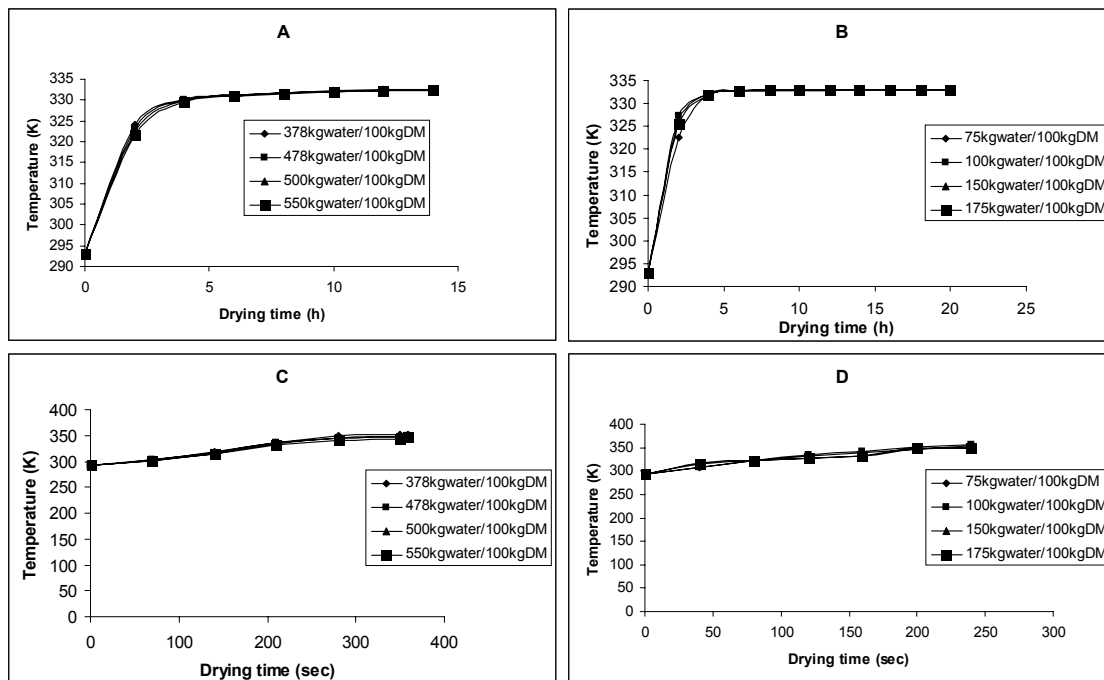


Figure 4.30. Effect of initial berry moisture content on the predicted temperature of berries during drying using the diffusional model (A: thawed berries during tunnel drying, B: infused berries during tunnel drying, C: thawed berries during FB drying, D: infused berries during FB drying).

The effect of the initial berry temperature on the predicted moisture contents of both berries during both drying conditions using the Luikov model is presented in Figure 4.31. The predicted moisture content of thawed berries was almost identical for the range of initial berry temperature of 5°C to 40°C. The infused berries showed slightly higher predicted moisture contents at the lower initial berry temperatures.

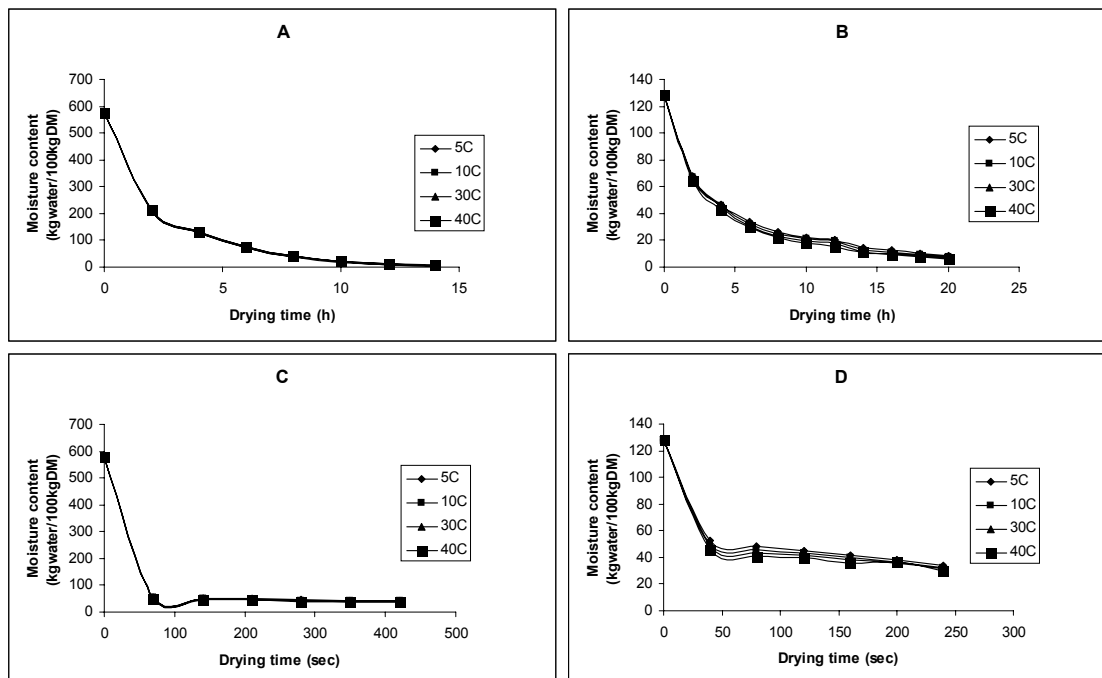


Figure 4.31. Effect of initial berry temperature on the predicted moisture content of berries during drying using the Luikov model (A: thawed berries during tunnel drying, B: infused berries during tunnel drying, C: thawed berries during FB drying, D: infused berries during FB drying).

Figure 4.32 shows the effect of the berry temperature on the predicted temperatures of the both berries during both drying conditions using the Luikov model. During tunnel drying, thawed berries reached equilibrium after 2 hours of drying for all four the initial berry temperatures, whereas for infused berries it took 8 hours to reach the equilibrium. For both drying conditions and both berries higher initial temperature values resulted in the higher predicted temperature values. The predicted temperature values for tunnel drying were very close after the equilibrium is reached.

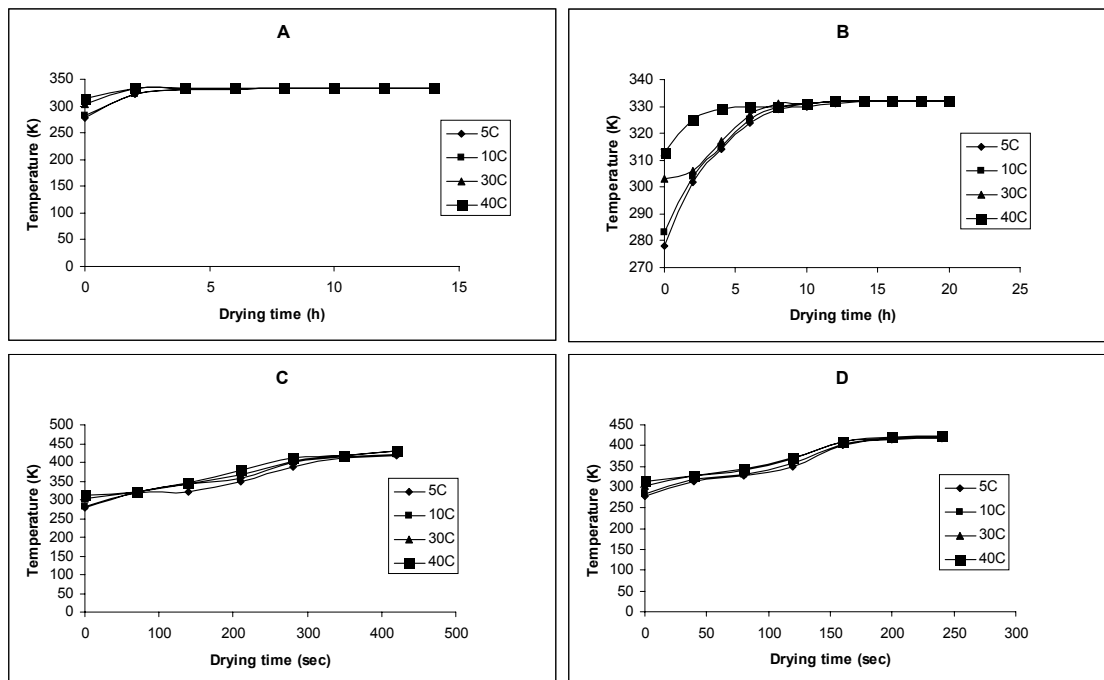


Figure 4.32. Effect of initial berry temperature on the predicted temperature of berries during drying using the Luikov model (A: thawed berries during tunnel drying, B: infused berries during tunnel drying, C: thawed berries during FB drying, D: infused berries during FB drying).

The effect of the initial berry moisture content on the predicted moisture content of the both berries during both drying conditions using the Luikov model is presented in Figure 4.33. The thawed berries resulted in very close predicted moisture content values for all the initial moisture contents during both the tunnel and the fluidized bed drying. The infused berries showed higher predicted moisture contents for the higher values of the initial moistures during both drying conditions.

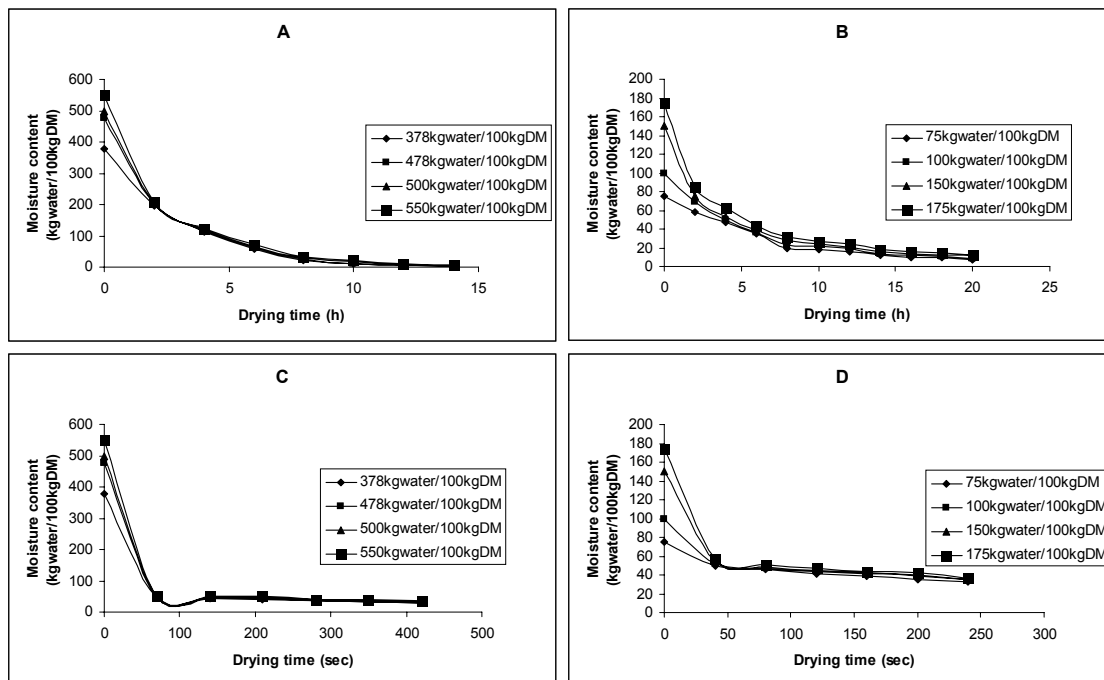


Figure 4.33. Effect of initial berry moisture content on the predicted moisture content of berries during drying using the Luikov model (A: thawed berries during tunnel drying, B: infused berries during tunnel drying, C: thawed berries during FB drying, D: infused berries during FB drying).

Finally, Figure 4.34 shows the effect of the initial berry moisture content on the predicted temperature of both berries during both drying conditions using the Luikov model. In the range of 378 to 550 kg water/100 kg DM of initial berry moisture content, both berries had very close predicted temperature values throughout the drying. In tunnel drying, interestingly, lower initial moisture contents resulted in the higher predicted temperature values and thawed and infused berries reached to equilibrium after 2 hours and 6 hours respectively.

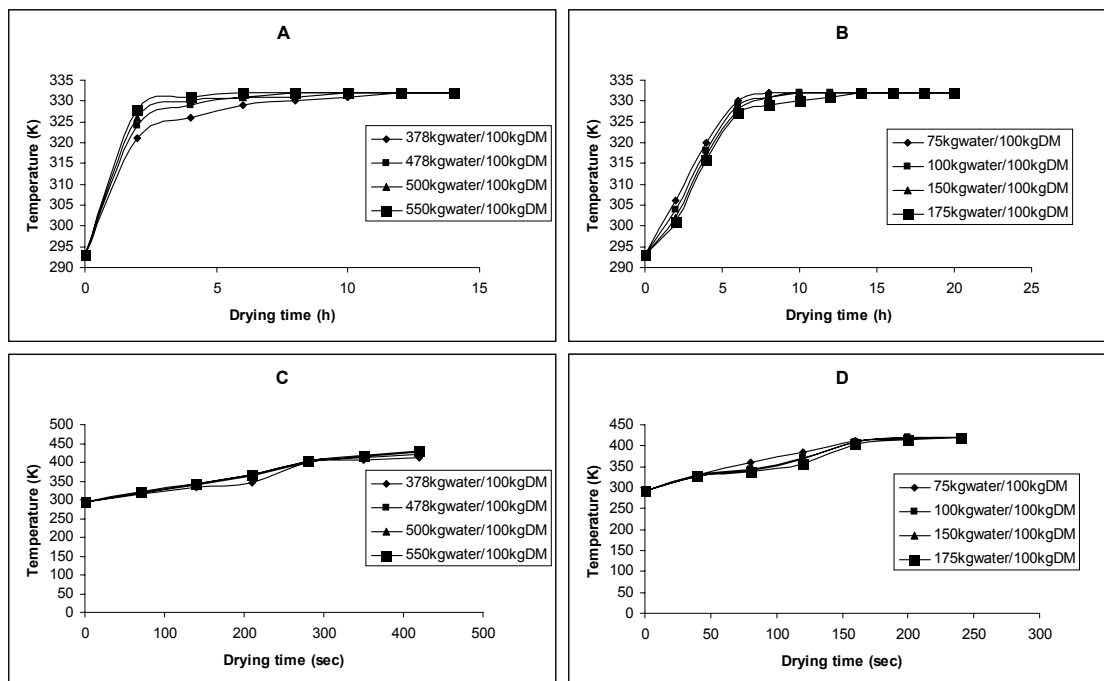


Figure 4.34. Effect of initial berry moisture content on the predicted temperature of berries during drying using the Luikov model (A: thawed berries during tunnel drying, B: infused berries during tunnel drying, C: thawed berries during FB drying, D: infused berries during FB drying).

CHAPTER 5

SUMMARY AND CONCLUSIONS

This research has been presented having two major objectives: mathematical modeling and the computer simulation of the thawed and infused blueberries during tunnel and fluidized bed drying. The mathematical modeling was based on both the diffusional model and the Luikov model along with the blueberry and transport properties and their calculations. Computer simulation was done using the finite element method for predicting moisture and the temperature histories and distributions of thawed and infused blueberries. The formulation and the solution procedures were applied to simulate the simultaneous heat and mass transfer in blueberries subjected to two drying methods. Verification of the both models was presented using the experimental data from Kim (1987). Both models were also used to simulate the separate set of experimental data on blueberries from Alma Experiment Station, Alma, GA. Sensitivity analyses on the two major parameters ($Deff$ and hm) were done. Effects of initial berry moisture content and temperature on the predicted moisture and temperature values were studied.

Temperature and moisture distributions in blueberry samples during drying were described by a set of coupled non-linear heat and mass transfer equations. The finite element formulation was developed using the Galerkin's weighted residual technique for spherical geometry in two dimensions. The diffusional model assumed that moisture diffused to the surface of the berry in the liquid form and evaporation took place on the surface whereas the Luikov model used an irreversible thermodynamics approach and accounted for the vapor diffusion along with the liquid diffusion.

The application of the finite element method to solve simultaneous heat and mass transfer equations in blueberries during drying was successful. The major conclusions of this research can be summarized as:

Mathematical modeling provided a useful way to validate the drying mechanisms of the simultaneous heat and moisture transfer in both thawed and infused blueberries with the relative accuracy.

Both models were satisfactory in predicting the drying curves for thawed and infused berries. However, the Luikov model predictions were found to be better than the diffusional model. These findings supported the hypothesis that there was considerable amount of vapor diffusion along with liquid diffusion.

Although Luikov's model provided better approximations of the moisture contents for both blueberries, it introduced three more parameters in the solution which complicated the model. In choosing the right model for describing the drying process this additional work on the solution procedure has to be considered along with the increased accuracy on the predictions.

In Luikov's model, higher relative standard deviations in fluidized bed drying at higher temperatures suggested that the pressure gradient might play an important role in the simultaneous heat and moisture transport due to the high temperatures as indicated by the earlier researchs (Irudayaraj and Wu, 1997; Irudayaraj and Wu, 1999a and Irudayaraj and Wu, 1999b).

Applications of two models to another set of experimental data were satisfactory. Sensitivity analysis revealed the importance of the De_{eff} and h_m determinations on the both model predictions. Especially, the method of determination of De_{eff} will have great effect on the model predictions. The selection of the drying air velocity will also affect

the h_m . Initial berry temperature and moisture contents also have somewhat importance in the model predictions therefore have to be considered.

Both models use the linear approximation functions for the solutions of the system of equations. The use of the quadratic or cubic approximation functions might improve the accuracy of the predictions. Inclusion of volumetric changes in the blueberries might also help improving the approximations.

In the literature, studies on drying of blueberries are limited. They are mostly related to the nutritional quality, optimization of drying pretreatments and rehydration (Ramaswamy and Nsonzi, 1998; Nsonzi and Ramaswamy, 1998 and Kim, 1987). This research is important for providing knowledge on the drying conditions.

High temperature drying of the blueberries may cause the damage reducing the nutritional quality and flavor of the berries. Therefore these two models can be used to understand and to control the drying processes and in process optimization.

It is very difficult to measure the material properties (e.g. De_{eff} , k_q , h , h_m) experimentally. But these models may be used in the numerical parameter estimations along with the reliable experimental drying curves.

NOTATIONS

c =specific heat(J/kgK)

c' =element capacitance matrix

c_m =mass capacity(kg moisture/kg dry body^oM)

[C]=capacitance matrix

ds =a small element along the surface S (m)

dx = a small element along the x-axis (m)

D =diffusion coefficient (m²/s)

f' =element force vector

{F}=force vector

h =convective heat transfer coefficient (W/m^{2o}K)

h_i =specific enthalpy (kJ/kg)

h_m =convective mass transfer coefficient (m/s)

I_i =volumetric capacity of the source (or sink) of material i, depending on the phase changes

j =unit vector in y direction

j_m =mass flux (kg moisture/m²s)

j_q =heat flux (W/m²)

k' =element conductivity matrix

k_q =thermal conductivity (W/m^oK)

K_{ij} =element of the conductance matrix in the ith row jth column

[K(T,M)]=temperature and moisture dependent conductance matrix

M =moisture content (%db)

M_0 =reference moisture content (%db)

N =shape function for linear triangular elements

n =number of the nodes in the element

n_j =normal vector to the boundary

q =flux (W/m^2)

r, z =cylindrical coordinates(m)

R =radius of the blueberry (m)

R_n =residual of the Galerkin formulation

S =surface

t =time (sec)

T =temperature ($^{\circ}K$)

T_0 =reference temperature ($^{\circ}K$)

U =moisture potential ($^{\circ}M$)

V =volume of the average blueberry (m^3)

X =first derivative of X with respect to time t

Greek letters

θ =deviation of the current temperature from the reference value T_0

Δt =time step (sec)

ρ =density (kg/m^3)

δ =thermogradiant coefficient (ratio of moisture gradient to the temperature gradient)

λ =latent heat of evaporation (J/kg)

APPENDICES

Appendix A: Matlab Code for Diffusional Model

```
Function [mois,temp,moisavg,tempavg]=time_tl(L,E,X,Y,...

Gheat,Gmass,Qheat,Qmass,Mmass,Smass,lambdaheat,lambdamass,deltatime,
g,BE);
%below function calculates the temperature and moisture values as
column vectors
m=length(E);n=length(X);
tempavg(1)=293; moisavg(1)=127.87;temp=zeros(g,n);mois=zeros(g,n);
temp(1,:)=(293*ones(n,1))'; mois(1,:)=(127.87*ones(n,1))';
for e=1:1:g %g=number of the time intervals

%Dxmass=-6*10^(-8)*(moisavg(e)/100)^3+8*10^(-
8)*(moisavg(e)/100)^2-10^(-8)*...
% (moisavg(e)/100)+10^(-9); %fb+tunnel, infused---
%Dxmass=-8*10^(-7)*(moisavg(e)/100)^3+10^(-6)*(moisavg(e)/100)^2-
3*10^(-7)*...
% (moisavg(e)/100)+2*10^(-8); %infused ,fb+fb
Dxmass=2*10^(-9)*(moisavg(e)/100)^3-3*10^(-
9)*(moisavg(e)/100)^2+2*10^(-9)*...
(moisavg(e)/100)+3*10^(-11); %infused,tunnel at 60C
%Dxmass=-8*10^(-9)*(moisavg(e)/100)^3+5*10^(-
8)*(moisavg(e)/100)^2-10^(-8)*...
% (moisavg(e)/100)+7*10^(-9);%thawed FB+tunnel

%Dxmass=(moisavg(e)/100)^3*10^(-12)+3*10^(-12)*(moisavg(e)/100)^2-
...
%10^(-10)*(moisavg(e)/100)+5*10^(-10); %for tunnel drying,
thawed
%Dxmass=exp(-3.5376*10^(-8))/tempavg(e)+1.1929*10^(-10); %from
dissertation
xwater=(moisavg(e)/100)/(1+(moisavg(e)/100)); %xi=mass fraction
of each component
xCH=0.138; xfiber=0.0389; %for fresh berries
rhowater=997.18+0.0031439*(tempavg(e)-273)-
0.0037574*(tempavg(e)-273)^2;
rhoCH=1599.1-0.31046*(tempavg(e)-273);
rhofiber=1311.5-0.36589*(tempavg(e)-273);
rho=1/((xwater/rhowater)+(xCH/rhoCH)+(xfiber/rhofiber));
xvwater=(xwater/rhowater)*rho; %xvi=volume fraction of each
component
xvCH=(xCH/rhoCH)*rho; %rho=composite density
xvfiber=(xfiber/rhofiber)*rho;
kwater=0.57109+0.0017625*(tempavg(e)-273)-6.7306*10^(-
6)*(tempavg(e)-273)^2;
```

```

kCH=0.2014+0.0013874*(tempavg(e)-273)-4.3312*10^(-6)*(tempavg(e)-273)^2;
kfiber=0.18331+0.0012497*(tempavg(e)-273)-3.1683*10^(-6)*(tempavg(e)-273)^2;
kqx=kwater*xvwater + kCH*xvCH + kfiber*xvfiber;

kDmass=Dxmass*stiff2d(0.01*[X Y],E);
kGmass=1/deltatime*mass2d(0.01*[X Y],E);
kmmass=Mmass*bound_mass(0.01*[X Y],E,BE);
Kmass=kDmass+kGmass+kmmass;
Cmass=1/deltatime*mass2d(0.01*[X Y],E);
Fmass=Smass*boundary(0.01*[X Y],E,BE);
mois(e+1,:)=(inv(Kmass)*(Cmass*mois(e,:)'+Fmass))'*1.32;
moisavg(e+1)=mean(mois(e+1,:));

%Mheat=106.8125-((1.4368*10^(-6)*(moisavg(e+1)-moisavg(e))/deltatime*rho*3470));
%Sheat=rho*(moisavg(e+1)-moisavg(e))/deltatime*2.1147*10^6*1.4984*10^(-6)-...
% rho*1.4984*10^(-6)*423*3470*(moisavg(e+1)-moisavg(e))/deltatime+423*106.8125;%fb drying,infused

Mheat=31.8656-((1.4368*10^(-6)*(moisavg(e+1)-moisavg(e))/deltatime*rho*3470));%/ (4*pi*(0.0071*10^(-2))^2);
Sheat=rho*(moisavg(e+1)-moisavg(e))/deltatime*lambdaheat*1.4984*10^(-6)-... %for tunnel drying infused
rho*1.4984*10^(-6)*333*3470*(moisavg(e+1)-moisavg(e))/deltatime+333*31.8656;

%Mheat=106.7618-((1.4368*10^(-6)*(moisavg(e+1)-moisavg(e))/deltatime*rho*3593.9));%/ (4*pi*(0.0071*10^(-2))^2);
%Sheat=rho*(moisavg(e+1)-moisavg(e))/deltatime*2.0539*10^6*1.4984*10^(-6)-...
%rho*1.4984*10^(-6)*443*3593.9*(moisavg(e+1)-moisavg(e))/deltatime+443*31.8656;%fb drying,thawed

%Mheat=31.8656-((1.4368*10^(-6)*(moisavg(e+1)-moisavg(e))/deltatime*rho*3593.9));
%Sheat=rho*(moisavg(e+1)-moisavg(e))/deltatime*lambdaheat*1.4984*10^(-6)-... %for tunnel drying thawed
%rho*1.4984*10^(-6)*333*3593.9*(moisavg(e+1)-moisavg(e))/deltatime+333*31.8656;

kDmass=kqx*stiff2d(0.01*[X Y],E);
kGmass=rho*3593.9/deltatime*mass2d(0.01*[X Y],E);
kmmass=Mheat*bound_mass(0.01*[X Y],E,BE);
Kmass=kDmass+kGmass+kmmass;
Cmass=rho*3593.9/deltatime*mass2d(0.01*[X Y],E);
Fmass=Sheat*boundary(0.01*[X Y],E,BE);
temp(e+1,:)=(inv(Kmass)*(Cmass*temp(e,:)'+Fmass))';
tempavg(e+1)=mean(temp(e+1,:));

end;

```

Appendix B: Matlab Code for Luikov Model

```

Function
[mois,temp,moisavg,tempavg,error]=time_tlthawed1(L,E,X,Y,...
    deltatime,g,BE,delta,lambda,c,h,hm,Tinf,Minf,moisexp);
%This function calculates the temperature and moisture values as
column vectors
%for nodes BE=[1 0 0;0 0 1;1 1 0;0 0 0;0 0 1;0 1 0;0 0 1];
m=length(E);n=length(X);
%initializing the moisture and temperature values
tempavg(1)=293;
moisavg(1)=578.99;temp=zeros(g,m+1);mois=zeros(g,m+1);
temp(1,:)=(293*ones(n,1))'; mois(1,:)=(578.99*ones(n,1))';
    cm=0.03
    for e=1:1:g %g=number of the time intervals

%calculating the Deff (D)
    D=10^(-12)*moisavg(e)^3+3*10^(-12)*moisavg(e)^2-10^(-
10)*moisavg(e)+5*10^(-10);

%calculating thermal conductivity (kq)
    xwater=(moisavg(e)/100)/(1+(moisavg(e)/100)); %xi=mass fraction
of each component
    xCH=0.138; xfiber=0.0389; %for fresh berries
    rhowater=997.18+0.0031439*(tempavg(e)-273)-
0.0037574*(tempavg(e)-273)^2;
    rhoCH=1599.1-0.31046*(tempavg(e)-273);
    rhofiber=1311.5-0.36589*(tempavg(e)-273);
    rho=1/((xwater/rhowater)+(xCH/rhoCH)+(xfiber/rhofiber));
    xvwater=(xwater/rhowater)*rho; %xvi=volume fraction of each
component
    xvCH=(xCH/rhoCH)*rho; %rho=composite density
    xvfiber=(xfiber/rhofiber)*rho;
    kwater=0.57109+0.0017625*(tempavg(e)-273)-6.7306*10^(-
6)*(tempavg(e)-273)^2;
    kCH=0.2014+0.0013874*(tempavg(e)-273)-4.3312*10^(-
6)*(tempavg(e)-273)^2;
    kfiber=0.18331+0.0012497*(tempavg(e)-273)-3.1683*10^(-
6)*(tempavg(e)-273)^2;
    kq=kwater*xvwater +kCH*xvCH + kfiber*xvfiber;

%calculating the constant variables of the Luikov model
    epsilon=(1.12-1.24*moisavg(e))/(1-moisavg(e));
    Kq=kq+((delta*epsilon*lambda*D)/cm);
    Cq=c*rho;
    Cm=rho;
    Km=D/cm;
    Kepsilon=(epsilon*lambda*D)/cm;
    Kdelta=(D*delta)/cm;
    jq=-kq*(Tinf-tempavg(e));
    Jq=(kq+(epsilon*lambda*D*delta)/cm)*(jq/kq)*10^(-2);
    jm=-hm*(-moisavg(e));
    Jm=jm-((D/cm)*delta*(jq/kq))*10^(-2);
    Aq=(kq+(delta*epsilon*lambda*D)/cm)*(h/kq);

```

```

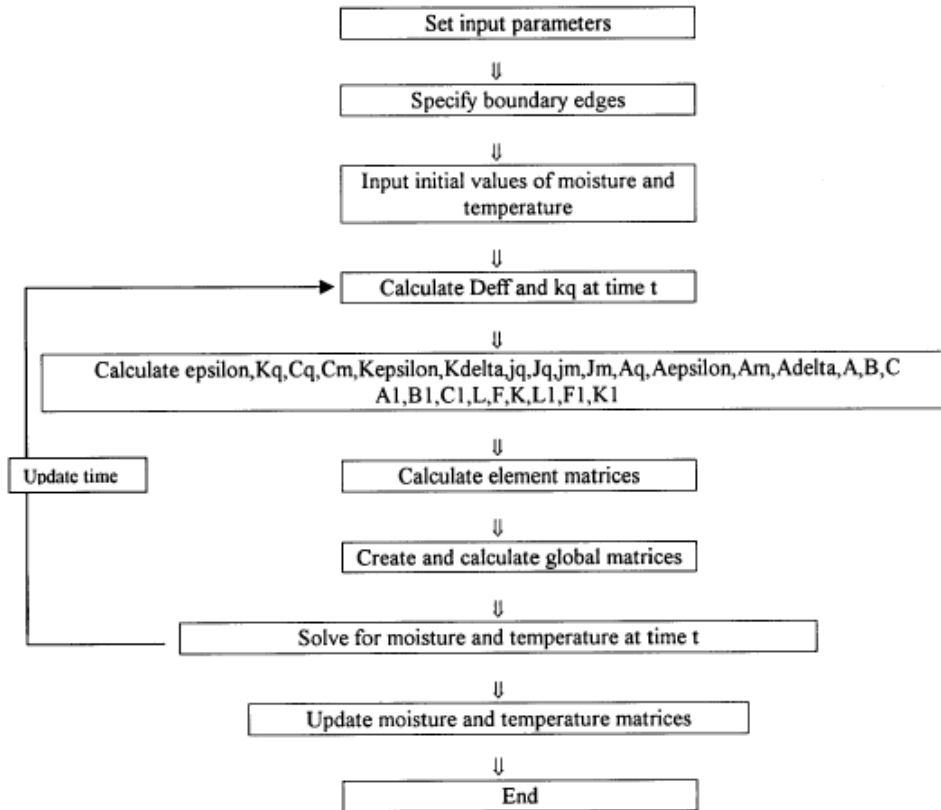
    Aepsilon=(kq+(delta*epsilon*lambda*D)/cm)*(lambda*hm*rho*(1-
epsilon)/kq);
    Am=hm*(rho-((1-epsilon)/kq)*lambda*(D/cm)*rho*delta);
    Adelta=- (h/kq)*(D/cm)*delta;
    A=-Jq-
Jm*(Kepsilon/Km)+Aq*Tinf+Aepsilon*Minf+(Kepsilon/Km)*Adelta*Tinf+(Ke
psilon/Km)*Am*Minf;
    B=-Aq-((Kepsilon/Km)*Adelta);
    C=-Aepsilon-(Am*(Kepsilon/Km));
    A1=((Kdelta/Kq)*(Aq*Tinf+Aepsilon*Minf-Jq))+Adelta*Tinf+Am*Minf-
Jm;
    B1=- (Kdelta/Kq)*Aq-Adelta;
    C1=-Am-Aepsilon*(Kdelta/Kq);

%calculating the global matrices
    K=(-Kq*stiff2d(0.01*[X Y],E)-Cq/deltatime*mass2d(0.01*[X
Y],E)+B*bound_mass(0.01*[X Y],E,BE));
    L=(C*bound_mass(0.01*[X Y],E,BE)-Kepsilon*stiff2d(0.01*[X
Y],E));
    F=(-A*boundary(0.01*[X Y],E,BE)-Cq/deltatime*mass2d(0.01*[X
Y],E)*temp(e,:));
    K1=(-Kdelta*stiff2d(0.01*[X Y],E)+B1*bound_mass(0.01*[X
Y],E,BE));
    L1=C1*bound_mass(0.01*[X Y],E,BE)-Km*stiff2d(0.01*[X Y],E)-
Cm/deltatime*mass2d(0.01*[X Y],E);
    F1=-A1*boundary(0.01*[X Y],E,BE)-Cm/deltatime*mass2d(0.01*[X
Y],E)*mois(e,:));

%solving for the moisture and temperature values for the each node
and averaging
    MT=[L K;L1 K1]^(-1)*[F;F1]*100;
    mois(e+1,:)=MT(1:n)';
    moisavg(e+1)=mean(mois(e+1,:));
    temp(e+1,:)=MT(n+1:2*n)';
    tempavg(e+1)=mean(temp(e+1,:));
end;

```

Appendix C: Flow diagram for procedure used in diffusional and Luikov Models



REFERENCES

1. Alvarez, C.A., Aguerre, R., Gomez, R., Vidales, S., Alzamora, S.M. and Gerschenson, L.N. (1995) "Air dehydration of strawberries: effect of blanching and osmotic pretreatments on the kinetics of moisture transport", *Journal of Food Engineering*, 25, 167-178.
2. Balaban M. (1989) "Effect of volume change in foods on the temperature and moisture content predictions of simultaneous heat and moisture transfer models", *Journal of Food Process Engineering*, 12, 67-88.
3. Balaban, M. and Pigott, G. M. (1988) "Mathematical model of simultaneous heat and mass transfer in food with dimensional changes and variable transport parameters", *Journal of Food Science*, 53, 935, 939.
4. Banga, J. R. and Singh, R. P. (1994) "Optimization of air drying of foods", *Journal of Food Engineering*, 23, 189-211.
5. Berger, D. and Pei, D. C. T. (1973) "Drying of hygroscopic capillary porous solids – A theoretical approach", *International Journal of Heat and Mass Transfer*, 16, 293-302.
6. Brennan, J. G. and Butters J. R. (Eds) (1990) "Dehydration" in *Food Engineering Operations*, 3rd Edition, Elsevier Applied Science, London, UK, pp 371-387.
7. Bruin, S. and Luyben, K. Ch. A. M. (1980) "Drying of food materials: a review of recent developments", in *Advances in Drying*, A. S. Mujumdar (Ed.), Hemisphere Pub, Corp., Washington, DC., pp 155-215.

8. Canovas, G. V. B. and Mercado H. V. (1996) *Dehydration of Foods*, Chapman and Hall, New York, NY.
9. Chang, W. and Weng, C. (2000) “An analytical solution to coupled heat and mass transfer in porous materials”, *International Journal of Heat and Mass Transfer*, 43, 3621-3632.
10. Chen, P. and Pei, D. C. T. (1983) “A mathematical model of drying process”, *International Journal of Heat and Mass Transfer*, 32, 297-310.
11. Chiang, W. C. and Petersen, J. N. (1987) “Experimental measurement of temperature and moisture profiles during apple drying”, *Drying Technology*, 5, 25-49.
12. Chou, S. K., Chua, K. J., Mujumdar, A. S., Hawlader, N. A., and Ho, J. C. (2000) “On the intermittent drying of an agricultural product”, *Trans IChemE*, 78, 193-203.
13. Comini, G. and Lewis, R. W. (1976) “A numerical solution of two-dimensional problems involving heat and mass transfer”, *International Journal of Heat and Mass Transfer*, 19, 1387-1392.
14. Cronin, K. and Kearney, S. (1998) “Monte Carlo modelling of a vegetable tray dryer” *Journal of Food Engineering*, 35, 233-250.
15. Ferraro, P., Figueiredo, A. and Freire, F. (1998) “Experimental analysis of the drying kinetics of a food product”, *Drying Technology*, 16(8), 1687-1702.
16. Fortes, M. and Okos, M. R. (1980) “Drying theories: their bases and limitations as applied to foods and grains”, in *Advances in Drying*, A. S. Mujumdar (Ed.), Hemisphere Pub, Corp., Washington, DC., pp 119-153.
17. Fortes, M. and Okos, M. R. (1981) “Non-equilibrium thermodynamics approach to heat and mass transfer in corn kernels”, *Trans. ASAE*, 24, 761-769.

18. Fowler, A. C. (1997) *Mathematical Models in the Applied Sciences*, Cambridge University Press, Cambridge, UK.
19. Franca, A. S., Oliveria, L. S., Haghghi, K., and Krutz, G. W. (1995) "The application of adoptive finite element analysis to heat and mass transfer problems", *Journal of Agricultural Engineering Research*, 62, 49-60.
20. Fryer, P. (1994) "Mathematical models in food processing", *Chemistry and Industry*, 4, 515-518.
21. Furuta, T. and Hayakawa, K.-I. (1992) "Heat and moisture transfer with thermodynamically interactive fluxes I. Mathematical model development and numerical solution", *American Society of Agricultural Engineers*, 35(5), 1537-1546.
22. Fusco, A. J., Avanza, J. R., and Gabitto, J. F. (1991) "A diffusional model for drying with volume change", *Drying Technology*, 9, 397-417.
23. Ghiaus, A. G., Margaris, D. P., and Papanikas, D. G. (1997) "Mathematical modeling of the convective drying of fruits and vegetables", *Journal of Food Science*, 62, 1154-1157.
24. Haghghi, K. and Aguirre, C. (1999) "Adaptive and stochastic finite element analysis in drying", *Drying Technology*, 17(10), 2037-2053.
25. Haghghi, K. and Segerlind, L. J. (1988) "Modeling simultaneous heat and mass transfer in an isotropic sphere – A finite element approach", *Transactions of the American Society of Agricultural Engineers*, 31, 629-637.
26. Haghghi, K., Irudayaraj, J., Stroshine, R.L. and Sokhansanj, S. (1990) "Grain kernel drying simulation using finite element method", *American Society of Agricultural Engineers*, 33(6), 1957-1965.
27. Harmaty, T. Z. (1969) "Simultaneous moisture and heat transfer in porous systems with particular reference to drying", *Ind. Engng. Chem. Fund.*, 8, 92-103.

28. Hayakawa, K. I. and Furuta, T. (1989) "Thermodynamically interactive heat and mass transfer coupled with shrinkage and chemical reactions", in *Food Properties and Computer-Aided Engineering of Food Processing Systems*, R. P. Singh and A. G. Medina (Eds.), pp 201-221.
29. Henderson, S. M. and Perry, R. L. (1967) *Agricultural process engineering*, 2nd edition, The AVI publishing company, Inc. Westport, CT.
30. Hernandez, J. A., Pavon, G., and Garcia, M. A. (2000) "Analytical solution of mass transfer equation considering shrinkage for modeling food-drying kinetics", *Journal of Food Engineering*, 45, 1-10.
31. Hong, Y. C., Bakshi, A. S., and Labuza, T. P. (1986) "Finite element modeling of moisture transfer during storage of mixed multicomponent dried foods", *Journal of Food Science*, 51, 554-558.
32. Hougen, O. A., McCauley, H. J., and Marshall, W. R. Jr. (1940) "Limitations of diffusion equations in drying", *Trans. Am. Inst. Chem. Eng.*, 36, 183-206.
33. Husain, A., Chen, C. S., and Clayton, J. T., and Whitney, L. F. (1972) "Mathematical simulation of simultaneous heat and mass transfer in high moisture foods", *Trans. ASAE*, 13, 732-736.
34. Husain, A., Chen, C. S., and Clayton, J. T. (1973) "Simultaneous heat and mass diffusion in biological materials", *J. Agric. Engng. Res.*, 18, 343-354.
35. Igbeka, J. C. (1982) "Simulation of moisture movement during a starchy food product-cassava", *J. Fd. Technol.*, 17, 27-36.
36. Incoropera, F. P. and DeWitt, D. P. (1996) *Fundamentals of Heat and Mass Transfer*, 4th edition, John Wiley and Sons Ltd., New York, NY.
37. Irudayaraj, J., Haghghi, K., and Strohine. R. L. (1992) "Finite element analysis of drying with application to cereal grains", *J. Engng. Res.*, 53, 209-229.

38. Irudayaraj, J. and Wu, Y. (1996) "Analysis and application of Luikov's heat, mass, and pressure transfer model to capillary porous media", *Drying Technology*, 14, 803-824.
39. Irudayaraj, J. and Wu, Y. (1997) "Modelling heat and mass transfer in coupled systems during absorption and desorption" In *Mathematical Modeling and Numerical Techniques in Drying Technology*, Ian Turner and Arun S. Mujumdar (Ed.), Marcel Dekker Inc., New York, NY.
40. Irudayaraj, J. and Wu, Y. (1999a) "Heat and mass transfer coefficients in drying of starch based food systems", *Journal of Food Science*, 64, 323-327.
41. Irudayaraj, J. and Wu, Y. (1999b) "Numerical modeling of heat and mass transfer in starch systems", *Transactions of the American Society of Agricultural Engineers*, 42, 449-455.
42. Jayaraman, K.S. and Das Gupta, D.K. (1992) "Dehydration of fruits and vegetables- recent developments in principles and techniques", *Drying Technology*, 10(1), 1-50.
43. Jia, C. C. and Sun D. (2000) "Mathematical simulation of temperature and moisture fields within a grain kernel during drying", *Drying Technology*, 18, 1305-1325.
44. Karathanos, V.T. (1999) "Determination of water content of dried fruits by drying kinetics", *Journal of Food Engineering*, 39, 337-344.
45. Karathanos, V.T. and Kostaropoulos, A.E. (1995) "Air- drying kinetics of osmotically dehydrated fruits", *Drying Technology*, 13(5-7), 1503-1521.
46. Keey, R. B. (1980) "Theoretical foundations of drying technology", in *Advances in Drying*, A. S. Mujumdar (Ed.), Hemisphere Pub, Corp., Washington, DC., pp 1-19.
47. Kiranoudis, C. T., Maroulis, Z. B., and Marinos-Kouris, D. (1992) "Model selection in air drying of foods", *Drying Technology*, 10, 1097-1106.

48. Kiranoudis, C.T., Maroulis, Z.B. and Marinos-Kouris, D. (1997) "Modeling and optimization of fluidized bed and rotary dryers", *Drying Technology*, 15(3&4), 735-763.
49. Kim, M. H. (1987) Fluidized bed and osmotic processes for dehydration of rabbiteye blueberries, Ph.D. dissertation, The University of Georgia.
50. Krischer, O. and Kast, W. (1978) Die Wissenschaftlichen Grundlagen der Trocknungstechnik, 3rd Edition, Berlin, Germany.
51. Kumar, A., Blaisdell, J. L., and Herum, F. L. (1982) "Generalized analytical model for moisture diffusion in a composite cylindrical body", *Transactions of the American Society of Agricultural Engineers*, 25, 752-758.
52. Lomauro, C. J., Bakshi, A. S., and Labuza, T. P. (1985) "Evaluation of food moisture sorption isotherm equations. Part I: Fruit, vegetable and meat products", *Lebensm. WissuTechnol.*, 18(2), 111-117.
53. Luikov, A. V. (1966) "Application of irreversible thermodynamics method to investigation of heat and mass transfer", *International Journal of Heat and Mass Transfer*, 9, 139-152.
54. Luikov, A. V. (1975) "Systems of differential equations of heat and mass transfer in capillary-porous bodies (review)", *International Journal of Heat and Mass Transfer*, 18, 1-14.
55. Mahmutoglu, T., Pala, M., and Unal, M. (1995) "Mathematical modelling of moisture, volume and temperature changes during drying of pretreated apricots", *Journal of Food Processing and Preservation*, 19, 467-490.
56. Markowski, M. (1998) "Air drying of vegetables: evaluation of mass transfer coefficient", *Journal of Food Engineering*, 34, 55-62.

57. Maroulis, Z. B., Drouzas, A. E., and Saravacos, G. D. (1990) "Modeling of thermal conductivity of granular starches", *Journal of Food Engineering*, 11, 255-271.
58. Maroulis, S. N., Karathanos, V. T., and Saravacos, G. D. (1989) "Effect of sugars on the water diffusivity in hydrated granular starches", *Journal of Food Science*, 54, 1496-15001.
59. Maroulis, Z. B., Kiranoulis, C. T., and Marinos-Kouris, D. (1991) "Simultaneous estimation of heat and mass transfer coefficients in externally controlled drying", *Journal of Food Engineering*, 14, 241-255.
60. Maroulis, Z. B., Kiranoudis, C. T., and Marinos-Kouris, D. (1995) "Heat and mass transfer modeling in air drying of foods", *Journal of Food Engineering*, 26, 113-130.
61. McMinn, W.A.M and Magee, T.R.A. (1999) "Principles, methods and applications of the convective drying of foodstuffs", *Trans IChemE*, 77, 175-193.
62. Miles, C. A., Beek, V. G., and Veerkamp, C. H. (1983) "Calculation of thermophysical properties of foods", in *Physical Properties of Foods*, Jowitt, R. Escher, F., Kent, M., McKenna, B., Rogues, M. (Eds.), Elsevier Science Publishing Co., Inc., New York, NY., pp 69-311.
63. Mukherjee, D., Puri, V.M. and Anantheswaran, R.C. (1997) "Measurement of coupled heat and moisture transfer coefficients for selected vegetables", *Drying Technology*, 15(1), 71-74.
64. Nsonzi, F. and Ramaswamy, H.S. (1998) "Osmotic dehydration kinetics of blueberries", *Drying Technology*, 16(3-5), 725-741.
65. Pabis, S. and Henderson, S. M. (1961) "Grain drying theory- II. A critical analysis of drying curve for shelled maize", *Journal of Agric. Eng. Res.*, 6, 272-277.

66. Pabis, S., Javas, D.S. and Cenkowski, S. (Eds.) (1998) "Mathematical theory of drying single solid bodies", in *Grain Drying*, John Wiley and Sons, Inc., NY.
67. Pandey, R. N., Srivastava, S. K., and Mikhailov, M. D. (1999) "Solutions of Luikov equations of heat and mass transfer in capillary porous bodies through matrix calculus: a new approach", *International Journal of Heat and Mass Transfer*, 42, 2649-2660.
68. Puri, V. M. and Anantheswaran, R. C. (1993) "The finite-element method in food processing: a review", *Journal of Food Engineering*, 19, 247-274.
69. Ramaswamy, H.S. and Nsonzi, F. (1998) "Convective-air drying kinetics of osmotically pretreated blueberries", *Drying Technology*, 16(3-5), 743-759.
70. Ratti, C. (2001) "Hot air and freeze-drying of high value foods: a review", *Journal of Food Engineering*, 49, 311-319.
71. Rossen, J. L. and Hayakawa, K. I. (1977) "Simultaneous heat and moisture transfer in dehydrated food: A review of theoretical models", in *Water Removal Processes; Drying and concentration of Foods and Other Materials*, AIChE Symposium Series 163, Vol 73, King, C. J. and Clark, J. P. (Eds.), pp 71-81.
72. Rovedo, C.O., Suarez, C. and Viollaz, P.E. (1995) "Drying of foods : evaluation of a drying model", *Journal of Food Engineering*, 26, 1-12.
73. Sabarez, H.T. and Price, W.E. (1999) "A diffusion model for prune dehydration", *Journal of Food Engineering*, 42, 167-172.
74. Sakai, N, and Hayakawa, K. I. (1992) "Two dimensional simultaneous heat and moisture transfer in composite food", *Journal of Food Science*, 57, 475-480.
75. Sakai, N. and Hayakawa, K. I. (1993) "Heat and moisture transfer in composite food – Theoretical analysis of influence of surface conductance and component arrangement", *Journal of Food Science*, 58, 1335-1339.

76. Saravacos, G. D. (1995) "Moisture transport properties of foods", In: Advances in Food Engineering. Proceedings of the 4th Conference of Food Engineering (COFE) by Narsimhan, G., Okos, M. R., and Lombardo, S. (Ed.), 53-57.
77. Saravacos, G. D. and Kostaropoulos, A. E. (1996) "Engineering properties in food process simulation", *Computers and Chemical Engineering.*, 20, S461-S466.
78. Segerlind, L. J. (1984) Applied finite element analysis, 2nd Edition, John Wiley and Sons, Ltd., New York, NY.
79. Sereno, A. M. and Medeiros, G. L. (1990) "A simplified model for the prediction of drying rates for foods", *Journal of Food Engineering*, 12, 1-11.
80. Sharaf-Eldeen T. and Hamdy, M. Y. (1987) "Falling rate drying of fully exposed biological materials: A review of mathematical models ", *American Society of Agricultural Engineers*, 79, 6522.
81. Simal, S., Mulef, A., Tarrazo, J., and Rosello, C. (1996) "Drying models for green peas", *Food Chemistry*, 55, 121-128.
82. Simal, S., Deya, E and Rossello, C. (1997) "Simple modeling of air drying curves of fresh and osmotically pre-dehydrated apple cubes", *Journal of Food Engineering*, 33, 139-150.
83. Simal, S., Rossello, C., Berna, A., and Mulet, A. (1998) "Drying of shrinkage cylinder-shaped bodies", *Journal of Food Engineering*, 37, 423-435.
84. Sokhansanj, S. and Gustafson, R. J. (1979) Finite element predictions of rice cracking during drying, Paper No 79-3547, American Society of Agriculture Engineers, St Joseph, MI.
85. Songtao, I. T., Xuquan, L., Guodan, L., Lering, L., and Lineng, L. (1999) "Cross-effect of heat and mass transfer of Luikov equation: measurement and analysis", *Drying Technology*, 17, 1859-1877.

86. Spiazzi, E. and Mascheroni, R. (1997) "Mass transfer model for osmotic dehydration of fruits and vegetables-I. Development of the simulation model", *Journal of Food Engineering*, 34, 387-410.
87. Suzuki, M., Keey, R. B., and Maeda, S. (1974) "On the characteristic drying curve" *Int. J. Heat Mass Trans.*, 17, 1455-1464.
88. Temple, S.J., Tambala, S.T. and Van Boxtel, A.J.B. (2000) "Monitoring and control of fluid-bed drying of tea", *Control Engineering Practice*, 8, 165-173.
89. Thorvaldsson, K. and Janestad, H. (1999) "A model for simultaneous heat , water and vapour diffusion", *Journal of Food Engineering*, 40, 167-172.
90. Toledo, R. (1991) *Fundamentals of Food Process Engineering*, Chapman and Hall, New York, NY.
91. Tomas, S. and Skansi, D. (1996) "Numerical interpretation of drying curve of food products", *Journal of Chemical Engineers of Japan*, 29, 367-370.
92. Tong, C. H. and Lund, D. B. (1990) "Effective moisture diffusivity in porous materials as a function of temperature and moisture content", *Biotechnol. Prog.*, 6, 67-75.
93. Tsukada, T., Sakai, N., and Hayakawa, K. I. (1991) "Computerized model for strain-stress analysis of food undergoing simultaneous heat and mass transfer", *Journal of Food Science*, 56, 1438-1445.
94. Vagenas, G. K. and Karathanos, V. T. (1991) "Prediction of moisture diffusivity in granular materials, with special applications to foods", *Biotechnol. Prog.*, 7, 419-426.
95. Vagenas, G. K. and Karathanos, V. T. (1993) "Prediction of the effective moisture diffusivity in gelatinized food systems", *Journal of Food Engineering*, 18, 159-179.

96. Vega-Mercado, H., Gongora-Niet, M. M., and Barbosa-Canovas, G. V. (2001) "Advances in dehydration of foods", *Journal of Food Engineering*, 49, 311-319.
97. Voudouris, N. and Hayakawa, K. (1994) "Simultaneous determination of thermal conductivity and diffusivity of foods using a point source probe: A theoretical analysis", *Lebensm.-Wiss. U.-Technol.*, 27, 522-532.
98. Waananen, K. M., Litchfield, J. B., and Okos, M. R. (1993) "Classification of drying models for porous solids", *Drying Technology*, 11, 1-40.
99. Wang, N. and Brennan, J. G. (1995) "A mathematical model of simultaneous heat and moisture transfer during drying of potato", *Journal of Food Engineering*, 24, 47-60.
100. Wang, Z.H. and Chen, G. (1999) "Heat and mass transfer during low intensity convection drying", *Chemical Engineering Science*, 54, 3899-3908.
101. Whitaker, T. B. and Young, J. H. (1972) "Simulation of moisture movement in peanut kernels: Evaluation of the diffusion equation", *Trans. ASAE*, 13, 163-166.
102. Wu, Y. and Irudayaraj, J. (1996) "Analysis of heat, mass and pressure transfer in starch based food systems", *Journal of Food Engineering*, 29, 399-414.
103. Yao, Z. and Le Maguer, M. (1994) "Finite element modeling of osmotic dehydration processes", *Food Research International*, 27, 211-212.
104. Yao, Z. and Le Maguer, M. (1996) "Mathematical modeling and simulation of mass transfer in osmotic dehydration processes. Part I: Conceptual and mathematical models", *Journal of Food Engineering*, 29, 349-360.
105. Yao, Z. and Le Maguer, M. (1997) "Mathematical modeling and simulation of mass transfer in osmotic dehydration processes. Part II: Simulation and model verification", *Journal of Food Engineering*, 32, 21-32.

106. Young, J.H.(1969) “Simultaneous heat and mass transfer in porous hgyroscopic solids”, *Trans ASAE*, 12, 720-725.
107. Young, J.H. and Whitaker (1971) “Evaluation of the diffusion equation for describing thin layer drying of peanuts in the hull”, *Trans ASAE*, 14, 309-312.
108. Zhou, L., Puri, V.M. and Anantheswaran, R.C. (1994) “Measurement of coefficients for simultaneous heat and mass transfer in food products”, *Drying Technology*, 12(3), 607-627.
109. Zogzas, N.P. and Maroulis, Z.B. (1996) “Effective moisture diffusivity estimation from drying data, A comparison between various methods of analysis”, *Drying Technology*, 14(7&8), 1543-1573.
110. Zogzas, N. P., Maroulis, Z. B., and Marinos-Kouris, D. (1994) “Moisture diffusivity methods of experimental determination. A review”, *Drying Technology*, 12 (3), 483-515.
111. Zogzas, N. P., Maroulis, Z. B., and Marinos-Kouris, D. (1994) “Moisture diffusivity data compilation in foodstuffs”, *Drying Technology*, 14 (10), 2225-2253.